615

CATALYSIS OF CARBON GASIFICATION

P. L. WALKER, Jr., M. SHELEF, and R. A. ANDERSON

MATERIALS SCIENCE DEPARTMENT
COLLEGE OF EARTH AND MINERAL SCIENCES
THE PENNSYLVANIA STATE UNIVERSITY
UNIVERSITY PARK, PENNSYLVANIA

I. INTRODUCTION

Carbon gasification, a group of reactions which encompasses the combustion of carbonaceous materials, was probably the first chemical process consciously employed in the service of man but remains as yet not completely understood in many aspects. This is hardly surprising if one realizes that it is a heterogeneous surface reaction in which the surface itself is continuously consumed and changed and that even simpler heterogeneous reactions in which surfaces remain supposedly unchanged offer considerable obstacles to theoretical treatments. Moreover, the gasification reactions are strongly influenced by impurities in the carbonaceous solid, impurities which are almost ubiquitous. The influences of these impurities are of a great practical significance whenever a faster gasification rate is desired, as, for instance, in energy-producing

processes or steel-making or whenever the prevention of gasification is the goal, as is the case in CO_2-cooled graphite-moderated nuclear reactors. New space technology and high-temperature applications of carbon and composite carbon–metal materials add further stimuli to research into catalyzed carbon gasification in an effort to determine the usefulness limits of these materials over a wide range of conditions. It appears that the probing of carbon gasification catalysis cannot wait until the non-catalyzed reactions become entirely deciphered, and, therefore, this field is being vigorously pursued in the meantime.

Until the middle 1930s, the majority of the investigations into carbon gasification dealt to a lesser or greater degree with, nolens volens, catalyzed reactions, because the carbons employed in these works always contained a certain amount of impurity capable of catalysis, usually not less than several hundredths of a per cent. The amounts of intentionally introduced catalysts were, in some cases, as much as several per cent or even tens of per cent. This, of course, helped to overshadow the effects of the impurities originally present in the carbons. The composition of the ashes in the carbon could encompass, besides the major ash components, almost the whole gamut of metallic elements, making a meaningful interpretation of the catalytic effect practically impossible.

Naturally, the detailed study of catalyzed carbon gasification gravitates more toward the use of well-defined carbons, purified to as high a degree as possible. This was to a large extent coincident with the technological trend to very pure materials as those used in nuclear reactors, electronic devices, etc. The intentional introduction of a controlled kind and amount of catalyst into a relatively pure and well-defined carbon sample generated data whose interpretation has culminated in a number of theories of catalysis of gas–carbon reactions. These theories are at present only qualitative rationalizations and still far removed from elegant, concise mathematical formulations; so is, for that matter, the theoretical state of heterogeneous catalysis. Nevertheless, their value is in stimulating new research which will eventually lead to better, more elegant theories.

Reviews on carbon gasification (*1–5*) have usually dealt with the catalysis of these reactions only in passing. One review devoted solely to the subject is that of Kröger published in 1939 (*6*). It covers mainly, in an extensive manner, work which has employed carbons of varying degrees of structural perfection and purity. The present review will refer to this early work only when very relevant to the context.

In this chapter, the authors have attempted to supply references to the majority of pertinent papers on catalysis of carbon combustion and

gasification. To the extent possible, we have attempted to unify the findings of different workers reporting catalysis results. We have then considered in detail our results on catalysis of the C—CO_2 reaction by Fe, Co, and Ni. Our results represent one of the few attempts which have apparently been made at identifying precisely the active catalyst phase or phases in a gasification reaction. We hope that consideration of these results will stimulate new and improved research directed at understanding more fully the mechanism of catalysis of carbon gasification.

II. LITERATURE ON CATALYSIS OF CARBON GASIFICATION

A. General Remarks

Since the publication of the review of Walker et al. on the gas reactions of carbon (*1*), further research has tended to confirm in general the mechanisms expounded therein. Specifically, with respect to the C—CO_2 and C—H_2O reactions, more evidence has been produced to support mechanism "B," i.e., the equilibrium retardation by product gases (*7–9*). It is, however, appropriate to mention that the simple Langmuir–Hinshelwood mechanism considered in (*1*) assumes a reacting surface which is energetically uniform, while the real surface is probably not. Thus several experimenters have reported that under certain conditions this mechanism does not hold (*9,10*). By and large at present the treatments of the noncatalyzed reactions are modifications of the Langmuir–Hinshelwood mechanism of surface reactions; and, consequently, any analysis of catalytic action attempts to explain the effect of the catalyst on one (or more) of the steps of this mechanism.

The limiting stage of the accepted Langmuir–Hinshelwood mechanism is not always obvious, except at extreme conditions of pressure. It can be safely supposed that at high pressures of the reacting gas the desorption step is rate-controlling, and conversely at very low pressures—the adsorption step. At intermediate pressure, both steps affect the coverage of the surface and, therefore, the gasification rate. The adsorption and desorption steps have different activation energies; and with the change of temperature, their relative effect on the gasification rate changes as well. It is to be anticipated that over a wide temperature range the rates of adsorption and desorption steps may cross over and the control pass from one step to another. It is, therefore, of utmost importance to specify the reaction conditions when asserting that a certain step of the mechanism is rate-controlling. Because the catalyst presumably affects the limiting

stage, it is plausible that the same agent may, or may not, catalyze the gasification rate depending on the conditions, or at least show an effect of varying magnitude.

It is sufficient to indicate at this point that the catalyst may affect any one of the steps in the mechanism on the prismatic planes of the carbon and do this either by lowering the activation energy or changing the number of active sites, say by affecting the chemisorption coverage on the prismatic planes, i.e., the preexponential factor. Then, it may affect both these parameters (see Section II.H). The possibility that more than one step of the mechanism is influenced must also be considered. Another mode of action of the catalyst is to induce pits in the carbon basal plane and thereby expose additional edge planes for the reaction. The combination of this possibility with the aforementioned can also not be overlooked.

One cannot exclude the possibility that the Langmuir–Hinshelwood mechanism is bypassed altogether and that the sequence of steps differs altogether. The various theories proposed touch on almost all the possibilities. We will discuss them in Section II.I.

We have referred above to the complexity of the catalyzed gasification of carbon. Now some of the pitfalls which the investigator is prone to overlook are enumerated. This will illustrate also the difficulty of bringing the published accounts of the catalysis of carbon gasification to a common basis.

The most obvious obstacle, of course, is the fact that carbon appears in an almost infinite spectrum of shades of structural perfection and frequently samples cut from the same specimen exhibit significant differences in their reactivity. This difficulty pertains to catalyzed and noncatalyzed reactions alike and will not be discussed further.

Then, unfortunately for someone trying to introduce a rigorous order into the phenomenon of catalysis, almost any inorganic impurity in a trace amount (less than 1 ppm) is capable of affecting gasification rates. The exact chemical state of the catalyst at the gasification conditions remains an enigma in many published accounts. This is mainly due to the fact that at elevated temperatures carbon is capable of reducing many of the added salts and oxides to the metallic state. Also the oxidizing gases are capable in certain conditions of oxidizing the metals. Few investigators have evaluated the thermodynamics of their carbon–gas–catalyst system at reaction conditions or at pretreatment conditions which often precede the reactions. It is not claimed that the thermodynamic data can provide a clear-cut answer, because they refer to bulk phases, while surface phases which are responsible for catalysis may have different stabilities; but at

least some gross misstatements may be avoided. Thus, in one instance, after treatment of graphite by Fe, Co, and Ni nitrates at 1100°C, the catalytic species are referred to as the corresponding oxides (*11*), while a part of the catalyst at least must have been reduced to the metallic state. This question of chemical state is very relevant to the mechanism. Some literature findings will be summarized below and the question will be considered at length when discussing our catalysis results in Section III.

Further obscure points are frequently concerned with the distribution and particle size and shape of the catalyst when added by solution impregnation or naturally present in the carbon. A less ambiguous picture is obtained when the catalyst is added in the form of discrete particles of known physical characteristics.

Another complication, taken into account in a few cases only, is that the amount of impurities originally present on the reacting surface increases very significantly with the amount of carbon burn-off. Presumably all the impurities which have been present in the burned-off volume do accumulate on the surface. To construct a model of this accumulation, the distribution and amount of impurities at zero burn-off and the size and shape of impurity particles and carbon particles before and after burn-off must be known. Heuchamps (*12*,*12a*), assuming a uniform distribution of impurities in the bulk, has calculated from surface area measurements, for a spectroscopic-grade Acheson graphite burned off in air and containing initially 1 ppm* of impurities, the surface impurity concentration change with burn-off. The results are given in Table I. The table clearly shows the large changes in surface concentration, especially at low initial levels of impurity; but even at modest burn-offs one might argue that the impurities may be rather loosely deposited on the fresh surface and not in such intimate contact with this surface as the impurities originally present at a given surface. It appears that if one has prepared a mixture of discrete impurity and carbon particles of commensurate size (as is the case in our studies described in Section III) the number of contact points is not greatly affected by burn-off, and if anything may even decrease with burn-off.

The latest studies (*7*,*8*,*12–16*) show that the same attention must be paid to the purity of gases as to the purity of the initial carbon. Thus minute quantities of impurities in the gases, such as hydrogen or water at the ppm level, are liable to influence the reaction to a considerable extent, possibly by the interaction with the catalyst in the solid.

* Unless indicated otherwise, the amount of impurity in the carbon is given on a weight basis.

TABLE I

Change of Surface Concentration of Impurities with Graphite Burn-Off in Air (*12,12a*)

Burn-off, %	Impurity concn., ppm
0	1
1	22
5	88
10	147
30	490
50	1,250
70	3,400
90	16,400

B. Relative Activities of Various Catalysts

A number of workers have investigated, some qualitatively and some quantitatively, the relative activities of various catalysts for accelerating the gasification of carbon. As we will see, these relative activities are by no means universal but depend strongly on the particular experimental conditions used. These experimental conditions determine such important parameters as size and porosity of catalyst particles (and thus their surface area), chemical state of the catalyst, intimacy of contact between catalyst and carbon surface, and relative amounts of catalyst on the carbon basal plane and prismatic faces. In the majority of investigations little is known about these important parameters, and thus the results, unfortunately, do not add significantly to our basic understanding of the catalysis of carbon gasification.

Letort and Martin (*17*) give the following activity for a series of metal catalysts in the combustion of graphite in air at 500°C in the presence of 0.12% of catalyst: Au > Na > Ca > Ag > Cu > Pb > Ni > Mn > Co > Fe. The strong catalytic capacity of noble metals is not isolated to this work but, as we shall see, has been observed by many. For example, Thomas and Walker (*18*) studied the influence of Fe, Ni, Co, Mn, Ta, Ti, Ag, Mo, and B on the etching of graphite single crystals. The most active catalyst was Ag; the least active catalyst was Ta.

Amariglio (*19*) introduced ca. 110 ppm of impurity into very pure nuclear graphite by impregnation with a water-soluble salt. The results are given as the ratio of the catalyzed rate to the rate of the noncatalyzed combustion in air at temperatures less than 600°C: Pb, 4.7×10^5; Mn, 8.6×10^4; Ag, 1.34×10^3; Cu, 500, Au, 240; Na, 230; Ba, 100; Cd, 90; Sr, 8; Mg, 6; Co, 4; Al, 3; Be, 1; and B, 1. This series differs

considerably from that of Letort and Martin. Activities of less than 10 were assumed to be insignificant because the catalysts themselves contained ca. 0.2% of impurities which would introduce ca. 0.2 ppm of unknown impurity into the carbon. This small amount could possibly increase the rate by a factor of 10.

Hering et al. (*20*) give still a different series of activities in the oxidation of purified graphites (<5 ppm impurity) in the 450–700°C temperature range. The catalysts were added by solution impregnation in the amount of <15 ppm. The catalysts were observed to accelerate pit formation in the basal planes. The ratio of the catalyzed to uncatalyzed rate, when 2.5 ppm of impurity were present during oxidation in air at 650°C were: $CuCl_2$, 10; $VOCl_3$, 8; $FeCl_3$, 4; NaCl, 3; Na_2CO_3, 3; NaF, 2; $MgCl_2$, 2; and $CaCl_2$, 1.5. It was not ruled out that the presence of halogen anions may have had an effect and changed the activity sequence which would have been observed, say in the presence of oxides (derived from nitrates, oxalates, etc.) (see Section II.E). Synergistic catalytic effects were noted. That is, the effect of two or three catalysts jointly exceeded the sum of the effects of each catalyst when present separately. The combinations studied were Fe + Na, V + Na, and Cu + Fe + V.

Gallagher and Harker (*21*) have studied the activity of Fe, Co, and Ni compounds in the oxidation of cellulose char by air in the 300–550°C temperature range and in the gasification by CO_2. The concentration of added impurities was as high as 5%. In general, Co compounds were more effective in reducing the ignition point of the char than Fe or Ni compounds, which would be predicted from the results of Letort and Martin. In the C—CO_2 reaction at 700–800°C one catalyst atom per 3730 atoms of carbon was added (ca. 0.15%), which is comparable to the amount of impurity present in the char. The relative catalytic activity found was Ni > Co > Fe. It is concluded that, in this case, only those compounds were effective which could be reduced at reaction conditions to the metallic state.

At higher temperatures, this sequence can be reversed. Tudenham and Hill (*11*) added Co, Fe, or Ni nitrates (ca. 0.14% reported as the oxide) to spectroscopic-grade graphite. They also added ammonium vanadate (ca. 0.03%). They obtained the following relative reaction rates with steam at 1100°C: Fe, 32; Co, 27; Ni, 19; and V, 22.

Harker (*22*) proposed a qualitative explanation for a series of relative activities observed during the measurements of ignition-point decrease in air of coconut charcoal admixed with 1% of alkali carbonates. A correlation of the increasing effect from Li to Cs with decreasing ionization potential was proposed, which in turn leads to a variant of the electronic

mechanism of catalysis discussed below (Section II.I). On the other hand, Patai et al. (*23*) report that at 367°C, in the case of chloride salts, the activity decreased sharply from Li to K and from Co to Sr. Again the anion effect of the halogens may have something to do with this discrepancy (see Section II.E).

Rakszawski and Parker (*24*) have extended this correlation to elements of the groups IIIA–VIA. They have reacted spectroscopic carbon originally containing 60 ppm ash, and admixed with 0.1 mole % (based on the element) of metal or oxide, with air at 700°C. Considering the periodic system of the elements and noting that the electropositivity of an element decreases in a given period from left to right and increases in a group from top to bottom, they arrange their catalysts in diagonal triads of increasing activity from top left to bottom right. Within each diagonal, the activity increases with the average ionization potential to produce the maximum oxidation state, which is contrary to the observation of Harker reported above (*22*). In fact, when one examines the authors' data, it is seen that within each group there is a tendency for activity to increase from top to bottom, i.e., with a lowering of the ionization potential, similarly to the case reported by Harker. Thus one may draw quite opposing conclusions.

To conclude, it seems to us that the series of relative activities reported are not very illuminating except, perhaps, for practical purposes. Such a route of study may shed light on the fundamentals of catalysis only when a limited number of closely comparable catalysts, i.e., transition metals or alkali metals, as done by Harker (*22*) and Tudenham and Hill (*11*), are compared in strictly similar conditions. Significantly, correlations of impurity effects with the recent indicators of catalytic activity, such as *d* character of transition metals, are still lacking.

C. Chemical State of the Catalyst

The question of the chemical state of the catalyst has been a point of controversy, especially since Long and Sykes (*26*) have, in formulating their electronic theory of catalysis, attributed the catalysis of the C—CO_2 and C—H_2O reactions to stoichiometrically deficient oxides of the transition metals.

An extensive study was made on the effect of Fe in its various states, on the reactivity of coal coke by King and Jones (*27*). The initial reactivity in CO_2 at 950°C depended strongly on the presence of Fe, the effect of as little as 0.3% of this element being already strongly manifested. The period during which a high reactivity persisted increased with the amount

of added Fe. It was observed that when a change in reactivity occurred from a high to a low value a corresponding change occurred in the state of oxidation of the active Fe. The amount of metallic Fe in the coke, after a certain amount of ferric oxide had been added and the sample heated for 1 hr in flowing N_2, was determined by the amount of H_2 formed on contact of the sample with HCl. A definite correlation was established between the amount of reducible Fe and the coke reactivity. It was ascertained that during the contact of CO_2 with Fe-containing coke at 950°C, the reducible Fe is gradually oxidized and a corresponding decrease in reactivity takes place. If a coke was so treated as to convert the reducible Fe to a nonreducible form, by mixing it at 1000°C with excess TiO_2 or SiO_2, the reactivity suffered an immediate decrease. Sulfiding of the Fe by H_2S had a similar effect.

It was calculated by King and Jones that at 950°C for a CO concentration $>74\%$, metallic Fe is the stable phase. When the CO concentration is between 20 and 74%, FeO is the stable phase; for a CO concentration $<20\%$, Fe_3O_4 is stable. They concluded that if the reacting gas contains $<74\%$ CO the iron will become an inactive catalyst. King and Jones observed that an Fe catalyst made inactive could be reactivated by cooling the coke in N_2 to room temperature prior to returning to reaction temperature. They suggested that this was a result of the solid-state reduction of FeO to Fe. They noted that if the cooling to room temperature was performed in CO_2, reactivation of the catalyst did not occur. Reactivation of the Fe catalyst could also be accomplished in H_2 or CO. Figure 1 shows reactivation in 1 atm of H_2 at 950°C. Following reactivation, the gasification rate in CO_2 steadily decreased to a limiting value as metallic Fe was reoxidized to an inactive state. Reactivation in CO was demonstrated for a run carried out in a closed system at 950°C as follows. At the commencement of the reaction, the CO/CO_2 ratio was low and FeO was the stable phase. As the reaction proceeded, the CO/CO_2 ratio increased and the gasification rate showed a marked increase. Fe had replaced FeO as the stable phase.

Goring and co-workers (*28*) studied the kinetics of gasification of coal char with steam and CO_2 at 870°C, following various pretreatment times in N_2 up to 24 hr at this temperature. They found that initial reactivity decreased sharply with increased pretreatment time and attributed this to the gradual deactivation of reducible Fe by combination with acidic oxides, like silica, in the ash.

Gulbransen and Andrew (*29*) incorporated 790 ppm of Fe into spectroscopic graphite. The Fe was added as the nitrate and decomposed to give

an oxide. Prolonged pretreatment at 700°C in vacuo, at which temperature the probability of reducing the oxide to the metal is low, did not produce a reactive sample in CO_2 at 700°C. In contrast, treatment in vacuo or in H_2 at 850°C gave samples which subsequently reacted rapidly with CO_2 at 700°C. Gulbransen and Andrew concluded that Fe must be present as the metal or carbide in order to enhance gasification.

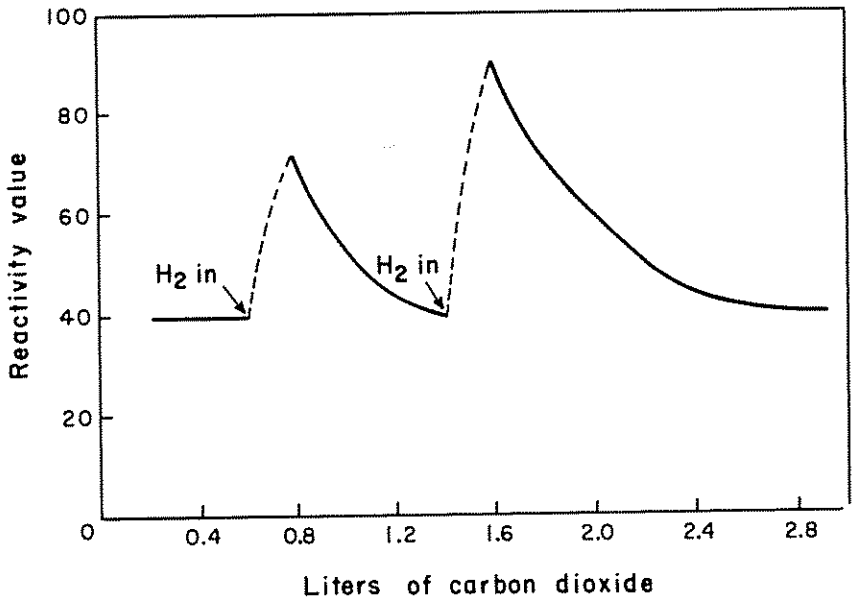

Fig. 1. Activation and deactivation cycles of Fe catalyst during reaction of coke with CO_2. Activation is achieved using H_2. [From King and Jones (*27*).]

Rakszawski et al. (*30*) concluded that for Fe to be an effective catalyst in the C—CO_2 reaction, it must be free of dissolved carbon. They added particulate Fe, Fe as ferric oxalate, and Fe as Fe_2O_3 to spectroscopic graphite and heated the mixtures in He at temperatures between 1400 and 1635°C prior to reactivity studies. They found that such a pretreatment sharply decreased the catalytic activity of the Fe and attributed the decrease to the solution of carbon in the Fe. Figure 2, for example, compares reactivity runs at 1000°C for Fe added as Fe_2O_3 for pretreatments in He at 1000°C for 1 hr and at 1400°C for 25 hr. On the basis of our studies, which will be discussed later, we conclude that the situation

is further complicated by extensive sintering and growth of the Fe particles at elevated temperatures. For example, we would suggest that the Fe in the sample pretreated in He at 1000°C for 1 hr also contained some dissolved carbon (ca. 1.7%), but that upon exposure to CO_2 this carbon was rapidly removed and the catalyst reactivated. Pretreating at 1400–1635°C (compared to 1000°C) would lead to more sintering and Fe particle growth, as well as increased amounts of dissolved carbon. The

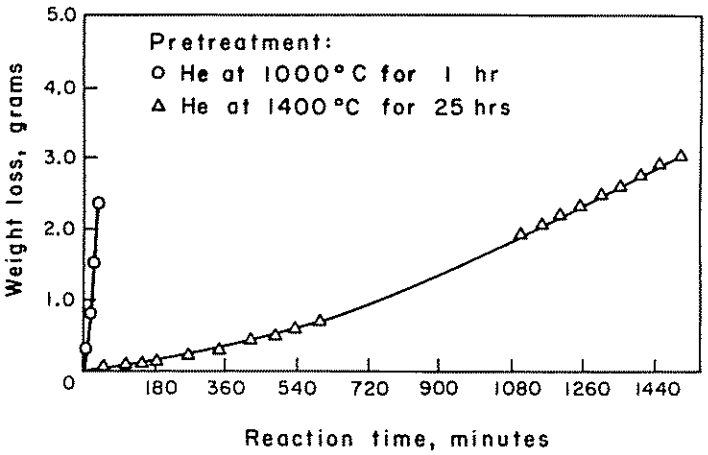

Fig. 2. Effect of pretreatment on reactivity of graphite in CO_2 at 1000°C. Graphite contains 100 ppm of Fe from Fe_2O_3. [From Rakszawski et al. (*30*).]

result would be a greater decrease in catalyst activity, as was observed. Rakszawski et al. (*30*) found that catalytic activity could be restored by treating the pretreated samples in H_2 at 1000°C or O_2 at 450°C prior to reaction with CO_2 at 1000°C. Catalyst activity was also restored, after some reaction time in CO_2 at 1000°C as seen in Fig. 3. Reactivation was attributed to gasification of the highly reactive carbon dissolved in the Fe by H_2, O_2, or CO_2.

Lothe and Melsom (*30a*) recently studied the gasification of spectroscopically pure graphite with steam, as catalyzed by Fe. They added Fe, Fe_3O_4, and Fe_2O_3 to the graphite. Fe was found to be a strong catalyst; the oxides were poor catalysts. The Fe catalyst was observed to be deactivated at high water-vapor pressures, which is consistent with the conversion of the active metal catalyst to the less active oxide. The presence of sufficient H_2 increased and maintained catalyst activity.

Lothe and Melsom conclude that catalysis by Fe is probably caused by interaction of Fe with the edges of the graphite crystals, thus weakening the bonds with neighboring carbon atoms. The activity of the catalyst is dependent upon its ability to move on the graphite. An immobile catalyst rapidly loses its contact with the edges of the basal plane where the attack takes place. According to these authors, the poisoning of the catalyst may be connected with formation of a carbide of Fe on the surface of the catalyst particle. This carbiding prevents the interaction of the

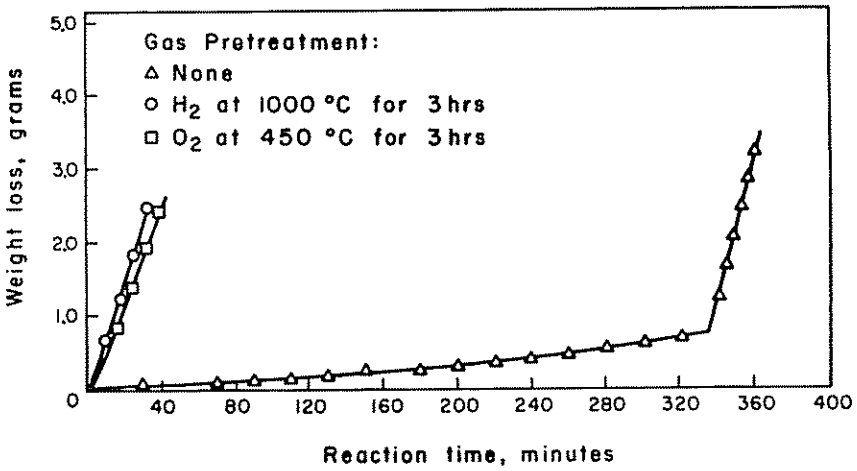

Fig. 3. Effect of secondary gas pretreatment in H_2 and O_2 on length of induction period for reaction of graphite in CO_2 at 1000°C. Graphite contains 510 ppm of Fe from ferric oxalate. Samples underwent primary pretreatment in He at 1635°C. [From Rakszawski et al. (*30*).]

catalyst particle with the graphite and probably reduced catalyst mobility. Deactivation by oxygen (or water) may possibly be explained by a similar mechanism. They suggest that a layer of chemisorbed oxygen may be formed on the catalyst and thus prevent the interaction between Fe and carbon.

We have mentioned above the results of Tudenham and Hill (*11*) using Fe, Co, Ni, and V catalysts. It appears to us that these elements were present as metals at the reaction temperature of 1100°C. The observed poisoning of Fe and V at lower temperatures was attributed to the H_2 produced in the C—H_2O reaction. As will be seen from our results (Section III) and the results of Lothe and Melsom (*30a*) just discussed, it appears that such a poisoning (at least in the case of Fe) may be simply

the outcome of the oxidation of the catalyst by H_2O at lower temperatures. Significantly Co and Ni are more resistant to oxidation than Fe.

That metals only are effective in the C—CO_2 reaction was noted by Gallagher and Harker (*21*) and Taylor and Neville (*31*). These latter investigators have shown iron oxide to be entirely ineffective at low temperatures, while Ni reduced to the metallic state by H_2 was a very effective catalyst even at 570°C. That in this reaction even an alkali metal may be the active entity was shown by Bach and Lewitin (*32,33*). They impregnated deashed, natural graphite with K vapors at 600°C and observed a marked increase in the burning rate in CO_2.

It appears that in the C—CO_2 and C—H_2O reactions, which usually take place at temperatures where at least some of the catalyst may be reduced to the metal by the CO and H_2 produced or by the solid carbon, the metal is the active entity.

The situation is considerably less clear in the C—O_2 reaction. On the one hand, there is ample evidence that at low temperatures oxides derived from a variety of salts are catalyzing the reaction. Employing thermodynamic calculations, Amariglio (*19*) showed that at his reaction conditions (C + air at 600°C) a catalyst such as Ba oxide could not be reduced to the metallic state in any significant amounts. On the other hand, microscopical studies show that metals are active catalysts. The metals employed were particulate Fe, Ni, Co, Mn, Ta, Ti, Ag, Mo (*18*), Pt (*34*), Fe, Au, Pb, Ni, and V (*35–37a*). Of these, Fe, Co, and Mn gradually lose their activity when exposed to oxidizing conditions at ca. 720°C (*18*). Reduction in CO restores the activity of the Fe, similarly to the case in the C—CO_2 reaction. Mo and V, on the other hand, appear to be active in the form of liquid oxides (*18*). Whether it is a necessary prerequisite for an oxide to be nonstoichiometric to be an active catalyst remains to be proved.

D. Effect of Amount of Impurities

Surprisingly, perhaps, there is not much relevant work published on the relation between amount of impurity and its catalytic effect. This is primarily due to the fact that many researchers either used impure materials to start with or employed an overdose of catalyst, i.e., addition to such a level that further changes in amount of catalyst have little, if any, additional effect.

Harker (*22*) studied the effect of adding a progressively increasing amount of alkali carbonates to carbons on the decrease of their ignition point in air. For small amounts added, the decrease in ignition temperature was large and roughly linear with concentration. However, a "saturation point" was observed, after which further addition gave little effect.

Figure 4 shows the influence of sodium carbonate on the ignition temperature of a 1000°C cellulose carbon. The amount of catalyst added before saturation was reached was found to depend on the particular carbon. For example, for an artificial graphite, saturation was reached at a sodium carbonate concentration of ca. 40×10^{-6} equiv./g, as compared to over

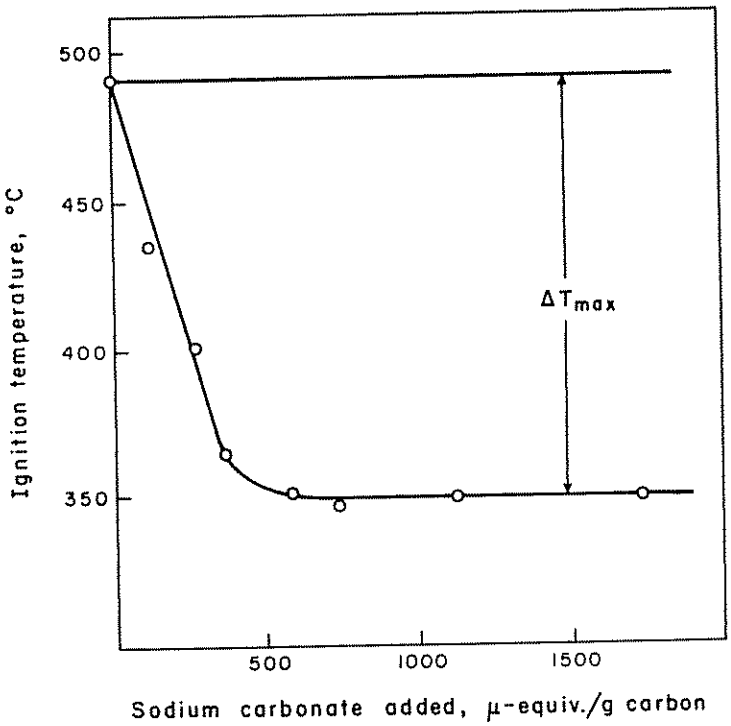

Fig. 4. Influence of Na_2CO_3 on the ignition temperature of cellulose carbon. [From Harker (*22*).]

500×10^{-6} equiv./g for the cellulose carbon. Presumably the surface area of the carbon would have an effect on the additive concentration at which saturation is reached—the larger the surface area the larger the concentration at saturation.

Amariglio (*19*) points out that the nonisothermicity of the data inherent in the choice of the criterion (ΔT_{ign}) invalidates results to a certain degree. He performed a detailed study of the effect of increasing amount of catalyst at ppm levels on the reaction of air with highly purified, artificial

graphite. The reaction rate increased linearly with Ba content up to ca. 130 ppm and with Na content up to ca. 150 ppm and then tended to level off. For Pb or Mn the rate-concentration curves had a sigmoidal shape, the catalytic effect increasing with increasing amount of catalyst in the low concentration range. The sigmoidal shape of the curves is the basis of the introduction by Amariglio of Kobozev's theory of active ensembles (*38*) to explain the catalysis of carbon gasification.

A linear relation between the oxidation rate and weight of catalyst added up to 15 ppm of Cu, V, Fe, or Na was reported in the oxidation of highly purified artificial graphite by air at 650°C (*39*).

Mukaibo and Yamauchi (*40*) studied the effect of V addition on the reactivity of highly purified artificial graphite with CO_2. They added V by immersing graphite plates into an aqueous solution of NH_4VO_3 at the boiling point for 20 min, drying at ca. 150°C and heating in vacuo at 1110°C. The above treatment was repeated a number of times to add increasing amounts of V. For reaction at 1100°C they found an increasing catalytic effect per unit of V added with increasing concentration up to ca. 550 ppm. It is suspected that the graphite plates were not uniformly impregnated with V and that the nonuniformity of impregnation increased with the number of impregnations used (that is, the total V content reported). Since the reactivity was undoubtedly in zone II at 1100°C (*1*), the increasing catalytic effect with increasing V concentration could be an artifact. That is, the reaction was preferentially occurring close to the outer surface of the graphite plate where the V particles were increasingly concentrated as the V content in the graphite increased.

Rakszawski (*41*) has studied the effect of Fe on the C—CO_2 reaction. Using natural graphite powder with <6 ppm impurity, he followed the effect of increasing concentrations of Fe, derived either from iron carbonyl or iron oxalate, on the reaction rate at atmospheric pressure and at temperatures between 900 and 1200°C. When adding Fe derived from iron carbonyl, he mixed Fe of known particle size with the graphite powder. When adding Fe as iron oxalate, a solution of ferric oxalate was added to the graphite at room temperature and the mixture dried under vacuum at 180°C. Following the addition of Fe, in both cases, the graphite was heated in helium at 1635°C prior to reactivity studies. Figure 5 shows the effect of Fe addition on the reactivity of the graphite at 1000°C. The graphite, with no Fe added, had a reactivity of 0.50%/hr. For both the 3-μ Fe, derived from iron carbonyl, and the Fe, derived from iron oxalate, the effect of Fe addition on increasing the gasification rate progressively decreased with increase in amount added. The Fe, derived

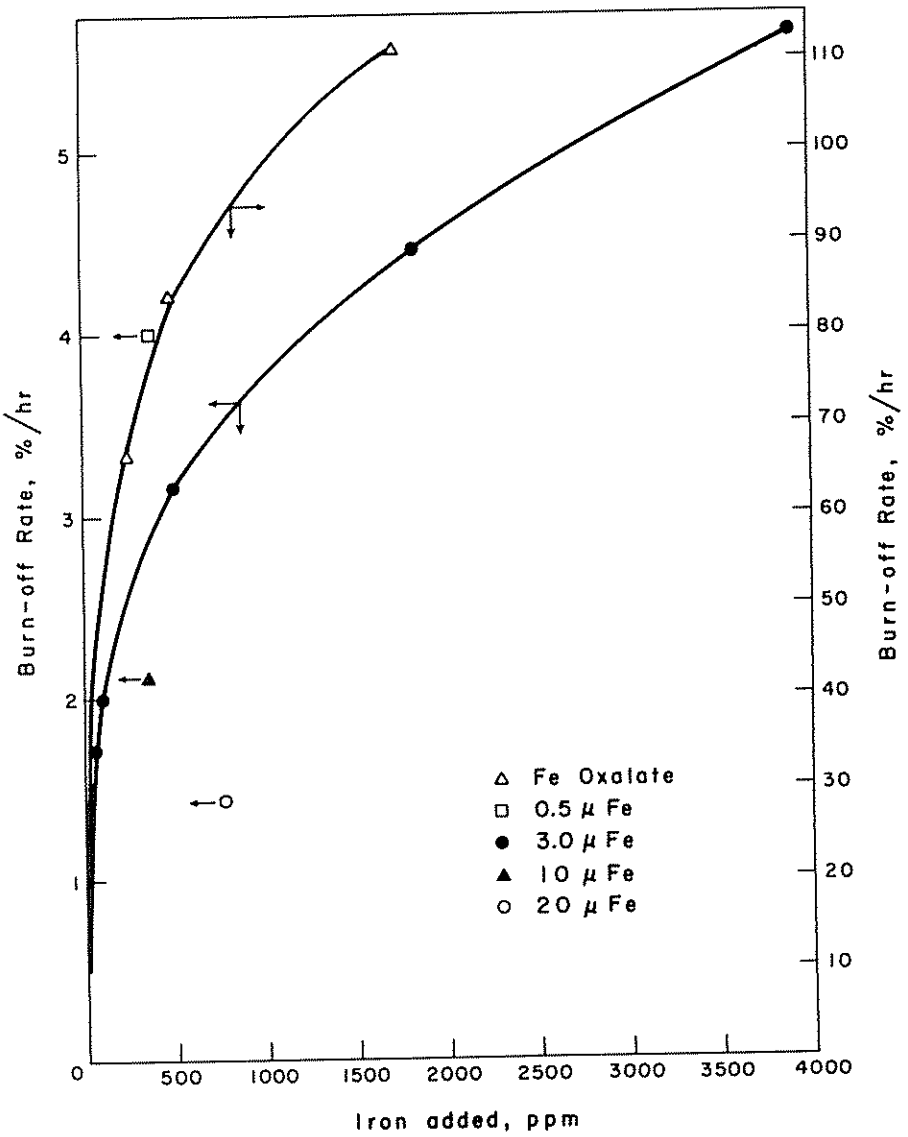

Fig. 5. Effect of amount of Fe addition on the rate of graphite gasification by CO_2 at 1000°C. [From Rakszawski (*41*).]

from iron oxalate, had a considerably greater effect on increasing graphite reactivity than did the 3-μ Fe, probably because of its smaller particle size. It is seen from results on other particle sizes of Fe, derived from iron carbonyl, that the extent of catalysis decreased with increasing particle size of the catalyst added.

The deviation from a linear relationship between catalyst concentration and gasification rate at higher catalyst concentrations is expected if for no other reason than catalyst efficiency should decrease as coverage of the carbon surface approaches a monolayer of particles and then exceeds this value. Further, as shown by Thomas and Walker (*18*), catalyst particles are highly mobile on carbon surfaces. They collide and agglomerate and thereby lose some of their catalytic activity. The possibilities for collision and agglomeration increase with increased catalyst concentration on the surface.

E. Anion Effect

When the catalyst is added to the graphite in the form of different salts, there are variations in its activity attributed by various authors to the anion of the salt.

Upon the addition of 0.0134 equivalent of potassium salts to carbon black (*23*), a spectrum of activities was observed upon oxidation in air at 367°C, the highest being shown by carbonate and the lowest by metaphosphate. This lowest activity for metaphosphate or any other phosphate salt is hardly surprising, because P compounds are among the few substances which inhibit carbon gasification (*24,42–44*). The differences between the activities of the other salts may be due to differences in the subdivision of their oxides resulting from salt decomposition. This was noted by Gallagher and Harker (*21*), when comparing the effect of Fe, Co, Ni oxides, chlorides, phosphates, citrates, and oxalates in the oxidation of charcoal at 300–450°C. The strongest catalysis was observed in the case of the organic salts, which presumably give the finest subdivision of the catalyst.

Nebel and Cramer (*44*) give a relative activity series for lead salts, added in the amount of 0.2 mole %, in reducing T_{Ign} of carbon in air as follows: CH_3COO^- > basic chloride > basic bromide > Br^- > monoxide > basic sulfate > NO_3^- > SO_4^{2-} > PO_4^{3-}. Here again the organic salts gave the greatest catalysis and the phosphate acted as an inhibitor.

The anion effect is particularly evident when halogen-containing compounds are added to the gas stream. Low amounts of halogen gases accelerated the gasification of high-purity graphite in CO_2, while higher

amounts inhibited the process (*45*). Bach and Lewitin (*32*) deduced from microscopical observations that HCl in CO_2 had no effect on basal-plane pitting of purified graphite but inhibited strongly pitting of impure graphite. Thus its effect is caused by interaction with the impurity in the solid, as for instance by volatilizing it in the form of a volatile halogenide, as is, in fact, the case in the purification of carbons. Hedden and co-workers (*45*) state, to the contrary, that they observed the effect of halogen impurities in gases even in the case of extremely pure graphites and that in the case of solid impurity contents of the order of 1 ppm this cannot be explained by interaction with solid impurities.

Mukaibo and Yamauchi found that the presence of iodine in the gas phase markedly retarded the gasification of impure graphite by CO_2 but accelerated gasification of a very pure graphite (*40*). Retardation, in the case of the impure graphite, was shown to be caused by removal of V, a strong catalyst, as the volatile iodide. We suggest two possible explanations for acceleration, in the case of very pure graphite. First, it has been shown that halogens can remove hydrogen from the edges of carbon crystallites by the formation of gaseous hydrogen halides (*46*). Concurrently, however, only partial substitution of halogen for hydrogen occurs on the exposed edge sites, leaving additional active sites available to undergo gasification reactions. Even very pure graphite contains some hydrogen (*47*), which could presumably be removed by iodine. Second, it has been shown that the presence of small amounts of gaseous halogen compounds enhances surface area development upon the gasification of graphite (*48*). Increased surface area could result in increased gasification rates.

It should be mentioned here that the much discussed effect of moisture in the gases on the rate of gasification (*12,15,16,36,49*) has been related in some instances to interaction with impurities in the solids (*13,50,51*). We will not discuss this matter, because it extends beyond the scope of this review.

F. Catalysis Effect on CO/CO_2 Product Ratio for C—O_2 Reaction

For combustion of very high purity graphites in 1 atm of very dry air at 637°C, the CO/CO_2 product ratio (r) is given as 1.30 (*13*). In "somewhat humid" atmospheric pressure air at 620°C, r is given as 1.6 ± 0.2 (*50*), again for very pure graphite. Since r varies with temperature and pressure (*52*), it is important to specify these experimental conditions when citing results.

One of the first studies on the effect of impurities on r was that of Arthur and Bowring (*53*). They noted that r decreased in the presence of Na, K, Cu, and Zn halides. It has been questioned as to whether impurities change r by changing the amounts of CO and CO_2 produced as primary products or by catalyzing the secondary combustion of CO to CO_2.

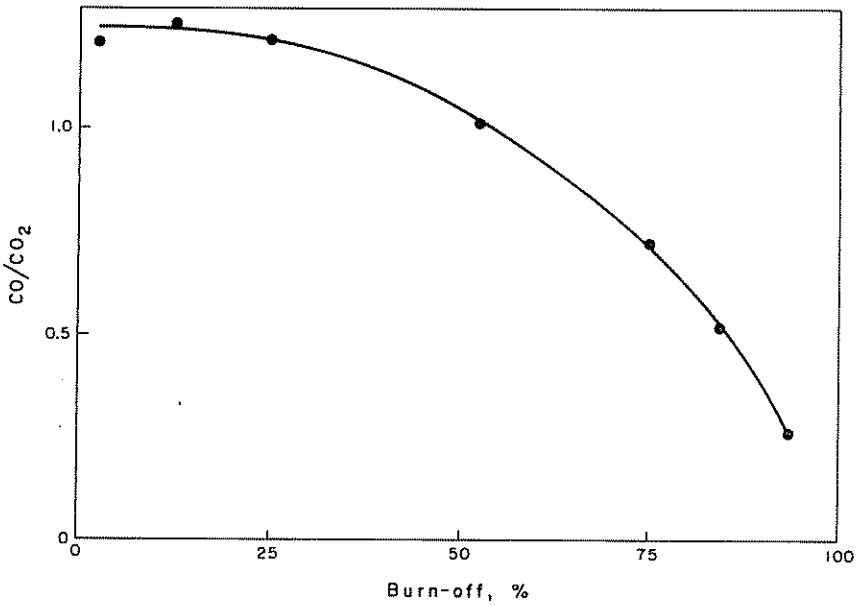

Fig. 6. Change in CO/CO_2 product ratio with burn-off of graphite of high initial purity in air at 630°C. [From Heuchamps (*12*).]

Heuchamps et al. (*13,54*) conclude that the primary ratio itself is affected by impurities. They measured r for a high-purity graphite (the graphite considered in Table I) as a function of burn-off, during its combustion in 1 atm of very dry air at 637°C. Figure 6 shows their results for the decrease in r as burn-off proceeds from zero to ca. 100%. The authors attributed the decrease in r with increasing burn-off to a concurrent increase in amount of impurities on the graphite surface. The fact that a plot of surface impurity concentration versus r would be essentially linear appears to support the authors' contention.

Heuchamps and Duval (*12a*) also studied the effect of contamination of a high-purity graphite with varying amounts of B, Na, and K on r and the relative gasification rate (F). With F equal to 1 for the pure graphite, Fig. 7 shows the results. As is seen, the presence of impurities produced a substantial increase in F and decrease in r. Heuchamps and Duval conclude

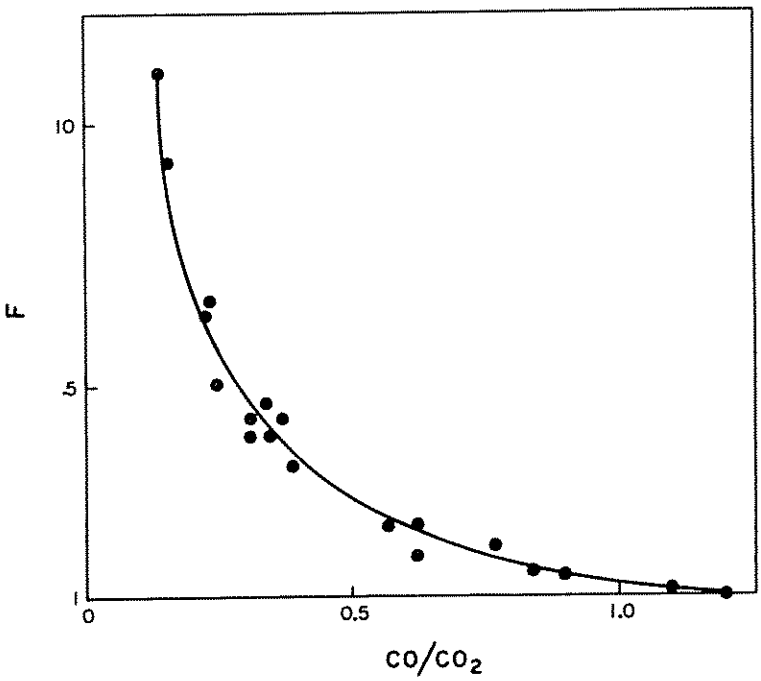

Fig. 7. Relation between the relative gasification rate and CO/CO_2 product ratio for reaction of graphite with air. Graphite contains varying amounts of added impurities. [From Heuchamps and Duval (*12a*).]

that combustion occurs simultaneously in two parts of the carbon surface. On one part, gasification is unaffected by impurities and CO is the main primary product. On another part, gasification is affected and catalyzed by impurities and CO_2 is the main primary product.

G. Catalysis Effect on Gasification of Single Crystals

This aspect of the subject was recently covered by Thomas (*55*) and Hennig (*56*) in the framework of extensive reviews of the microscopic study

of graphite gasification. The use of microscopy to study gasification of graphite single crystals is a powerful technique, since it permits direct observation of the process and direct evaluation of catalyst activity in different crystallographic directions, using specimens of the highest structural perfection.

The basic points emanating from the large body of studies summarized in the aforementioned reviews (*55,56*) and relevant to the present subject can be summarized. There is a certain occurrence of basal-plane pitting in the absence of catalysts. There is a small, but detectable, anisotropy of gasification rate in oxygen of the different prismatic faces. For example, the rate of attack of the "armchair," or $11\bar{2}l$, face is usually different from that of the "zigzag," or $10\bar{1}l$, face. The relative rates are functions of temperature and gas purity. The anisotropy of the oxidation between the directions parallel to the *a* axis (r_a) and *c* axis (r_c) is usually much larger than the anisotropy between the rates on various planes in the *a*-axis direction. Values of r_a/r_c, quoted, vary from 26 to 10^{13} for the gasification of single crystals in oxygen, apparently depending primarily on the defect concentration in the basal plane. The larger the defect concentration, the lower r_a/r_c is.

The origins of the noncatalyzed etch pits on the basal plane have been ascribed to point defects on the basal planes, as vacancies (*35,57*), vacancy clusters (*35*), impurities incorporated in the carbon lattice (boron) (*35*), or emergent points of nonbasal dislocations (*35,58*) on the basal plane. These defects can be induced by neutron bombardment (*35,59*), mechanical deformation (*35*), or rapid quenching (*35*). The accumulated evidence indicates, nevertheless, that in the absence of surface impurities the amount of basal plane pitting is much smaller than in their presence (*18,32,34*). Pit formation is affected also by impurities in the gas phase. Thus H_2 pretreatment reduces the pit-formation tendency (*60,62*), while H_2O enhances spontaneous pitting (*37a*). The gas impurities have a profound influence on the reaction in the prismatic planes and may inhibit (or promote) selectively the gasification of carbon atoms exposed on "armchair" or "zigzag" planes (*60–62*).

The question which has been recently discussed by several authors is whether the promotion of pitting by catalyst particles requires as a prerequisite a defect in the basal plane of graphite or is the catalyst capable of inducing an etch pit on a flawless region of the plane. Glenda Hughes et al. (*58*) deduce that the catalyst alone cannot produce an etch pit. This is also the conclusion of Hennig and Kanter (*63*). Hennig

(*36*) distinguishes clearly by means of microscopic observation between the catalytic action on defect-free single crystals and on crystals in which defects were induced. In the first case the catalysis is confined to the prismatic planes and is localized at the catalyst–carbon contact surfaces. In the second case, pitting of the basal plane is induced. However, there are always structural imperfections in nonideal specimens to enable the catalyst to exhibit its promoting action on the gasification process in both ways.

Microscopic studies have also shown that for low-temperature (200°C) oxidation of graphite by atomic oxygen, iron particles behave as inhibitors, serving as recombination centers for the oxygen atoms (*64*). It is demonstrated that atomic oxygen reacts with the entire basal plane and not only at points of structural imperfections. This fact is very important in support of the hypothesis (*37*) which regards the role of metallic catalysts primarily as dissociation centers for the gas molecules. One has to remember that at high temperatures the probability of dissociation increases very sharply.

H. Catalysis Effect on Kinetic Parameters

1. Activation energy

In recent years a series of investigations have been published which quote fairly unanimous figures as to the overall activation energies of the C—CO_2 and C—O_2 reactions for highly purified carbons. The values given are 87 ± 3 kcal/mole for the C—CO_2 reaction (*7,45,50,65–67*), and 61 ± 3 kcal/mole for the C—O_2 reaction (*12,24,50,55,65*). These figures, in part quoted earlier (*1*), provide a suitable reference point to assess changes in activation energies in the catalyzed processes. There are relatively few data on activation energy changes during catalysis in the C—H_2O reaction.

Table II compiles published data on activation energies for the gas–carbon reactions. The table indicates the kind of carbon employed, the temperature range, and kind and amount of impurities added. An examination of Table II shows that in the majority of cases there occurs in the catalyzed reaction a decrease in E. It appears that even very feeble concentrations of catalysts decrease, somewhat, the E values (*50*) and that the effect increases with concentration of impurity up to a certain level. This is also illustrated by Heuchamps et al. (*54*) in Fig. 8. They relate the decrease in E from 63 to ca. 40 kcal/mole as combustion of graphite in air proceeds to a progressive increase in surface impurity concentration from 1 ppm to several per cent. The change is monotonic and smooth. On the

other hand, Amariglio (*19*) (another worker from Duval's school) presents data supporting the view that the drop in E is achieved by the very first addition of impurity, far below the saturation of the surface by catalyst (i.e., below 1.4 and 0.8% of surface coverage by Na and Pb catalyst, respectively). It is not apparent whether Amariglio has taken into account the increase of the surface concentration with burn-off, which would have increased the surface coverage far beyond the figures quoted. The author indicates that burn-off ranges of 25 or 40% were achieved in his experiments, depending on temperature. It is apparent from (*12*) and (*54*) that at such high degrees of burn-off the surface could have become completely covered with catalyst, even if the initial addition of catalyst was of the order of several ppm. The important question of the change of activation energy with amount of impurity remains at present obscure and careful experimentations involving measurements taken over extremely narrow burn-off ranges are required to establish an unambiguous picture.

Recently, Heintz and Parker (*68*) studied catalysis of the C–air reaction by 47 3*d*, 4*d*, and 5*d* transition metals. The metals, all of $<44\ \mu$ particle size, were added at a 0.1 mole % level to natural graphite powder, which had a total ash content of <60 ppm. The E found for the reaction of the graphite powder between 600 and 800°C was 48.8 ± 3.5 kcal/mole, determined from 50 separate runs. Using the usual techniques (*1*), it was confirmed that the reaction was located in zone I. The effect of the metal additives on E has been related to their atomic number, which reflects the number of electrons entering the particular $(n-1)$ d level involved. Figure 9 shows the results for the 3*d* metals. Also included in Fig. 9 is the relationship between the lattice energy, $-U$, of the monoxide of the metals and atomic number. The "double-humped" curves seen in Fig. 9 were also obtained for the 4*d* metals. It was suggested that these curves are typical of the $(n-1)$ d level in which 0, 5, and 10 electrons in the $(n-1)$ d orbitals (i.e., empty, half-filled, and completely filled, respectively) impart unusual stabilities to the particular oxidation state involved (*69*). For the 3*d* metals, minima in E were observed for Ca, Mn, and Zn; for the 4*d* metals, minima were observed for Sr, Tc, and Cd. Since the lattice energies of the monoxides of the 3*d* and 4*d* metals followed the same pattern as did E, this was taken as an indication that the divalent state of the metal entered into the oxidation mechanism of the graphite, probably as an oxygen acceptor–donor species.

No simple correlation between E and atomic number was found for the 5*d* metals, because, it was suggested, the valence orbital (5*d*) is

TABLE

Effect of Catalysts on Activation

Ref.	Carbon characteristics	Reaction	Temp. range, °C	Kind and amount of impurity in pure sample
(*50*)	Pechiney EDF	C + air	580–640	<1 ppm total
(*50*)	Pechiney spectro.	C + air	580–640	Na, 0.5; V, <0.1 ppm
(*50*)	Natural Madagascar agglomerated	C + air	560–620	Na, 0.1; Mn, $<0.5 \times 10^{-3}$; Ta, $<10^{-4}$ ppm
(*35*)	Natural Ticonderoga single crystals, prismatic planes	C + O_2	550–700	?
(*19*)	Nuclear graphite	C + air	<600	~1 ppm total
(*24*)	United ultrapurity graphite	C + O_2	700–800	<60 ppm ash
(*68*)	United ultrapurity graphite	C + air	600–800	<60 ppm ash
(*50*)	Pechiney EDF	C + CO_2	In zone I	<1 ppm total
(*73*)	Coke made from humic acid	C + CO_2	700–900	2.5% ash
(*45*)	A whole series of carbons including very pure	C + CO_2	~1000	Varies
(*70*)	Charcoal	C + CO_2	700–900	400 ppm, mainly B and Si
(*70*)	Charcoal	Adsorption step	700–900	400 ppm, mainly B and Si
(*70*)	Charcoal	Desorption step	700–900	400 ppm, mainly B and Si
(*70*)	Charcoal	C + H_2O, desorption step	700–900	400 ppm, mainly B and Si
(*71*)	High-purity sugar C	C + CO_2, desorption step	600–900	0.07% ash
(*71*)	High-purity sugar C	C + CO_2, desorption step	600–900	0.07% ash

II

Energy of Carbon Gasification

E for pure sample, kcal/mole	Mode of addition (or removal) of impurity	Kind and amount of impurity in catalyzed sample	*E* of catalyzed reaction, kcal/mole
64	Chlorination, 2700°C; heating, 3500°C	V, 38; Fe, 6; Na, 0.5; Mn, 0.2 ppm	60
64	Heating, 3500°C	Na, 3; V, <0.1 ppm	58
64	Heating, 3500°C	Na, 9; Mn, 0.46; Ta, 0.1 ppm	59
46	Deposition on surface	Colloidal Fe	10
62	Impregnation from solutions	~100 ppm of Ba, Cu, Mn, or Na	40 ± 3
63	Added as powders	0.1 mole % of IIIA–VIA	29–52
49	Added as powders	*3d*, *4d*, *5d* transition metals	See Fig. 9
87 ± 3	Chlorination 2700°C; heating 3500°C	V, 38; Fe, 6; Na, 0.5; Mn, 0.2 ppm	87 ± 3
95	Admixing	Large amounts of Na, Fe, or Al	Lowered by 25–40 kcal/mole
81–92.5	Added to gas	1–2% $POCl_3$	59.0–47.5
74	Extraction by HCl and HF	3.5% ash, mainly Na_2O, K_2O, Fe_2O_3, Al_2O_3, SiO_2	68.0
68.4	Extraction by HCl and HF	3.5% ash, mainly Na_2O, K_2O, Fe_2O_3, Al_2O_3, SiO_2	58.8
66.0	Extraction by HCl and HF	3.5% ash, mainly Na_2O, K_2O, Fe_2O_3, Al_2O_3, SiO_2	38.0
83 ± 5	Extraction by HCl and HF	3.5% ash, mainly Na_2O, K_2O, Fe_2O_3, Al_2O_3, SiO_2	55 ± 7
61.2	Impregnation from solutions	7% Fe	22.8
61.2	Impregnation from solutions	5% Al	55

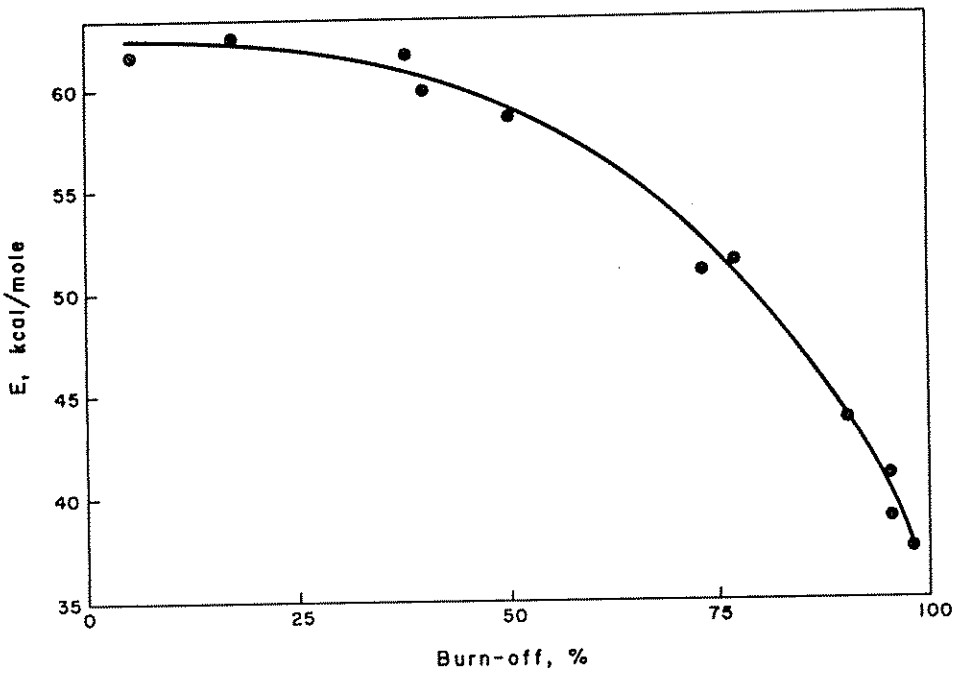

Fig. 8. Change in activation energy with burn-off of graphite of high initial purity in air at 630°C. [From Heuchamps et al. (*54*).]

sufficiently removed from the nucleus so that the regularity of the "double-humped" variation is usually not observed (*69*). While the occurrence of divalent species was taken to be quite probable for the 3*d* and 4*d* metals, especially in a thousand-fold excess of graphite, the existence of divalent species of the 5*d* metals was considered to be less certain. It was postulated that the 5*d* metals enter into the C–air reaction in the same manner as the 3*d* and 4*d* metals, but not necessarily via the divalent state.

Results in Table II show that addition of catalysts also decrease the overall E for the C—CO_2 reaction. In addition, workers have concerned themselves with the effect of impurities on the E for the individual steps in the C—CO_2 reaction. According to Long and Sykes (*70*), the E for the desorption step was affected much more than the E for the adsorption step. Semechkova and Frank–Kamenetskii (*71*) also found that the addition of catalysts decreased the E for the desorption step. Long and Sykes

(*70*) report that the presence of catalysts also produced a significant decrease in E for the desorption step in the C—H_2O reaction.

There are results for the C—CO_2 reaction discussed later, where insignificant differences in E were observed for samples having wide variations in impurity content.

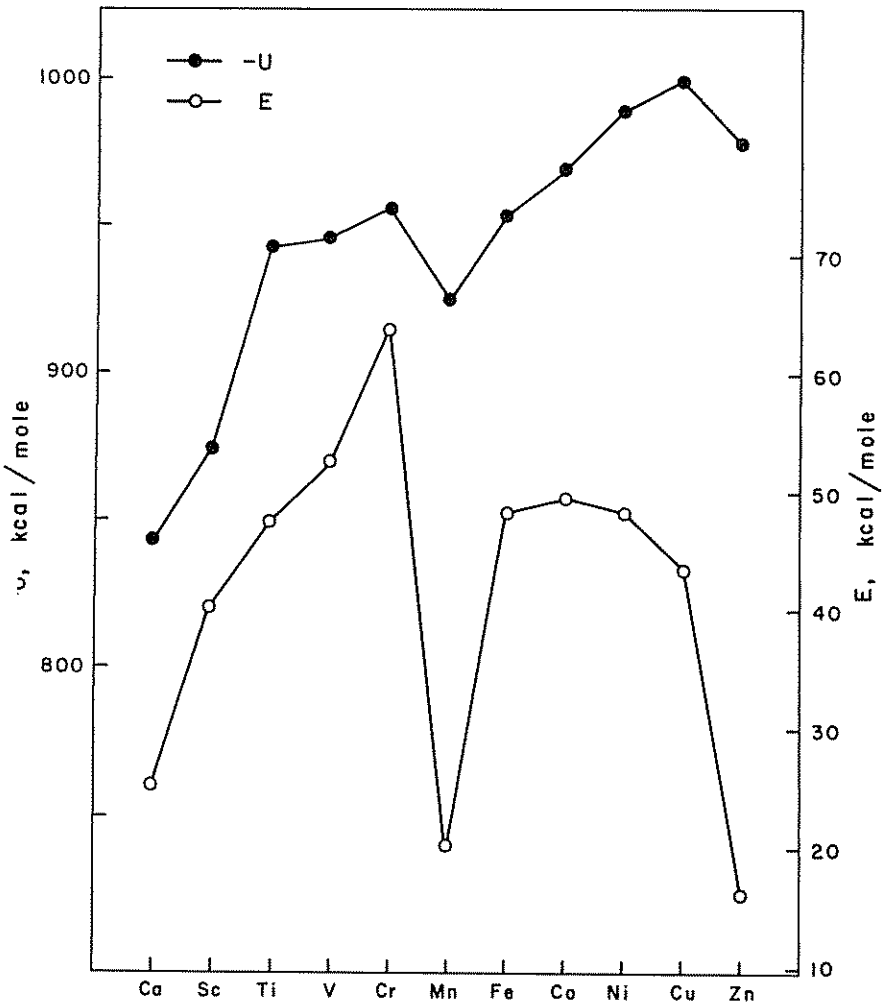

Fig. 9. Effect of 3*d* transition metals on activation energy of reaction of graphite with air. Also shown are lattice energies of the monoxides of the 3*d* transition metals. [From Heintz and Parker (*68*).]

2. Preexponential Factor and Compensation Effect

Frequently for a catalyzed reaction the change in E, when using a series of catalysts or different amounts of the same catalyst, is accompanied by a corresponding change in the preexponential factor in such a manner as to satisfy approximately the equation $mE - \ln A = \text{constant}$, where m is a proportionality constant and A is the preexponential factor in the Arrhenius expression, rate $= A \exp(-E/RT)$. This equation expresses what is known as the "compensation effect" and is a widely encountered, although not universal, phenomenon of catalytic reactions (*25*,*72*). Bond (*25*) summarizes the physical models and mathematical formulations pertaining to the compensation effect.

There are scattered data in the literature indicating that the compensation effect is also a feature of the catalyzed gas–carbon reactions. Thus in single crystals oxidized by O_2 (*35*), the decrease of E from 46 to 10 kcal/mole (Table II) was accompanied by a decrease of the preexponential factor by 10^8. Kawana (*73*) reported that a decrease of E in the C—CO_2 reaction of 25–40 kcal/mole, upon the addition of large amounts of Na, Fe, or Al (Table II), was accompanied by a 6-order-of-magnitude drop of A.

Biederman has compiled in his thesis (*8*) literature values of E and A relating to the rate constant of the chemisorption step of the C—CO_2 reaction, as described by the Langmuir–Hinshelwood mechanism. These data clearly indicate a compensation effect, although the exact nature of the catalysts causing the compensation effect is not known.

In studying the compensation effect in the carbon–gas reactions, the researcher must be extremely wary of diffusion effects, since their manifestation is evidenced in a fashion similar to that of the compensation effect: a decrease of E and a decrease of A. Regrettably little systematic work, under well-controlled conditions, has been devoted to a study of the compensation effect in the gas–carbon reactions. One of the few studies reported is that of Heuchamps (*12*). He studied this effect in the C–air reaction, using the graphite previously described (Table I and ff.). As seen in Fig. 10, the relation between $\log A$ and E was found to be linear over most of the range investigated, which is in line with the expected compensation effect. Heuchamps showed that his results are well explained by Constable's model [see, for instance, Bond (*25*)] entailing a heterogeneous surface with the catalyzed reaction taking place on some of the more energetic sites.

Semechkova and Frank-Kamenetskii (*71*), in studying the reaction of CO_2 with low ash sugar carbon and samples contaminated with Fe and

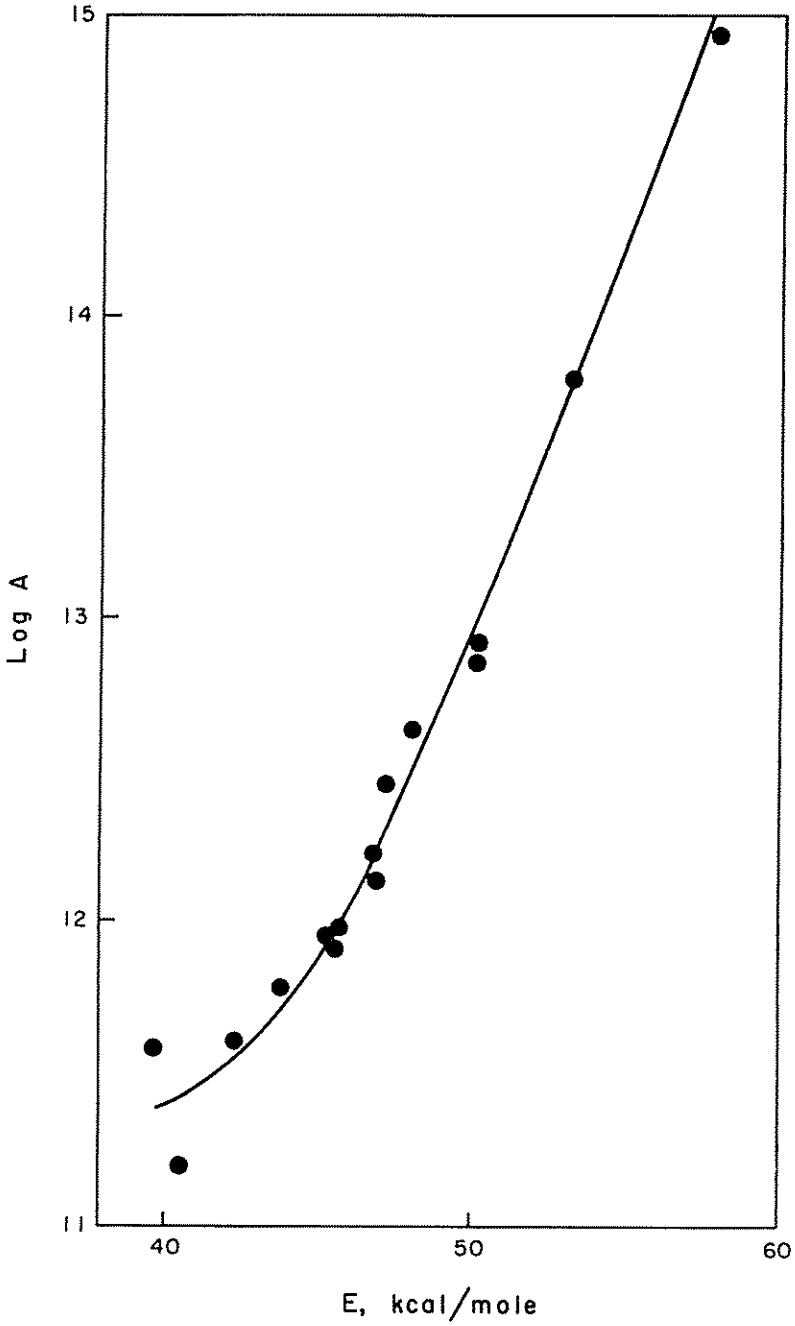

Fig. 10. Compensation effect for reaction of graphite of high initial purity with air. Pre-exponential factor and activation energy both change with burn-off. [From Heuchamps (*12*).]

Al, found the compensation effect to be present for the desorption step. They expressed all their results by the equation E(kcal/mole) = 9.5 + 5.6 log A, where A has the units of sec^{-1}.

As is unfortunately the case in the gas–carbon reactions in many aspects, we have also contradicting evidence, i.e., examples of no compensation effect. Ergun (*74*) reports the same E for what in his opinion is the rate-determining step (desorption) in the C—CO_2 reaction, for carbons which are of widely different purity and react at very different rates. The rate differences are attributed to widely differing preexponential factors, i.e., to the larger number of active sites present in the less pure carbons. Wicke (*65*) has reported the same E for high-purity carbon and less pure charcoal reacting with CO_2. Rusinko and Walker (*75*) heat-treated impure natural graphite at 2600°C, reducing its ash content from 2.1 to <0.01%. This heat treatment reduced the reaction rate of the graphite by a factor of ca. 10 in CO_2 at temperatures between 900 and 1100°C, without producing any significant change in activation energy. It should be noted that for all these results just cited the reaction was carried out at atmospheric pressure. Therefore, it is presumed that the gasification rate was controlled by the desorption step. Thus these results are in direct contradiction to the findings of Long and Sykes (see Table II), who observed a large increase in E for the desorption step when the impurity level in the carbon was decreased.

There are no indications that the second type of no-compensation effect, namely, a constant preexponential factor and a changing E is operative in gas–carbon reactions. Neither has an anticompensation effect, in which both E and A change in an opposite sense, been reported.

I. Proposed Mechanisms of Catalysis

The theories advanced to account for the experimental facts of catalysis presented in the preceding sections fall broadly into two categories, which may be termed oxygen-transfer and electron-transfer theories. Although in the previous sections the data pertaining to all the gas–carbon reactions were lumped together, it does not necessarily mean that the same theory must account for all the reactions. As the mechanisms of the noncatalyzed C—O_2 and C—CO_2 reactions are essentially different and the reactions occur in widely differing temperature ranges (*1*), it is conceivable that the mechanisms for their catalyzed reactions may differ also. This possibility has been largely obscured by the tendency of individual researchers to present an all-embracing, unifying, and elegant picture.

Conversely, it cannot be excluded a priori that the same reaction may

undergo different modifications under catalytic influence, if the reaction conditions and the catalysts employed differ. Thus one scheme of a catalytic action does not necessarily, even for the same reaction, exclude all other explanations.

1. Oxygen-transfer mechanism

Historically, this was the first mechanism proposed to explain catalysis results for carbon gasification. This mechanism appears to have been first advanced by Neumann et al. (*76*) in 1931 and then by Milner et al. in 1943 (*77*). The scheme below was formulated by Cobb and collaborators, where RO represents a metallic oxide:

$$RO + CO_2 \rightarrow RO{\cdot}CO_2$$

$$RO{\cdot}CO_2 + C \rightarrow RO + 2CO$$

More recently, Amariglio (*19*) and Vastola and Walker (*78*) have expressed views which are similar in principle, differing only in the chemical entity of the intermediate compound. Amariglio stresses the localized action of the catalyst particles which appears to be a well-established experimental fact.* The catalysts on the surface are regarded as oxygen carriers by an oxidation–reduction cycle. Thus the catalyst is assumed to undergo a cycle between two oxidation states such as metal–oxide or lower oxide–higher oxide. Metals which cannot undergo such cycles at the experimental conditions, because of thermodynamic restrictions, do not exhibit catalytic action. Thus the views of Amariglio extend those of Cobb and collaborators to include metals as well as lower oxides into the class of catalytic compounds. Vastola and Walker write, for the case of the C—CO_2 reaction catalyzed by Fe, the following equations as representing the mechanism:

$$xCO_2 + yFe = Fe_yO_x + xCO$$

$$Fe_yO_x + xC = yFe + xCO$$

This again is an oxidation–reduction–cycle as above.

It is to be emphasized that while the "chemical" schemes do account for the experimental fact of the catalyst action at the catalyst–graphite contact, no attempt has been made hitherto to substantiate this mechanism by a detailed kinetic study. The "chemical" mechanism does not explain

* Amariglio discusses the gasification of graphite by O_2; the arguments may be extended, however, to the C—CO_2 reaction.

in what way the limiting stages of the noncatalyzed mechanisms are bypassed. The mechanism more or less tacitly assumes that the limiting step of the noncatalyzed reaction is the chemisorption step and that a catalyst particle serves as an "active" chemisorption center. Thus, if the catalyst "active" center is situated at an otherwise inert basal plane of graphite, it may start a gasification process. It is usually assumed (see Section II.G) that the presence of an imperfection (vacancy, dislocation end, etc.) is necessary for the process to start.

It should be pointed out that the observation of contact action does not necessarily mean that the oxygen abstracted from CO_2 en route to the establishment of the carbon–oxygen bond has established previously a stable bond with the catalyst, as is implied by the "chemical" mechanism. The actual migration of surface oxygen from the metal to the carbon has apparently not been investigated. The metal–oxygen entity (in the case of metallic catalysts) or the "higher" metal oxide (in the case of metal oxide catalysts) may conceivably be a relatively unstable surface state. It is not ruled out that the decomposition of this state gives rise to atomic oxygen which immediately reacts with the carbon both on prismatic and basal planes (*64*). Thus effectively the catalyst may act as a dissociation center. This possibility was considered by Hennig (*37*) but was ruled out because he failed to observe a Brownian motion of the colloidal metal particles, which should have accompanied such a phenomenon. The Brownian motion of catalyst particles was observed by Thomas and Walker (*18*) in their cinematographic study of a catalyst and indicates that the dissociation center role of catalyst must still be considered. This approach is only a nuance in the general framework of the oxygen-transfer mechanism. As seen from the above, to account for the catalytic phenomena, the oxygen-transfer theory has undergone refinements concerning mainly the decreasing stability of the catalyst–oxygen intermediate from a stable oxide to a chemisorbed state (surface oxide) to a dissociation center. The ideas of Rossberg (*66*), which attribute to the dissociation of the reacting gas the limiting role in gas–carbon reactions, agree conceptually with the dissociation center role of the catalyst. For criticism of Rossberg's ideas see (*1*).

The assumption of a relatively unstable intermediate in the oxygen-transfer mechanism allows the explanation of the catalytic activity of noble metals which has been a challenging detail resisting explanation by theories postulating stable oxide intermediates.

The main objection to the oxygen-transfer mechanism comes from the

fact that were it operative the sequence of steps leading to the Langmuir–Hinshelwood mechanism would have been bypassed altogether, while the majority of authors apply this mechanism when dealing with the reactivity of relatively impure carbons. The answer to this question is still absent. Recently some authors, for instance, Hennig (*35*), have expressed the view that catalytic oxidation of graphite probably bypasses the usual sequence of steps.

To summarize, the essential features of the oxygen-transfer mechanism are (a) catalyst–oxygen interaction, (b) exclusion of carbon–catalyst interaction.

2. Electron-transfer mechanism

The interpretation of the catalysis of gas–carbon interactions by means of an electronic mechanism is a ramification of the modern theories of heterogeneous catalysis on metals and semiconductors which assigns a major role to the electronic structure of the solids involved in the process, i.e., to their ability to accommodate additional electrons in the unfilled energy bands or conversely to donate electrons to the adsorbed surface species.

The systems involved in the catalyzed gas–carbon reactions are, with the exception of the case where the catalyst or inhibitor is added to the gas phase, at least three-phase: two solids and a gas phase. The gas phase is composed of two, or more, components, i.e., at least the reactant and products. This in the general picture of heterogeneous catalysis is analogous to systems consisting of gas mixtures reacting on solids containing a catalyst and a promoter. The first in our case corresponds to the carbon itself and the second to the impurity in the carbon.

The electronic theories of catalysis of gas–carbon reactions envisage as the central point of the mechanism a transfer of electrons between the two solid phases. This takes place in addition to, and has an effect on, the gas–solid interactions. A carbon–catalyst interaction (bonding) has been observed by Hennig (*35*) by microscopic techniques. Essentially, the role of the impurity in the carbon gasification reactions is regarded in the electron-transfer mechanisms as that of an electronic promoter. The extremely feeble amounts of impurity exhibiting large catalytic activities is taken to support this viewpoint.

Long and Sykes (*26,70*) made the first and as yet the most detailed attempt to formulate an electron theory of catalysis of carbon gasification. By retaining the Langmuir–Hinshelwood sequence of steps, a mechanism

is proposed, which accounts for the authors' experimental data. The summary of the mechanism is as follows:

1. The catalysts influence the general energy levels of the reacting systems.
2. The active sites are considered to be the less firmly bound carbon atoms situated at the edges of graphitic lattice planes.
3. When an oxygen atom is adsorbed at such a site, two types of distribution of the π electrons may be distinguished as seen in Fig.

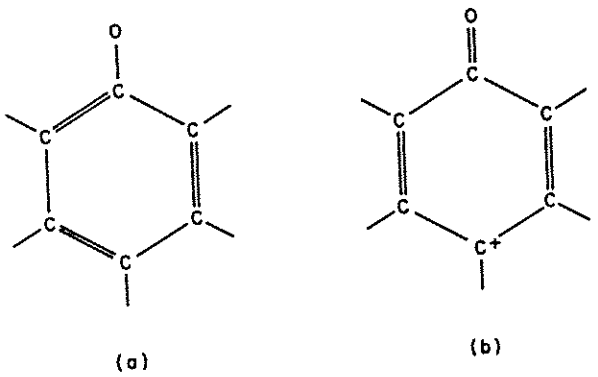

Fig. 11. Two types of distributions of π electrons. [From Long and Sykes (*26*).]

11. Type (b) requires less energy to break the carbon–carbon bonds to release a CO molecule.

4. The action of the catalyst is thought to be such as to induce type (b) distribution of the π electrons; therefore, the activation energy of the last stage will be decreased by the catalyst.
5. If the last stage is the controlling step, the overall activation energy will also be reduced.
6. The first stage of the reaction will also be facilitated if the oxygen is attached to the carbon by a double bond.
7. The mobility of π electrons provides a means whereby catalysts situated at various points in the carbon lattice may influence events at the active sites.
8. The probable mode of action of a catalyst is explained by its accepting electrons from the carbon planes in order to facilitate both adsorption by increasing the carbon–oxygen bond strength and desorption by weakening the adjoining carbon–carbon bonds.

9. It is immaterial from which part of the conjugated system the electron is removed. The catalyst needs not be situated at an active site; it needs only be in contact with the same plane of the carbon lattice from which the electron is removed.
10. The ability of the transition metal oxides to accept electrons is explained by arguments of catalysis on semiconductors. Thus wüstite should be a catalyst because of its metal deficit structure, while the metal itself is not supposed to have catalytic activity.

Therefore, the Long and Sykes theory predicts a decrease in the activation energies of both the adsorption and desorption steps. It limits the number of active sites, even in the case of catalyzed reaction; only to that corresponding to edge carbon atoms. It does not explain the effect of catalysts on the basal planes. It excludes metals as the active catalysts. Subsequent electronic theories are to a large extent modifications of the Long and Sykes approach, trying largely to explain experimental facts which cannot be rationalized by this theory.

Rakszawski (*41*) extends the apparent validity of the Long and Sykes theory to include metals. The argument is that transition metals with unfilled *d* bands do satisfy the basic requirements of serving as electron acceptors and hence are capable of forming surface carbon–metal bonds; even into this scheme the noble metals may be fitted. Filling of the *d* band of transition metals occurs during bulk carbide formation (*79*), and Rakszawski showed that the penetration of carbon into the iron particles impaired their catalytic activity. An investigation into the effect of the degree of filling of the *d* band, as characterized by the *d* character of the metal catalyst or by the use of alloyed catalysts, in the catalysis of gas–carbon reactions has apparently not as yet been made.

The observed facts seem also to belie point 9 of the above-enumerated points of the Long and Sykes mechanism. That is, the action of the catalysts is considered overwhelmingly to be confined to their immediate vicinity. The treatment of Heuchamps given below tries to accommodate this fact within the electron-transfer mechanism of catalysis.

Hedden et al. (*45*) present a modification of the Long and Sykes theory to explain their experimental facts, namely, that small amounts of halogen in the gas catalyze carbon gasification by CO_2, while large amounts inhibit gasification. The deviation from the Long and Sykes mechanism consists in the introduction of negatively and positively charged surface entities, $(CO_2) + C \rightarrow (CO)^+ + C[O]^-$. The brackets represent a strongly chemisorbed oxygen atom, the parentheses a weakly chemisorbed CO molecule. The formation of the strongly chemisorbed negatively charged

oxygen is accompanied by the formation of a positively charged chemisorbed CO molecule. This step is postulated to be the rate-controlling process, contrary to the desorption step in the Long and Sykes mechanism. The oxygen atom, being a strong acceptor, is initially always able to find excess π electrons from the lattice; and, therefore, the limiting factor is the chance of formation of the positively charged $(CO)^+$ groups. Thus electron acceptors at low concentrations will act as catalysts and donors as inhibitors. This, in the view of Hedden and co-workers, explains the marked initial inhibition of the C—CO_2 reaction by small amounts of CO in the gas. Halogens, which are strong acceptors, will at low concentrations catalyze the gasification. With increasing concentrations of chemisorbed halogens, the removal of electrons from the lattice becomes increasingly more difficult and the formation of the $C[O]^-$ surface complexes becomes rate-controlling. This coupled with the physical blockage of the surface by halogens leads to the inhibition displayed by these species at higher concentrations. The concentration at which the maximum catalytic effect was noted varied as: $I_2 > Br_2 > Cl_2$. This is in accordance with the electronegativities of the halogens: $I_2 < Br_2 < Cl_2$.

The ideas of Harker (*22*) employed for the rationalization of the catalytic action of alkali metals in the C—CO_2 reaction rest on the same presumptions of electron transfer, although the interpretation is diametrically opposite to that of Hedden and co-workers. That is, the depletion of the carbon of π electrons upon oxygen adsorption and the concomitant formation of acceptor levels in the carbon are assumed to be the controlling factors from the outset of the process. The function of the alkali metals is explained by their ability to remove these additional acceptor levels.

Heuchamps (*12*) also discussed an electronic theory of catalysis which is based on a model for the distribution of charges at the prismatic planes in graphite. In this model, Fig. 12, most atoms at the edge of the prismatic surface (terminated by the "zigzag" configuration) carry a pair of electrons and are negatively charged. Thus the prismatic planes possess a double layer of charge which is negative outward. The active sites are the carbon atoms with a single electron. Oxygen which is adsorbed on the active sites is assumed, as is the case in the previous electronic theories of catalysis, to localize a π electron from the bulk. The work of Ubbelohde (*80*) and Walker and co-workers (*81*) on the thermoelectric power changes of graphite upon oxygen adsorption and thermochemical calculations of Strange (*7*) further support this phenomenon of electron localization. This localization of the π electrons increases further the height of the

potential energy barriers to adsorption, which existed already on the clean carbon surface. The observed adsorption kinetics, according to the Elovich equation (*82*), is ascribed to an increase in the potential energy barrier as adsorption proceeds.

Heuchamps concludes that adsorbed impurities which have low ionization potentials, like the alkali metals, will form positive ions at the surface, decrease the potential energy barrier to oxygen adsorption, and catalyze carbon gasification. By analogy he concludes that adsorbed impurities which have high electron affinities, like the halogen gases, will

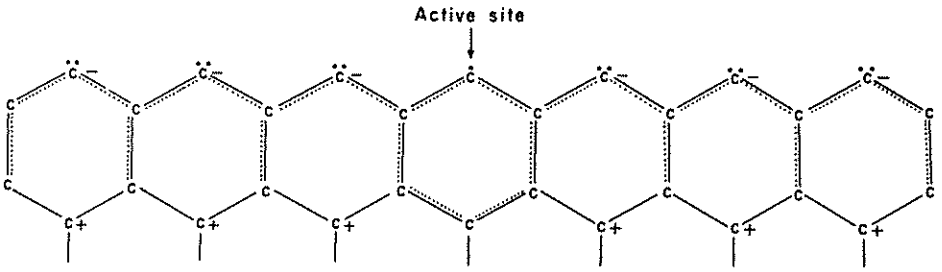

Fig. 12. Possible configuration of electrons on edge carbon atoms in graphite. [From Heuchamps (*12*).]

form negative ions at the surface, further increase the potential energy barrier to oxygen adsorption, and retard carbon gasification. Heuchamps feels that some surface impurities can catalyze gasification without necessarily becoming positive ions. Specifically, he suggests that the transition metals, with holes in their *d* bands, can accept an electron from a free electron doublet, producing an active site and at the same time lowering the height of the potential barrier.

A verification of the electronic theory of catalysis of carbon gasification has been attempted by Sykes and Thomas (*83*) by following the gasification of diamond by CO_2 in the presence of an Fe catalyst. The absence of π electrons in diamond was hoped to provide a clear-cut answer for the choice between the rival oxygen-transfer and electron-transfer mechanism. No unambiguous conclusion, however, could be drawn because at the reaction temperature (900°C) diamond undergoes graphitization. Then the diamond itself possesses in its electronic structure donor and acceptor levels satisfying, per se, the basic requirements of the electronic interpretation of combustion catalysis.

In summary, there is no overwhelming evidence on the basis of the

literature covered in this section to justify the exclusion of either the oxygen-transfer or the electron-transfer mechanism to explain catalysis of carbon gasification. There have been attempts to decide between these mechanisms by subjecting one of them to a crucial test, but an unambiguous decision has proved so far exceedingly elusive. There remains much room for fertile imagination in devising crucial experiments to tip the scales of acceptance in favor of one or the other mechanism. Our recent research, which makes an attempt in this direction, will be discussed in detail in the next section of this chapter.

III. CATALYSIS OF THE C—CO_2 REACTION BY GROUP VIII METALS

A. General Remarks

A detailed study has been made of the catalysis of the C—CO_2 reaction by Fe, Ni, and Co, three of the more important group VIII metals. In the case of Fe, additional studies have been conducted to identify its chemical phases which are active as catalysts. Iron has one property which has often been used as a means of detecting its presence as an impurity in other materials; it is strongly ferromagnetic. By measurement of the magnetic susceptibility of a specimen at several magnetic field strengths, trace quantities of ferromagnetic impurities can be detected in diamagnetic or paramagnetic substances (*84,85*). The magnitude of the ferromagnetism will depend upon the amount and the chemical form of the Fe. If the magnetic moment of the Fe phase can be quantitatively determined when it exists as an impurity in carbon, valuable information in precisely defining the catalyst system should be at hand. The development of the procedure for this quantitative measurement will be described in detail in this section, since it emphasizes the lengths to which one must go if he is really to understand the catalytic phenomenon.

B. Experimental

1. Materials

Materials used in this investigation were selected on the basis of their purity and well-defined physical form. SP-1 graphite, obtained from the Carbon Products Division of Union Carbide Corporation, is a highly purified natural graphite with a guaranteed maximum impurity content of 6 ppm. The particles of this graphite are flakes with an average diameter of 20–30 μ and a thickness of about 0.3–0.5 μ (*81*). The particles either

approach single crystals closely or, in any case, are composed of large crystals which are highly aligned. This graphite can be pelletized under pressure at room temperature without a binder. Its surface area in powder or pelletized form is 1.8 to 2.0 m^2/g, as determined by the BET method.

The Fe, obtained from the General Analine and Film Corporation, consists of roughly spherical particles having a fairly narrow size distribution. It is prepared by the decomposition of iron carbonyl. Powders of average particle size of 20, 10, and 3 μ were used. The Ni, obtained from the International Nickel Corp., is prepared by the decomposition of nickel carbonyl. The Co was obtained from A. D. Mackay, Inc. Ni and Co powders of 10 μ average particle size were used. In all cases, the metal powders were of >98.0% purity.

2. Sample preparation

A 90% graphite–10% metal mixture was prepared and diluted with additional graphite to obtain mixtures containing about 300 ppm of metal. Mixing of 150-g batches for 1.5 hr in a Patterson–Kelley twin shell blender was found to yield quite a uniform dispersion of metal upon comparison of 1-g aliquots by magnetic analysis. Ten-gram portions of the graphite–metal mixes were compressed at 100,000 psi and room temperature into rectangular blocks about 2 in. long by $\frac{1}{2}$ in. wide by $\frac{1}{4}$ in. high. This molding pressure was found to give somewhat more reproducible and machinable samples than lower molding pressures. Subsequently the blocks were cut in half lengthwise, and each half was machined into a cylinder 30 mm long and 4.7 mm in diameter. The apparent density of the compressed samples was 2.15 g/cm^3, giving a porosity of about 5%.

3. Heat treatment and reactivity measurements

Figure 13 represents the apparatus used for heat treatment of pure and metal-doped graphite cylinders and subsequent reactivity studies. The globar-heated furnace contained a $1\frac{1}{8}$ in. i.d. vertical mullite tube. It had a temperature gradient, as indicated in the plot of typical data obtained when the constant-temperature region, position H, was maintained at 1000°C.

Gases, dried to a moisture content of ca. 125 ppm water vapor by Linde 13X molecular sieves at room temperature, deoxidized by passage over Cu turnings at 600°C, and preheated by mullite chips at 750°C, flowed up the mullite tube around the sample. All gases used had purities of >99.8%.

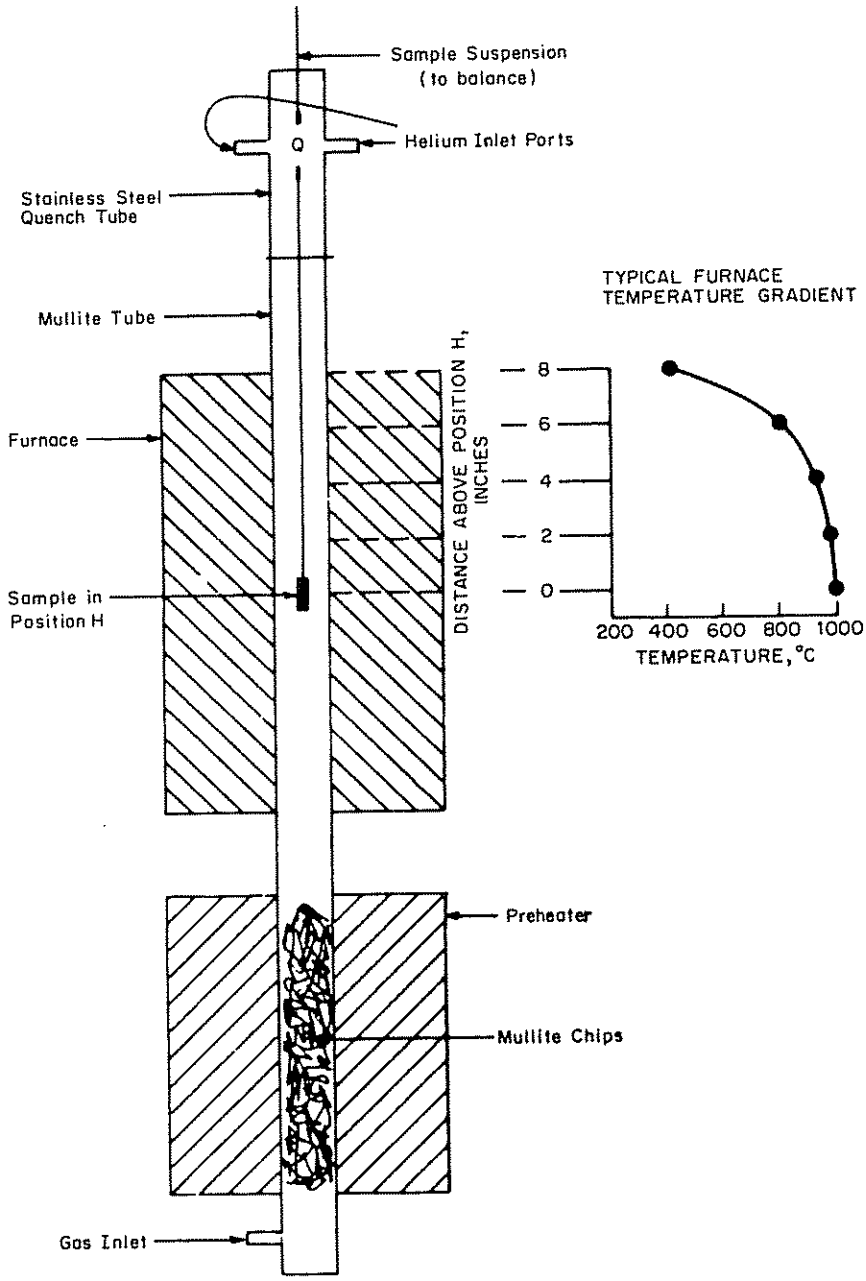

Fig. 13. Diagram of heat-treatment and reactivity apparatus.

The sample was held in a mullite container. To prevent thermal shock damage to the furnace and container during heating, it was found necessary to lower the sample slowly into the furnace. With temperatures of 800–900°C the sample was lowered to position in two equal steps and held at each position for 1 min. At 1000–1300°C, the sample was lowered in eight steps over an 8-min period. Reaction rates, measured as weight loss of carbon per unit time, were determined by suspending the sample from a Sartorius Selectra Automatic single-beam balance which had a sensitivity of 2 mg. Since the graphite samples weighed ca. 1 g, the least amount of burn-off which could be detected was ca. 0.2%.

When the sample was to be cooled by rapid removal from position H to position Q, He was admitted through the upper inlet ports and was impinged on the sample through six uniformly spaced slots in the quenching jacket. The sample was thus cooled to room temperature in ca. 3 min.

4. Measurement of magnetic susceptibility

The specific magnetization or magnetic moment per gram of a ferromagnetic substance approaches a constant and characteristic value for that substance at sufficiently high magnetic field strengths (*84–86*). This value is called the saturation magnetization. The magnetic susceptibility χ, the ratio of magnetic moment M to applied field H, of a ferromagnetic material at saturation is thus a function of the applied field, i.e., $\chi = M/H$. For a diamagnetic material such as carbon, the magnetization is induced in direct proportion to the applied field so that the susceptibility is independent of the applied field. These facts constitute the basis for separating the diamagnetic contribution to the observed susceptibility of a mixed sample from that of the ferromagnetic contribution. Standard texts on magnetism (*84–86*) present the general form of the relationship thus derived. Henry and Rogers (*87*) derive the relation for a system essentially the same as that used in the present research, that is, susceptibility measurements on samples containing traces of ferromagnetic impurities by the technique described below. The expression obtained is $\chi_H = \chi_G + 2CM_S/(H_2 + H_1)$, where χ_H is the magnetic susceptibility per gram of sample at a given field strength, H; χ_G is the specific susceptibility of pure graphite; C is the concentration of ferromagnetic component in mass units; M_S is the saturation magnetization of the ferromagnetic component; and H_2 and H_1 are applied field strengths at the bottom and top of the sample, respectively.

The observed susceptibility is thus a linear function of $(H_2 + H_1)^{-1}$ with slope of $2CM_S$ and intercept of χ_G. In this way both the diamagnetic

susceptibility of the graphite and the saturation magnetization of the ferromagnetic constituent can be determined from susceptibility measurements at several different field strengths. Slopes and intercepts were determined in this study from a least-squares calculation for χ_H versus $(H_2 + H_1)^{-1}$ at five values of the applied field.

Figure 14 is a schematic representation of the apparatus used for susceptibility measurements. It is a modification of the Gouy apparatus and closely resembles that used by Henry and Rogers (*87*). It offers several advantages over conventional Gouy measurements. First, relatively small samples can be used, since H_2 at the bottom of the sample and H_1 at the top are homogeneous over an appreciable volume, and a field gradient exists between. Second, the entire sample can be maintained in a

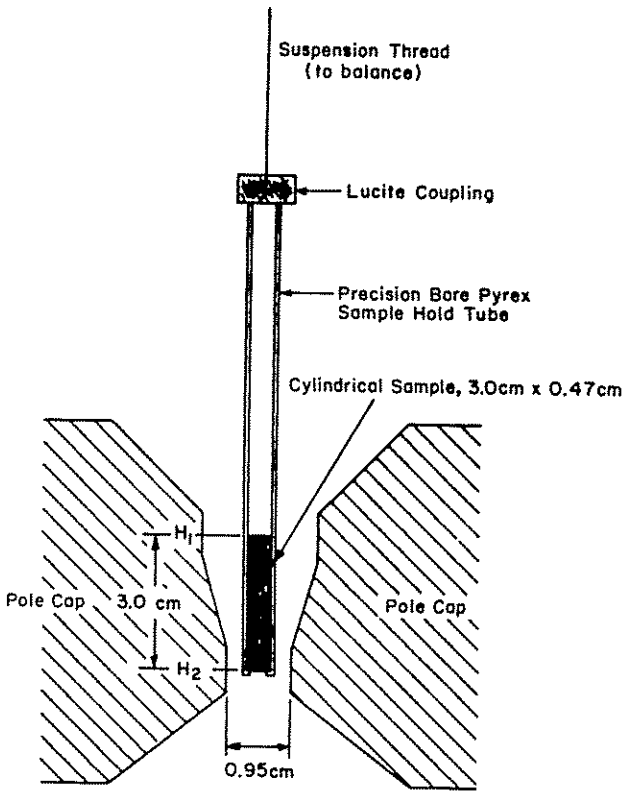

Fig. 14. Diagram of magnet pole caps and sample suspension.

magnetic field of sufficient strength to assure saturation of the ferromagnetic component, as opposed to the usual Gouy technique, which requires that one end of the sample be in a zero field.

The pole caps were 4-in. constant-gradient caps V-4086-1, manufactured by Varian Associates. The magnetic field was controlled by Varian Model V-2300 power supply and V-2301 current regulator. Magnetic current settings on the regulator were found to give a reproducible magnetic field strength. The pole gap used was 0.952 cm ($\frac{3}{8}$ in.). Figure 15 shows the field strength distribution in the vertical direction between the poles at the 0.952-cm gap for five different current settings. These measurements were made by carefully moving a Rawson Lush rotating coil fluxmeter through a vertical distance of 6.8 cm between the poles and recording the field strength every 2 or 4 mm. The fields at H_2 and H_1 are seen to be homogeneous over several millimeters even at the highest field strengths. It was expected that the lowest field strength employed, 7000 Oe, would be sufficiently high to attain saturation of the ferromagnetic components.

An Ainsworth Type TY double-beam balance with magnetic damper was used to measure apparent changes in weight when the sample was placed in the magnetic field. The sample was contained in a thin-walled, precision-bore, 4.7-mm-i.d. Pyrex tube with a Lucite bottom. This sample holder was suspended from the balance by thread. In most cases the sample holder was weighted by a 50-g weight suspended below it to prevent lateral displacements. Weight changes of the empty sample holder were recorded at each of the magnetic field strengths used in the susceptibility determinations and subtracted from the weight changes of sample plus holder observed at corresponding field intensities to obtain a corrected weight change. χ_H was then determined from the corrected weight change and magnetic field values by the equation $\chi_H = 2gl\,dw/m(H_2^2 - H_1^2)$, where g is the gravitational constant, 980 dynes; l is the sample length, 3.0 cm; m is the sample mass in grams; and dw is the corrected weight change in grams.

Since the above computation requires taking the difference between the squares of the two large measured homogeneous field strengths, which could introduce excessive error, final calibration of the integral susceptibility apparatus was made using a pure Cu cylinder of known susceptibility. This material was obtained from the same source as the Cu examined by other workers (*87*), who found it free of ferromagnetic impurity and determined its susceptibility to be -0.0859×10^{-6} g^{-1}. The susceptibility of a rod of Cu from which the calibration standard was

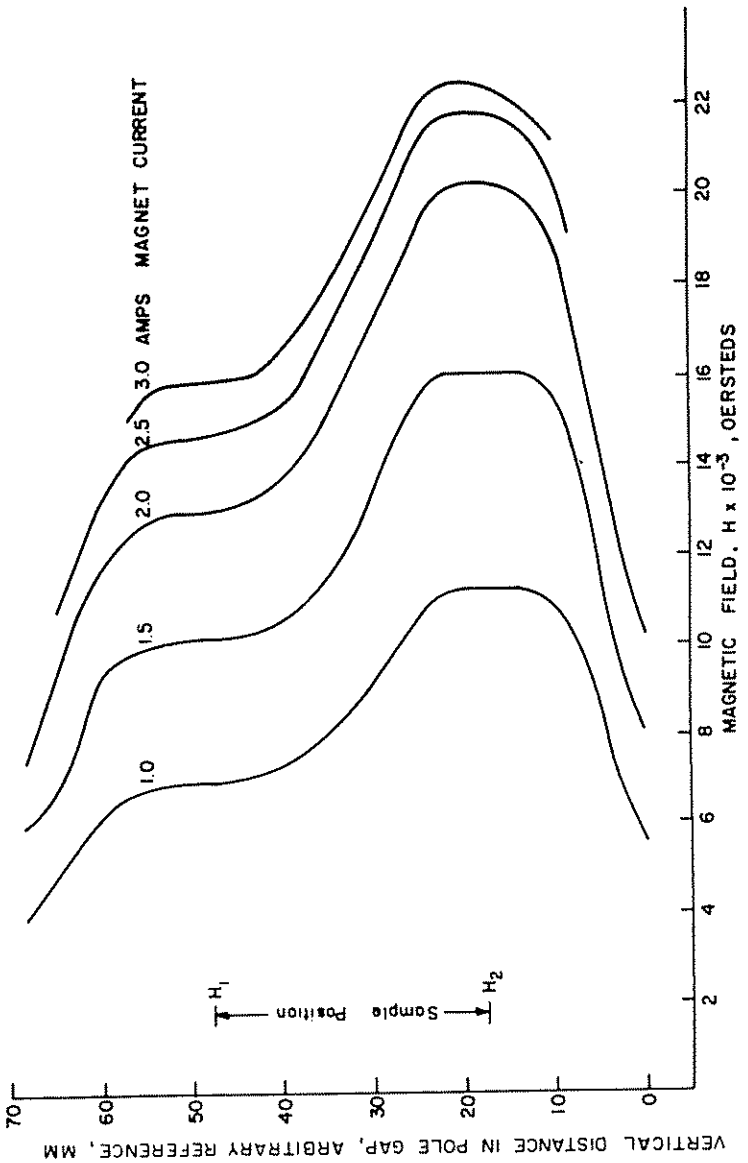

Fig. 15. Magnetic field distribution with $\frac{3}{8}$-in. pole gap.

obtained was measured by the standard Gouy method and found to be -0.086×10^{-6} g^{-1} with no ferromagnetic contribution. The quantity $H_2^2 - H_1^2$ was thus calculated from measurements on this standard.

Duplicate susceptibility measurements on pure graphite samples indicated typically a standard deviation of $< \pm 1\%$. For several Fe-doped samples, duplicate susceptibility measurements gave standard deviations of $< \pm 1\%$ for the intercept (χ_G) and $< \pm 0.5\%$ for the slope ($2CM$) for the data treated as a function of $(H_2 + H_1)^{-1}$ as described.

It should be noted that the values reported for graphite susceptibility in either pure or doped samples will not be absolute, but representative of a given sample only. The diamagnetic susceptibility of graphite is markedly anisotropic (*88*), being some 40–80 times more intense in the *c* direction (normal to the layer planes) of a single crystal than in the *a* direction (parallel to the layer planes). The graphite flakes described previously are also markedly anisotropic in shape and will tend to align under compression with the normal to the flake diameter (corresponding to the *c* direction of crystallites) parallel to the pressing direction (*89*). This results in a preferred orientation of crystallites such that, in the cylindrical graphite samples, observation in one direction will reveal primarily layer-plane surfaces, while rotation by 90° will reveal primarily layer-plane edges.

When placed in a magnetic field, such an anisotropic sample will seek the position of lowest potential energy (*84,85*), in this case with the majority of layer-plane normals perpendicular to the major direction of the applied field. With the cylinder free to rotate about its axis, this behavior assures that the sample will always be oriented in the same direction with respect to the magnetic field. Since the distribution of crystallites will not be precisely the same in each sample, however, the measured susceptibility will vary from sample to sample.

5. Phase identification from magnetization data

In utilizing the magnetization data to establish the catalyst composition, it is necessary to consider possible phase transformations occurring during cooling from heat-treatment temperatures as well as the effect of heat treatment alone. Thus Gumlich (*90*) has shown that the C retained in solid solution with Fe is more effective in diminishing the saturation magnetization of Fe than the same amount of C combined as cementite (Fe_3C). The major features of the Fe–C phase diagram, presented in Fig. 16, have been quite well established (*91–93*). Reliance on the phase diagram alone, however, might prove misleading as the "equilibrium" phase Fe_3C is in reality metastable and decomposes to Fe and graphite

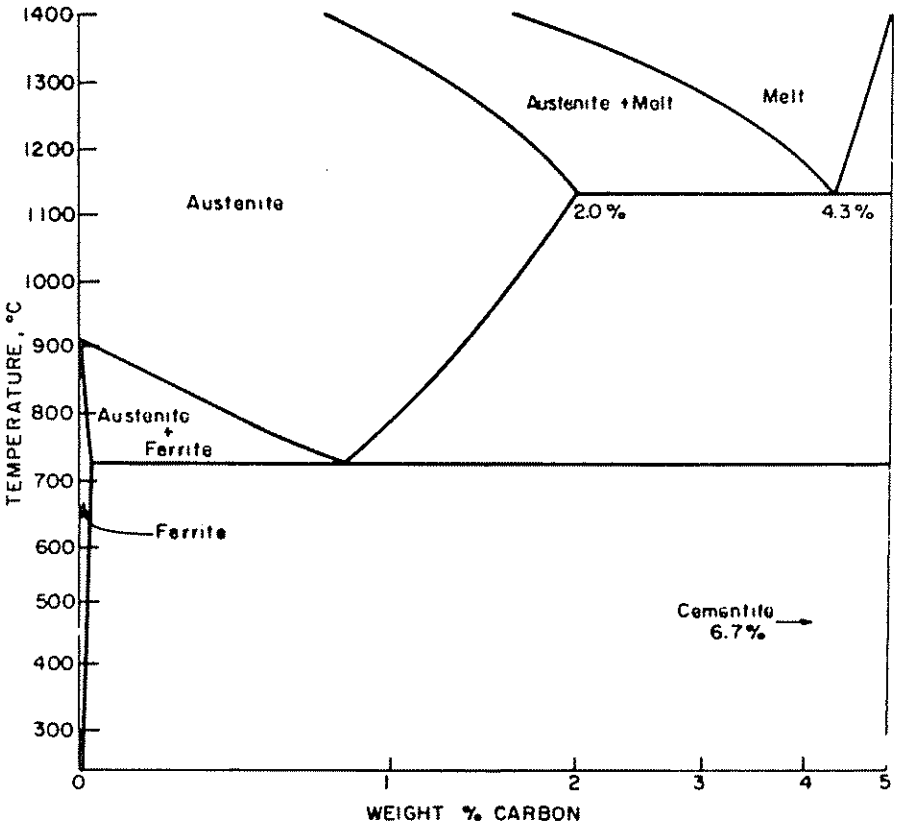

Fig. 16. Fe–C phase diagram.

under certain conditions (*93–96*). Neither are other metastable phases such as Fe_3C carbides or martensite represented on the diagram. Moreover, the rates of attainment of equilibrium and of other possible phase transformations must be considered in any practical situation. Thus the ferromagnetic phase formed upon cooling the Fe-doped graphite samples from heat treatment to room temperature undoubtedly is not the same phase that existed at the higher temperature. It will be shown, however, that identification of the high-temperature phase can be established through its relation to the room-temperature phase.

The time required for C to saturate the Fe particles used in this study is estimated by the methods of Darken and Gurry (*97*) using the data of

Smith (*98*) to approximate the diffusion coefficient of C in Fe under appropriate conditions. A fractional saturation (amount of C in Fe at time t divided by the amount at infinite time) of 0.9999 should be attained in 9 sec at 800°C for the 20-μ-diameter particles. Higher temperatures and smaller particles considerably reduce this time.

Following formation of the solid solution of C in γ-Fe (austenite), cementite precipitation occurs (*95*) to maintain the concentration of dissolved C at the saturation level for that temperature. The cementite may decompose forming Fe and graphite again. At 1100°C cementite decomposition is very rapid (*93,94*), while below about 700°C the decomposition rate is quite slow and cementite is found to be a persistent phase, although thermodynamically unstable. The Fe–C phase formed during heat treatment at temperatures of 800–1100°C will, therefore, consist of austenite and cementite. Austenite is a stable phase at 723–1123°C, and the solubility of C in it increases somewhat with temperature. Cementite, being unstable, will be found in decreasing amounts as the temperature of heat treatment is raised above 700°C and the rate of its decomposition becomes increasingly larger relative to the rate of its precipitation from saturated austenite. Above 1123°C the system becomes molten, and the solubility of C in Fe increases somewhat.

Consider now what occurs upon cooling from the 723 to 1123°C temperature range to below 723°C.

1. For slow cooling rates, decarburization of austenite can occur as C precipitates in the form of cementite to attain the lower equilibrium solubility. Again the cementite, being unstable, will decompose at some rate with the net effect being a decrease in the amount of C combined with Fe. At 723°C a ferrite–cementite eutectoid with 0.8% C is formed. Ferrite is a solid solution of C in α-Fe.

2. Faster cooling rates result in the retention of all the C dissolved in austenite; i.e., the austenite becomes supersaturated by failing to attain equilibrium at the lower temperature. If the cooling rate is very fast, i.e., quenching, the supersaturated austenite can undergo the instantaneous, diffusionless transformation to martensite (supersaturated ferrite). At intermediate rates the austenite is transformed into a system of ferrite and cementite.

Of importance is the fact that some transformation must take place on cooling, but that the amount of C combined with Fe in the low-temperature phase can be the same as that combined at the higher heat-treatment temperature.

The cooling procedure used in this investigation has been described.

The martensite transformation occurs only with much more rapid cooling rates (*99*) and can be eliminated from consideration. The formation of the ferrite–cementite system from austenite occurs rapidly [e.g., ca. 5 sec at 600°C for relatively pure Fe containing 0.9% C (*100*) but at cooling rates slower than required for the martensite transformation (*96,100*)]. The experimental procedure should allow adequate time for this transformation to be completed.

In making use of magnetization data for phase identification in the Fe–C system, the amount of C combined with Fe is calculated on the basis that it is in the form of ferrite and cementite at room temperature. Assuming no serious decarburization has taken place during cooling, this carbon content will be representative of the austenite or austenite–cementite system which existed at heat-treatment temperature. The details of such an analysis are now given.

For a mixture of phases the specific magnetization (per gram of mixture) is the sum of the weighted contributions from each phase (*84*). It has been shown that this generalization applies to the case of Fe combined with C as the two-phase system ferrite and cementite (*90,101*). With M_M, M_F, and M_{CEM} designating the specific magnetizations of the mixture, of ferrite, and of cementite, respectively, and μ_M, μ_F, and μ_{CEM} representing the mass in grams of mixture, of ferrite, and cementite, respectively, this can be written

$$M_M = \mu_F M_F + \mu_{CEM} M_{CEM} \tag{1}$$

with

$$\mu_F + \mu_{CEM} = \mu_M = 1 \tag{2}$$

M_F and M_{CEM} are known (*86,101*) and M_M is obtained from the susceptibility measurements previously described. These values are $M_F = 218$, $M_{CEM} = 128$. From the known composition of ferrite and cementite, the following can be written with μ_C designating the mass of combined C:

$$\mu_C = 0.0002\mu_F + 0.0669\mu_{CEM} \tag{3}$$

Combining (2) and (3), we obtain

$$\mu_{CEM} = (\mu_C - 0.0002)/0.0667 \tag{4}$$

Substituting (2) and (4) and the values for M_F and M_{CEM} into (1),

$$M_M = 2.7 - 1349\mu_C \tag{5}$$

or

$$\% = (217 - M_M)/13.49 \tag{6}$$

Equation (6) gives the per cent C in the ferrite–cementite system as a function of the specific magnetization of that mixture. Previously described magnetic susceptibility measurements yield the product $2C_M M_M$ as the slope, S, of the linear plot of χ_H versus $(H_2 + H_1)^{-1}$. It is only necessary for the concentration, C_M, of the ferrite–cementite mixture in the graphite sample to be known before this measurement can be used to analyze for the per cent combined carbon. C_M is calculated from C_{Fe}, the known Fe concentration in the unheated sample. Equation (2) can be alternatively expressed by

$$\mu_C + \mu_{Fe} = \mu_M = 1 \tag{7}$$

Then

$$C_{Fe} = (1 - \mu_C)\mu_S \tag{8}$$

with $\mu_S \equiv$ mass of sample per gram of Fe. Also

$$C_M = \mu_M/\mu_S = 1/\mu_S \tag{9}$$

C_M can then be expressed in terms of the known value C_{Fe} and the yet-unknown combined C concentration:

$$C_M = C_{Fe}/(1 - \mu_C) \tag{10}$$

By taking the ratio of the slope, S_M, of the heat-treated sample to that of the unheated sample, S_0, the dependence of Fe concentration is eliminated:

$$S_M/S_0 = 2C_M M_M/2C_{Fe}M_{Fe} \tag{11}$$

Making use of (6) and (10) gives

$$S_M/S_0 = 217 - 13.49(\%C)/218 - 2.18(\%C) \tag{12}$$

Figure 17 is a plot of this function from which the per cent C can be read directly after obtaining the ratio of slopes from susceptibility measurements.

Consider now magnetic identification of the Fe oxide phases. Of the three Fe oxides, wüstite (FeO), magnetite (Fe_3O_4), and hematite (Fe_2O_3), only magnetite is ferromagnetic* with a specific magnetization of 95 (*84*). Wüstite is antiferromagnetic, and the stable form of Fe_2O_3, hematite, is paramagnetic; their contribution to the overall susceptibility of samples in which they are contained in trace quantities would be undetectable. Mixed Fe oxide systems would have an apparent specific magnetization

* Magnetite is more properly described as ferrimagnetic, but for the purpose of this investigation no distinction need be made.

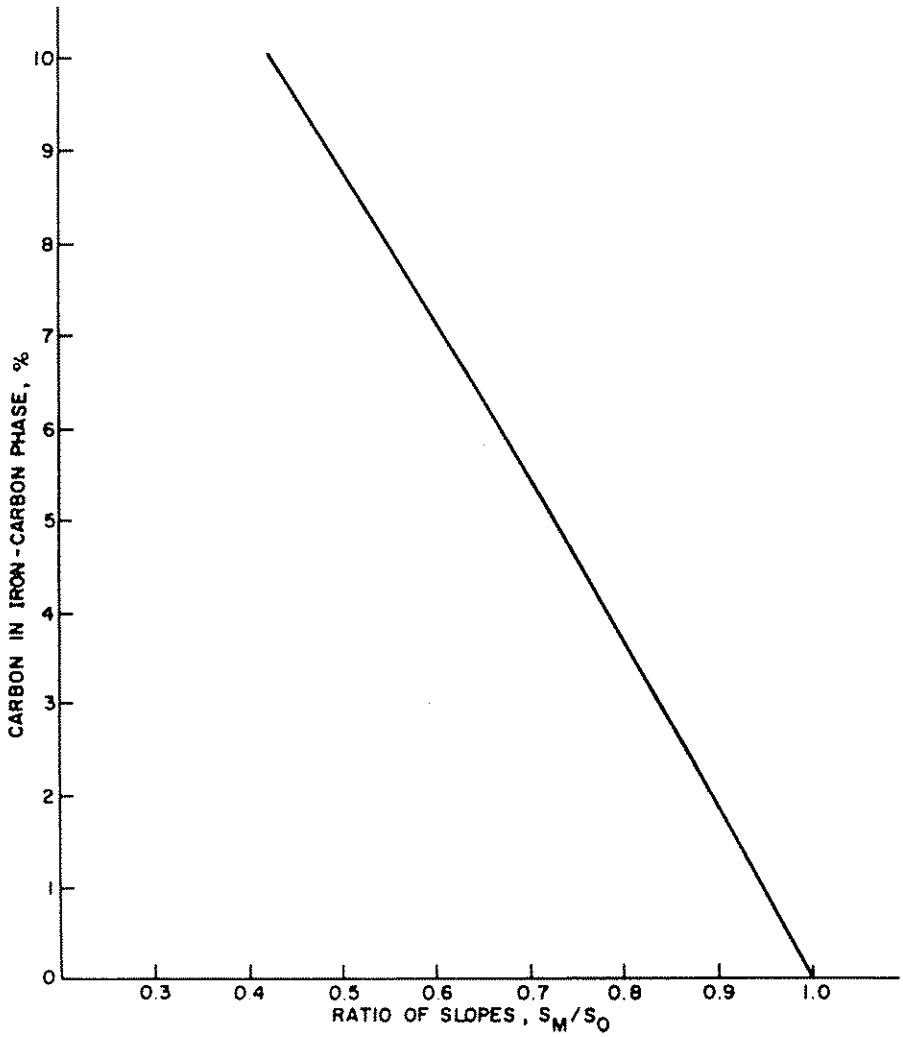

Fig. 17. Calibration curve for relating magnetic data to Fe–C phase composition.

with an upper limit of 95 unless some free Fe were also included. Complete oxidation of the Fe will, therefore, lower the observed magnetization substantially more than complete carbiding.

For magnetite, the observed magnetization is compared with the known magnetization of that oxide after converting the original Fe concentration

to the concentration in terms of that oxide. This requires simply the multiplication of the Fe concentration by the ratio of 3 Fe to Fe_3O_4, or 1.38.

Several sources of error are possible in the calculation of specific magnetization from magnetic susceptibility data. It is assumed that the amount of Fe impurity remains constant during gasification runs, i.e., reaction results in the removal of graphite only and thereby increases the concentration of Fe remaining. If a small amount of Fe is lost during the gasification process as some supporting graphite is removed, the assumed concentration will be too high and the calculated magnetization, therefore, too low. A second possible cause for variation in calculated magnetization values is the nonhomogeneity of the oxide phases, for example, the inclusion of small amounts of Fe or nonferromagnetic oxide phases in a predominantly magnetite system. For these reasons, calculated magnetization values within 10% of the value accepted for magnetite are considered to be in good agreement with the latter value and indicative of primarily a magnetite phase. It was thus observed that low burn-off runs in which adequate time was allowed for steady state to be reached were in better agreement than relatively high burn-off runs during which treatment times were dictated by the type of reactivity data sought.

C. Results

1. Typical magnetic susceptibility data

Figure 18 is a typical plot of χ_{II} versus $(H_2 + H_1)^{-1}$ obtained from magnetic susceptibility measurements on a pure graphite, an Fe-doped unheated graphite sample, and an Fe-doped heat-treated sample. The pure graphite has no detectable amount of ferromagnetic impurity. For the Fe-containing samples, the remarkably good linearity of the plots indicates that the assumption regarding the attainment of saturation magnetization is valid even for the lowest applied fields. The intercept, χ_G, is seen in Fig. 18 to be different for the pure graphite and the Fe-doped graphite and also to be affected by heat treatment.

The variation in χ_G from sample to sample is to be expected and has been described in the experimental procedure as being the result of variations in crystallite orientation. Table III gives χ_G values obtained from a number of pure graphite samples pelletized at different pressures and indicates the extent of the variation observed with undoped samples because of the above factor. Two samples were obtained from each pressed block of graphite; one-half is designated simply by a number; the

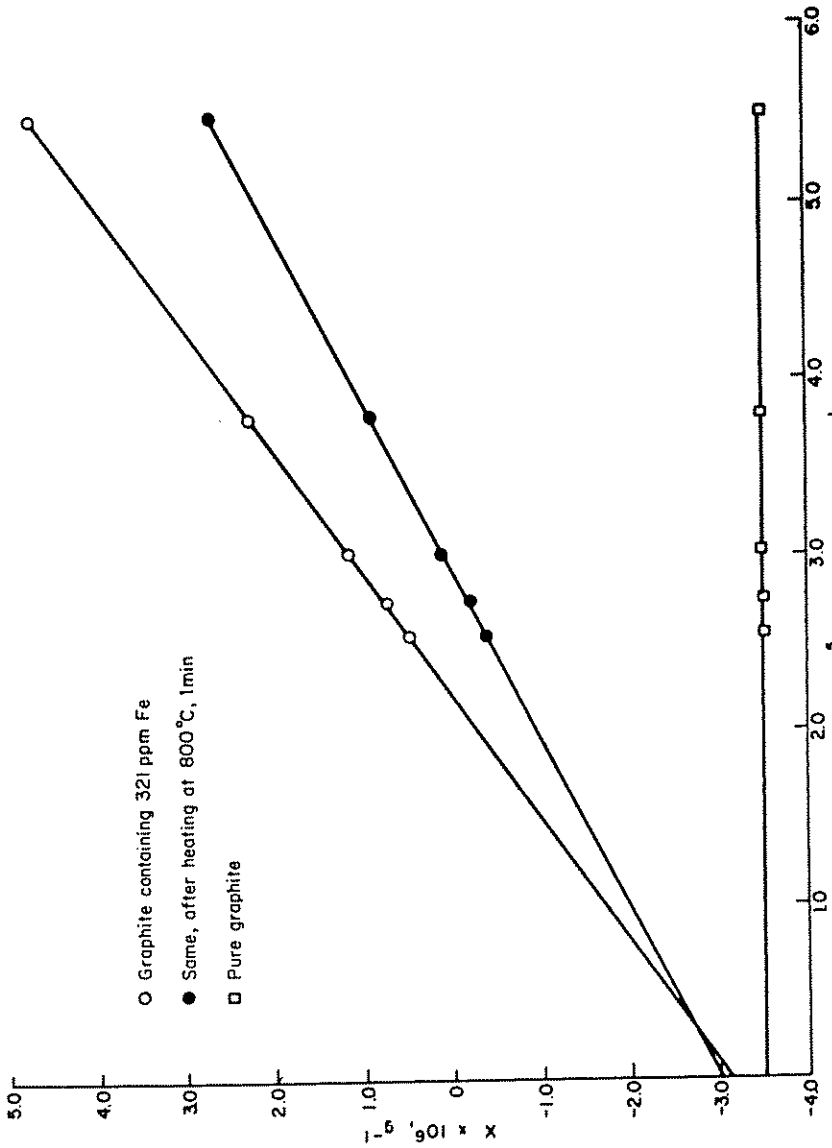

Fig. 18. T al plot of magnetic susceptibility data.

TABLE III

Effect of Molding Pressure and Rate on Graphite Susceptibility

Sample	$-\chi \times 10^6$, g^{-1}	Molding pressure, psi	Molding rate[a]
13	3.52	30,000	A
13A	3.03	30,000	A
14	3.88	30,000	B
15	3.10	60,000	B
15A	4.02	60,000	B
16	3.80	60,000	A
16A	3.00	60,000	A
17	3.57	90,000	A
17A	3.50	90,000	A
18	3.53	90,000	B
18A	3.40	90,000	B
19	3.47	120,000	B
19A	3.66	120,000	B
20A	3.67	120,000	A

[a] A, 60,000 psi/min; B, 15,000 psi/min.

other sample from the same block is designated by the same number suffixed by "A." At low molding pressures nonuniform crystallite distribution is more marked than at higher pressures, as indicated by wide divergence of χ_G values between one sample and its mate from the same block and by variations from block to block. At higher pressures the samples appear more uniform, but by no means is a reproducible bulk susceptibility attained. Undoubtedly the crystallite orientation is not uniform within a given sample either. The previously described precision of measurement on a given sample is, however, good.

For 16 samples containing ca. 300 ppm of Fe and all pelletized at 100,000 psi, the range of χ_G values was -2.92×10^{-6} to -4.01×10^{-6} g^{-1}. The differences between the apparent graphite susceptibilities of pure samples and doped samples were not significant.

An effect of heat treatment on the measured bulk susceptibility of graphite was observed for pure samples as well as those containing Fe. It is attributed to small changes in crystallite orientation, suggested by the fact that some expansion of the graphite samples occurred during heat treatment. This could occur, for example, by supplying sufficient thermal energy to reorient particles locked in high-energy positions during pressing. Walker et al. (*81*) have shown that the thermoelectric power of

graphite is unaffected by the presence of Fe, so that an intrinsic electronic change in the graphite is highly improbable.

2. Transformations in the iron phase on heat treatment

The graphite samples were doped with about 300 ppm of metallic Fe powder. The following descriptions of the Fe–C or Fe–O systems pertain, therefore, to the Fe as it exists in the graphite matrix. The major part of the matrix does not in general participate in the formation of the Fe-containing phases; the Fe–C system thus does not refer to the Fe–graphite

TABLE IV

Per Cent C in Fe–C Phases at Various Temperatures

	Temp., °C				
	1100	900	850	800	500
%C analyzed	1.2–1.8	1.8	2.4	3.7	6.2–9.0
%C in austenite (*91*)	1.9	1.3	1.2	1.1	0.02[a]
%C in cementite (*91*)	6.7	6.7	6.7	6.7	6.7

[a] Ferrite.

mixture but to the Fe impurity and C combined with it in solution or as chemical compounds.

Table IV presents results of heat treatment in He at temperatures from 500 to 1100°C as determined by magnetic analysis. Equilibrium data from the phase diagram are included for comparison. At 1100°C the amount of C in the Fe–C phase was slightly less than that existing in saturated austenite at that temperature. As expected, cementite was found to be unstable and not persistent at 1100°C. The remaining austenite apparently underwent a small amount of decarburization in cooling from this temperature. At 900°C the analyzed per cent C at steady state was slightly above that for saturated austenite. For the two-phase system previously described, C in excess of that which is soluble in Fe as austenite must be combined as cementite. At 850 and 800°C the total amount of combined C and, therefore, the amount of cementite at steady state, further increased, indicating the increased persistence of cementite with decreasing temperature because of the decreased rate of decomposition. Finally, at ca. 500°C, where essentially all combined C should exist as cementite, the total combined C analyzed corresponded closely to the per cent C in cementite. The fact that on some occasions C was found combined with

the Fe in proportions greater than that in cementite probably indicates the existence of other carbides, e.g., Fe_2C, which have magnetic moments similar to cementite and have been found to exist in this low-temperature range (*84*).

To further characterize the behavior of the system as regards cementite persistence, some runs were made in series at 1100 and 500°C with the results given schematically in Fig. 19. At 1100°C only austenite was found. When the 1100°C heat treatment was followed by heating at 500°C, cementite was formed; the formation proceeded relatively slowly at the lower temperature as indicated by the increase in per cent C in going from 6 to 20 min soak time. Upon subsequent heating to 1100°C, the cementite was decomposed; if followed by a second heating at 500°C, cementite (and possibly higher carbides) formation again resulted. If the initial heating was done at 500°C cementite was similarly formed, and the

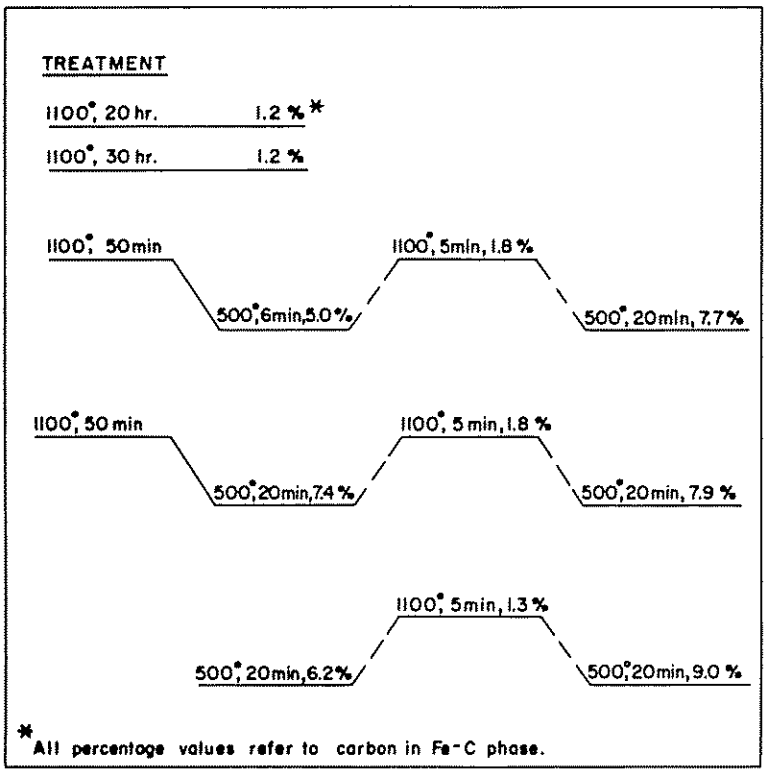

Fig. 19. Schematic of heat treatment results at 1100 and 500°C.

behavior during subsequent treatment followed that just described for other samples. In order to allow the sample to be rapidly changed from one temperature to the other, the constant-temperature zone of the furnace was maintained at 1100°C, and the lower temperature was attained by placing the sample in a higher position. As Fig. 13 has indicated, the sample was thus in a temperature gradient, in this case of about 100°C/cm. The 500°C temperature is the mean temperature in this gradient.

The persistence of the cementite phase at 500°C suggested that a decomposition rate might be observable at somewhat higher temperatures. This is illustrated in Fig. 20 for temperatures of 800, 850, and 900°C. Each point indicates that the sample was quenched after heat treating in the constant temperature zone for the period given on the time coordinate, the specific magnetization determined, and the sample returned to the furnace for further treatment. The cumulative heat-treating time, exclusive of the time required to pass the sample through the temperature gradient zone of the furnace, is plotted versus the ratio S_M/S_0, which decreases as the total combined C in the Fe–C system increases. This parameter is used rather than per cent C directly so that an easier comparison can be made with the results in Fig. 21 on the oxide systems to be presented shortly.

The behavior was qualitatively the same at all temperatures. As the sample entered the furnace and was maintained several minutes below heat-treatment temperature, cementite was formed and persisted fo. short heating periods giving a large initial C concentration. Holding for extended times at heat-treatment temperatures resulted in cementite decomposition. Finally, a steady state was reached wherein the rates of cementite formation and decomposition were equal. As indicated by the 500 and 1100°C runs, the decomposition rate becomes relatively faster than the formation rate as the temperature increases, so that the steady-state concentration of cementite decreased at higher temperatures. Figure 20 illustrates both the increased decomposition rate and decreased steady-state cementite concentration as temperature increased from 800 to 900°C.

A predictable behavior for the Fe–C system under the conditions of this investigation was thus established. The observed behavior was in accord with the established equilibrium data and other considerations already discussed. A primary use of this information will be to correlate Fe catalyst activity to its chemical composition.

Figure 21 illustrates the behavior of samples heated at 800, 850, and

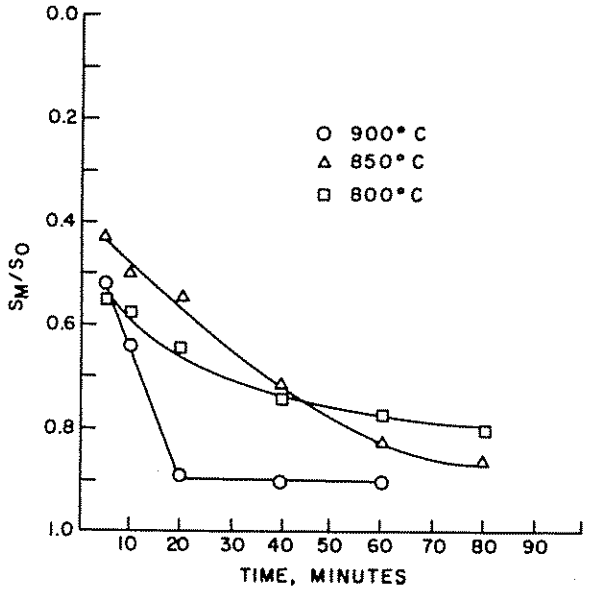

Fig. 20. Effect of heat treatment of Fe-doped graphite in He on magnetic susceptibility.

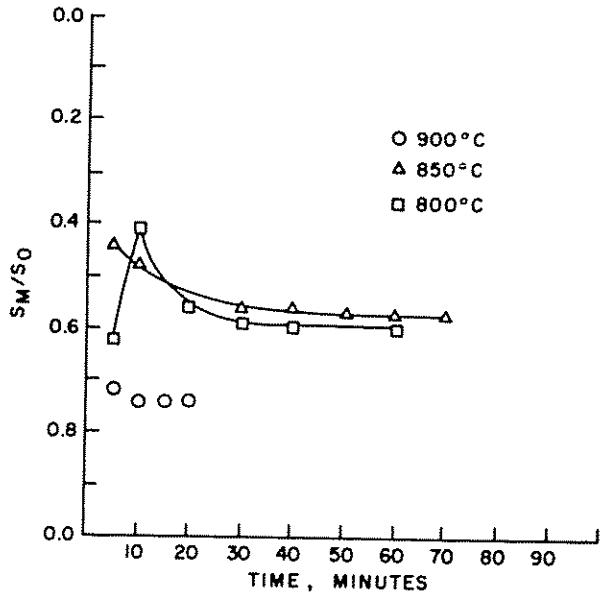

Fig. 21. Effect of heat treatment of Fe-doped graphite in CO_2 on magnetic susceptibility.

900°C in CO_2 by a procedure exactly analogous to that used for the heat treatments in He represented in Fig. 20. The following observations are made:

1. Initial stages of heat treatment in CO_2 resulted in a large decrease in magnetization, except at 900°C.
2. Additional periods of heat treatment at 800 and 850°C caused the magnetization to rise again and become constant at a value less than that of either pure Fe or carburized Fe at steady state. At 900°C the magnetization remained nearly constant with time.
3. The specific magnetization at steady state for treatment at 800 and 850°C are essentially the same. In both cases it corresponds closely to the specific magnetization of magnetite, i.e., 95.

A general similarity of the shape of the 800 and 850°C curves to those in Fig. 20 is also observed and can be attributed to several phenomena. The initial large magnetization change could be ascribed to cementite formation such as occurs during the He heat treatments. Second, the formation of nonmagnetic wüstite during initial stages of Fe oxidation would also account for the decrease. Still a third possibility exists: rapid and complete oxidation to paramagnetic hematite at the lower temperatures encountered during placement of the sample in the furnace could be followed by reduction to magnetite by reaction with C at heat-treatment temperature. The resolution of this problem will be undertaken in Section III.D.

The identification of phases existing at steady state is more clear-cut. There is no doubt that the phases obtained by treatment in CO_2 are not those found when heat treatment is carried out in He. The specific magnetizations of 94 and 91 found for phases formed at 800 and 850°C are taken as real evidence that the phase is magnetite. Additional results will firmly establish this. Regardless of which of the three above paths is selected for the ultimate formation of magnetite, it is necessary to conclude that at 900°C the Fe is also in an oxidized state. In this case, however, either less Fe is oxidized or more Fe oxide is reduced than at 800 or 850°C. Clearly the phase is not an Fe–C system.

The feasibility of a magnetite phase existing under these conditions is demonstrated by consideration of the approximate equilibrium conditions listed below for Fe oxides in the 800–900°C temperature range (*102,103*):

P_{CO_2}/P_{CO}	<0.3	0.3–3.0	3.0–3.0 × 10^4	>3.0 × 10^4
Equilibrium phase	Fe	FeO	Fe_3O_4	Fe_2O_3

These conditions apply to the system Fe–CO_2 at atmospheric pressure. Under experimental conditions with the Fe contained in a graphite matrix, the equilibrium for C gasification, i.e., for $C + CO_2 = 2CO$, must also be considered. For example, at 900°C the equilibrium ratio P_{CO_2}/P_{CO} is about 0.05 for this reaction. Therefore, although the CO_2 reactant gas should oxidize the Fe to hematite at equilibrium, a lower oxide should result if even a relatively small CO pressure is developed by reaction of CO_2 with the graphite. These considerations are introduced here to show the compatibility of existing equilibrium data with experimental observations of oxide phases.

Several experimental characterizations of the behavior of Fe oxides were made. The addition of about 300 ppm of magnetite powder to the graphite resulted in the following:

1. No change in magnetization occurred after treatment in CO_2 at 850°C for 20 min, showing the persistence of this phase.
2. A marked increase in magnetization was observed after treatment in CO at 850°C for 13 min, indicating partial reduction to Fe.

The following observations were made on a sample of graphite to which about 300 ppm of hematite powder had been added:

1. In the unheated sample no ferromagnetic constituent was detectable indicating the expected paramagnetism of hematite.
2. Heating in CO_2 at 850°C for 20 min produced a strong ferromagnetic contribution.
3. Subsequent heating in CO at 850°C for 13 min produced a further increase in magnetization.

Since the hematite was originally paramagnetic, the usual magnetic analysis of impurity concentration could not be made, so that observations 2 and 3 are not given quantitatively. However, they do show that hematite was reduced to a magnetite phase in the presence of C and CO_2 at 850°C and that this phase was partially reduced by CO to Fe for the following reasons. Fe, Fe_3O_4, and γ-Fe_2O_3 are ferromagnetic. The latter cannot be formed by heating α-Fe_2O_3, the paramagnetic form (*84*), and, therefore, is not formed by the CO_2 treatment at 850°C. If it is assumed that Fe was formed under these conditions, the effect of CO, which could only reduce the magnetization of Fe by carburization, in the subsequent treatment cannot be explained. By elimination of these two possibilities it is concluded that magnetite must be responsible for the observed ferromagnetism after CO_2 treatment. Moreover, the persistence of magnetite in the same environment has already been established.

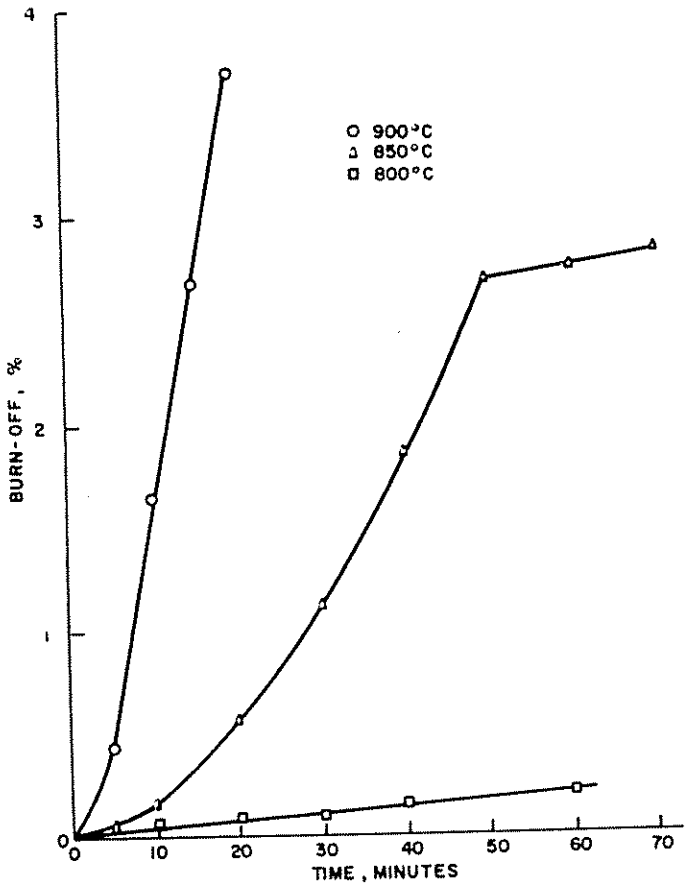

Fig. 22. Extent of graphite burn-off incurred in CO_2 during heat treatment described in Fig. 21.

3. Iron state and catalytic activity

The results in Fig. 21 have been used to show the formation of oxide phases during exposure to CO_2 at 800–900°C. Preliminary reactivity results were also obtained in these experiments by measurement of the sample weight before and after each run. Figure 22 illustrates the marked differences in reactivity or catalyst activity at the several temperatures. At 900°C a relatively large burn-off was observed for each run. At 850°C reactivity first increased with appreciable gasification occurring, then

suddenly dropped almost to zero. At 800°C only 0.2% burn-off was attained after a total reaction time of 60 min, indicating essentially no catalytic activity of the Fe phase. A remarkable correlation was found between this behavior and changes in catalyst composition. At 900°C the Fe was not oxidized to magnetite and was catalytically active. At 800°C the Fe was oxidized to magnetite and exhibited essentially no

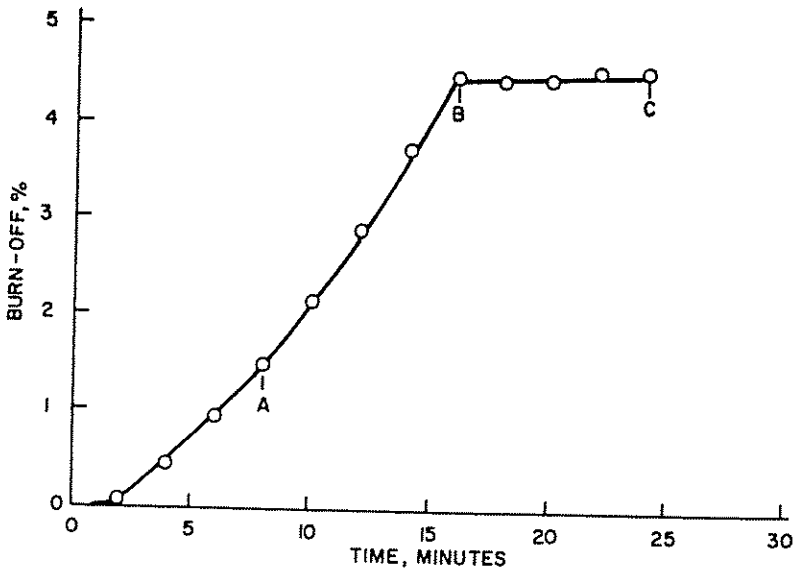

Fig. 23. Graphite reactivity at 850°C showing the result of catalyst deactivation.

activity as a catalyst at any point in the transition. At 850°C both situations occurred. During initial stages of Fe oxidation, the catalyzed gasification reaction proceeded readily; upon completion of Fe oxidation to magnetite, the catalyst simultaneously lost its activity. These results were the grounds for a more detailed investigation.

Figure 23 is constructed from data obtained by reacting a sample doped with ca. 300 ppm of 3-μ Fe at 850°C in CO_2. This experiment verifies the type of reactivity behavior previously observed at 850°C, although conducted in a slightly different manner. The usual methods for placing the sample in the furnace and removing it were used, but in this case the gasification rate was measured over longer periods of time with the sample in the furnace and suspended from the Sartorius balance. Points A, B, and C indicate the times at which the sample was removed

from the furnace for susceptibility measurements. The magnetization of the ferromagnetic phase measured at C following the unreactive run was 91, again agreeing well with the magnetization of magnetite. At A and B the magnetization relative to Fe, proportional to S_M/S_0, was 0.78, whereas Fig. 21 in conjunction with Fig. 22 indicates values of S_M/S_0 of 0.44 to 0.57 for the catalytically active phase at 850°C. These results are analyzed in Section III.D, but several direct observations can be presented now. A range of Fe oxide composition exists wherein some catalytic activity is exhibited. S_M/S_0 values greater than that for magnetite (i.e., >0.60) indicate the existence of some metallic Fe in the oxide. S_M/S_0 values less than that for magnetite suggest the inclusion of a relatively larger volume of wüstite but could be indicative of other phases as previously noted. Although in both cases catalytic activity was observed at 850°C, the relative magnitudes of graphite gasification incurred over a given time, as shown in Figs. 22 and 23, indicate that the more reduced phase ($S_M/S_0 > 0.60$) is the more active.

The second point of interest to be introduced here is that although nearly the same intermediate oxide phases apparently were formed at 800 and 850°C preceding oxidation to magnetite, catalyzed gasification was observed at 850°C, while the gasification rate at 800°C was extremely slow. The relative inertness of phases at 800°C, which were found active at 850°C, will also be the subject of later discussion.

The intermediate phase formed appears to be related to the extent to which the gasification reaction proceeds during a run. This implies th in addition to the varying activity of various phases previously suggested, the occurrence and extent of gasification may be a deciding factor in the stabilization of a given phase. This would occur by alteration of the composition of the gaseous atmosphere in contact with Fe and, therefore, the constitution of the Fe oxide phase. Where S_M/S_0 values lower than that of magnetite were found for intermediate phases, little or no gasification occurred during each treatment in CO_2; and the gaseous environment of the solid phases was probably different than where gasification was allowed to proceed to greater extents. The former situation occurred in the 800 and 850°C runs in Fig. 22. Similarly, S_M/S_0 values of 0.39 and 0.51 were found for intermediate phases in a sample containing ca. 300 ppm of 20-μ Fe when the Fe was gradually converted to magnetite by successive heating in CO_2 at 850°C with only 0.7% C burnoff occurring over 170 min. In all runs where more extensive gasification occurred during a given treatment, however, S_M/S_0 values greater than that of magnetite were found as has been pointed out in connection with Fig. 23.

The suggestion that a catalytically active phase was maintained by the very occurrence of the gasification reaction as well as the occurrence of the gasification reaction being dependent on the persistence of an active catalyst was examined experimentally. The following hypotheses were tested:

1. If the catalyzed reaction occurs, it should continue unimpeded at constant temperature without deactivation of the catalyst by oxidation to magnetite.
2. An active catalyst can be rendered inert by oxidizing the Fe to magnetite at low temperatures.
3. If a sample containing a catalyst, deactivated by preoxidation, is exposed to a reducing atmosphere the catalyst activity will be regenerated.

Results of testing the first hypothesis are given in Fig. 24, which also illustrates the effect of catalyst particle size and concentration on reaction rate and general reactivity behavior. In these runs the samples were placed in the CO_2 atmosphere at 900°C and allowed to react undisturbed for as much as 30%. The reactivity did not decrease but increased to a nearly constant value at about 20% burn-off. The 3-μ catalyst particles were found to be more active per unit concentration than the 20-μ particles. The 400-ppm concentration of 3-μ catalyst particles produced a higher rate than the 300-ppm concentration. S_M/S_0 values obtained at the completion of these reactivity runs were 0.76 and 0.77 for the two samples containing 3-μ particles and 0.70 for the one containing 20-μ particles, showing that oxidation to magnetite was not completed and that an appreciable fraction of metallic Fe was maintained.

The second hypothesis already appears well founded on the basis that samples could ultimately be rendered inactive under conditions where they had formerly been reactive by slow passage of the sample through the low-temperature region of the furnace into the reaction-temperature zone, the sample all the while being in CO_2. This procedure resulted in the formation of magnetite. As an additional test, the temperature was lowered during a reactivity measurement until reaction ceased. The temperature was then raised to the level where reaction had initially been observed. Figure 25 presents the results of this experiment, obtained with the sample containing 20-μ iron already discussed in connection with Fig. 24, and is plotted as a continuation of the per cent burn-off for Fig. 24. The initial reaction rate at 900°C was nearly constant but somewhat lower than the rate at the end of the previous run, possibly as a result of oxidation of some of the catalyst particles during placement of

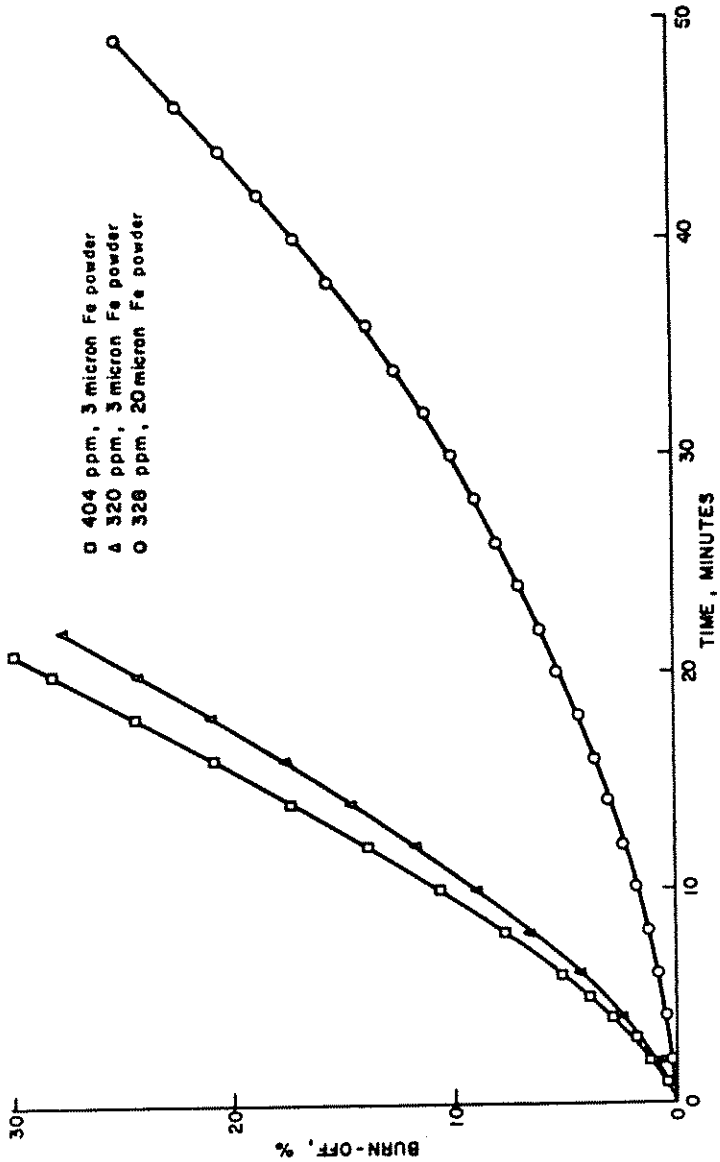

Fig. 24. Graphite reactivity at 900°C showing effect of particle size and concentration of catalyst.

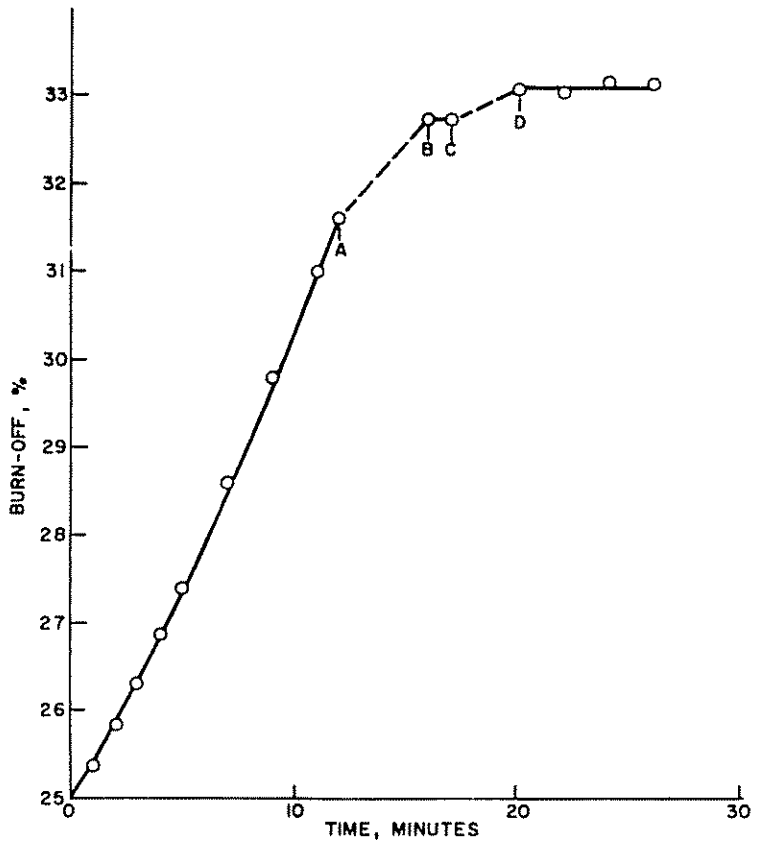

Fig. 25. Graphite reactivity at 900°C showing the result of catalyst deactivation.

the sample in the furnace. The time given is again exclusive of the time elapsed in lowering the sample to the constant-temperature zone. Between the origin and point A the sample was maintained at 900°C. Between points A and B the temperature was decreased from 900 to 850°C; from B to C the temperature was held at 850°C; between C and D the temperature was raised to the former level of 900°C and maintained there for the remainder of the run. During the transitions from A to B and C to D, the sample weight could not be measured accurately because of changes in buoyancy with temperature, but the loss of catalytic activity is apparent. The weight change in going from C to D is attributed wholly to the buoyancy effect, since at constant temperature of either 850 or 900°C

immediately before and after this transition no weight loss was observed. A specific magnetization of 87 measured at the conclusion of this run again indicates the presence of magnetite.

The persistence and noncatalytic behavior of magnetite at temperatures above that at which it was formed is illustrated by results from the sample containing 3-μ Fe, oxidized to magnetite at 800°C by the treatment shown in Fig. 21. Essentially no C gasification occurred during this catalyst transformation or in a reoxidation following reduction by CO at

TABLE V

Effect of H_2 and CO on Magnetite and Fe–C Phases

Initial phase	Initial S_M/S_0	Treatment conditions			Resulting S_M/S_0
		T, °C	t, min	Gas	
Fe_3O_4	0.58	850	10	H_2	0.89
Fe_3O_4	0.60	850	30	CO	0.78
Fe_3O_4	0.59	850	10	CO	0.72
Fe_3O_4	[a]	850	13	CO	0.87
Fe–C	0.87	850	10	H_2	0.92
Fe–C	0.80	800	30	CO	0.73

[a] This sample was initially doped with magnetite powder. In other cases magnetite was formed in situ by oxidation of Fe or Fe–C alloy with CO_2.

800°C. A 30-min treatment in CO_2 at 850°C did not produce appreciable C gasification subsequently, nor did a 15-min treatment at 900°C. The magnetization remained constant at 94, showing that no magnetite reduction resulted from these treatments. Only when the catalyst was reduced by CO at 900°C did gasification subsequently take place. This type of catalyst activation is the next subject for consideration.

Hypothesis 3 regarding catalyst regeneration under reducing conditions was verified in several ways. Specific magnetization changes resulting from treatment of samples in H_2 and CO were first determined. Table V also contains data on a carburized catalyst for comparison with the oxidized catalysts. Both H_2 and CO were effective in partially reducing magnetite to metallic Fe, as shown by the increased magnetization after heat treatment. This was true of magnetite that had been added to the graphite directly as well as the oxide formed from Fe in the oxidizing CO_2 atmosphere. It is possible that complete reduction was effected and that

the magnetization following treatment in H_2 or CO represents an Fe–C phase.

The austenite–cementite phase existing at steady state at 850°C was affected by H_2 to a much smaller degree than magnetite with some decarburization apparently occurring. A second treatment under the same conditions produced no further change. At 800°C the magnetization of the austenite–cementite phase was decreased by CO treatment in contrast to the increase observed with magnetite. The decrease probably indicates that the Fe was carburized to a higher level by CO than by direct reaction with graphite, presumably by affecting the relative rates of cementite formation and decomposition. Smith (*104*) gives equilibrium data for Fe carburization in CO—CO_2 atmospheres.

Having shown that magnetite is readily reduced by H_2 and CO, the effectiveness of these reactions in regenerating catalyst activity was next examined. The reactivity of the first sample listed in Table V was found to be revived following the reduction of magnetite by H_2. Reaction was carried out to about 20% burn-off at 850°C over a period of 50 min with no anomalous reactivity behavior being exhibited. In a second treatment in CO_2 at 850°C using normal procedures, this sample was found to be unreactive with the catalyst reoxidized to magnetite.

Figure 26 represents typical results from runs in which the deactivated catalyst was treated with CO and the subsequent reactivity measured. This sample had initially been found to be reactive at 850°C and was about 24% reacted before the catalyst was deactivated by oxidation to magnetite by passage through the low-temperature zone of the furnace. The magnetization of the oxide phase thus formed was 83, the relatively low value indicating either the presence of some wüstite or an error in concentration as discussed in the experimental procedure. The sample containing this deactivated catalyst was placed in the furnace at 850°C and held for 5 min (A to B) in CO_2 during which no reaction was observed. The CO_2 gas flow was replaced with CO for the next five min (B to C), after which CO_2 was readmitted and the CO flow stopped (point C). The resultant high reactivity in CO_2 following point C is apparent from Fig. 26. Following this run the catalyst was again oxidized to magnetite in a subsequent treatment in CO_2 with consequent loss of catalytic activity.

Results in Fig. 27 were then obtained with the same sample at 850°C. The sample was lowered into the furnace and maintained for 5 min in a He atmosphere, after which CO_2 was admitted and the He flow stopped (point A, Fig. 27). This treatment resulted in catalyst reactivation, apparently by direct reduction of the Fe oxide by graphite, with over 4%

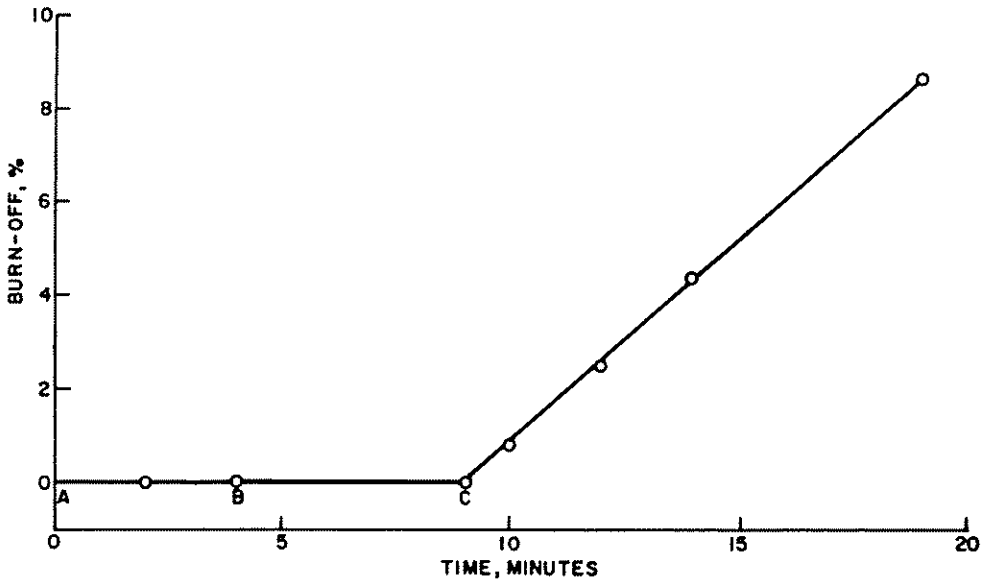

Fig. 26. Graphite reactivity at 850°C showing effect of CO regeneration of the active catalyst.

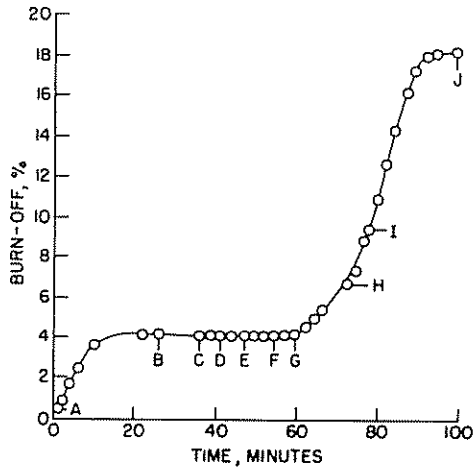

Fig. 27. Graphite reactivity at 850°C showing effect of CO_2—CO mixtures on catalyst activity.

burn-off occurring between A and B. However, after a short time the rate of C gasification decreased and reaction finally ceased, at B. A second 10-min treatment in He (B to C) was not effective in reviving the reactivity, no burn-off being observed from C to D. At this point a total of about 38% of the graphite had been previously gasified, so that catalyst–graphite contacts may have been somewhat reduced and direct reduction of the Fe oxide thereby rendered more difficult. Since reduction by CO gas should not be limited by this consideration, catalyst reactivation should be possible. The remainder of this run shows that this was so. The CO_2 flow was maintained at a diminished rate as CO was admitted in successively higher concentrations. The following concentrations of CO were maintained between points demarked on Fig. 27: D to E, 15%; E to F, 54%; F to G, 66%; G to H, 82%; H to I, 42%; I to J, 0%. With a gas composition of 82% CO–18% CO_2, the gasification reaction was resumed. This phenomenon is especially interesting in view of the known inhibiting effect of CO on the uncatalyzed C–CO_2 reaction (*1*). Gasification continued with the CO concentration reduced to 42%, but shortly after returning to 100% CO_2 the reaction again ceased. Because of the exceedingly large total burn-off, this sample disintegrated before magnetic susceptibility measurements could be made. In view of all previous results and the phenomena observed here, however, there is little doubt that the catalytically inactive phase was magnetite.

In two cases catalyst activation was observed in the CO_2 atmosphere. The catalysts had been carburized initially by heating at 1300°C in He for 50 hr in one case (A) and 15 hr in the other (B). Sample A was subsequently heated at 900°C in CO_2 for 90 min during which only 0.5% carbon burn-off was observed; the catalyst was converted to magnetite. The sample was then replaced in the furnace at 950°C in CO_2 with only 0.7% burn-off occurring in 90 min at this temperature. Raising the temperature in 25°C increments did not appear to increase the catalytic activity at 975 or 1000°C. At 1025°C an induction period of about 22 min was followed by a sudden increase in gasification rate of tenfold over that observed in the induction period.

Sample B was found to be highly reactive when placed in CO_2 at 950°C, but reaction was quenched by lowering the temperature to 820°C and maintaining the CO_2 atmosphere. Increasing the temperature subsequently to 950°C in CO_2 and maintaining these conditions for 11 hr did not revive the catalytic activity. Increasing the temperature subsequently to 1000°C, however, resulted in a rather sudden increase in gasification rate by a factor of 5 after an induction period of about 30 min.

Results similar to those observed above have been reported by Rakszawski (*41*) and were attributed to decarburization of the Fe catalyst by CO_2. This is obviously not the case here since the Fe–C phase had been readily oxidized to magnetite at lower temperatures. As in all previous cases cited in this study, catalyst activation is evidently the result of reduction of the magnetite phase. S_M/S_0 was 0.24 for sample B following reaction at 1000°C, indicating a largely wüstite phase. Because the

TABLE VI

Oxidation of Precarburized Catalysts

Carburization temp., °C	Oxidation temp., °C	Resultant magnetization
1300	850[a]	88
1300	850	98
1300	850	94
1300	850	82
1300	900[b]	99
850	850[a]	80
850	850[a]	83
850	850[a]	85

[a] This sample was reacted in CO_2 at oxidation temperature before oxidation of the Fe to magnetite was completed by subsequent treatment in CO_2.

[b] This sample was heated in H_2 for 1 hr at 1000°C after carburization and before oxidation.

inherent graphite reactivity becomes appreciable in this temperature range, the concentration of CO will increase in the sample resulting in reduction and activation of some of the catalyst particles. This in turn produces more CO and rapid activation of more oxide particles, resulting in the observed sudden increase in gasification rate.

The effect of a CO_2 atmosphere on the composition of the Fe–C phase formed by heating the Fe-doped graphite samples at 1300°C in He has been introduced above. The conversion of the Fe–C phase to an Fe–O phase was typical behavior, as evidenced by the data in Table VI. The magnetite phase formed by oxidation of precarbided or precarburized Fe particles was similar in all respects to that formed directly in un-heat-treated samples. Thus formation of this phase again was found to render the catalyst inactive. Once formed it remained stable at higher temperatures in CO_2. It could be reduced either by H_2 or CO and subsequently reoxidized by CO_2.

Referring again to the data in Table VI, it is noted that in all cases but one, samples originally heated at 1300°C were unreactive at 850 and 900°C, whereas when carburization was accomplished at 850°C, the samples were initially reactive. The one sample carburized at 1300°C that was reactive (the first sample in Table VI) had been heated only 1 hr; heating times for the other samples ranged from 20 to 60 hr. Loss of some Fe as a result of the extended heating times at 1300°C was noted and undoubtedly should be accompanied by a decrease in catalytic activity, but complete deactivation is not expected. It is believed that agglomeration of the catalyst particles during heating at 1300°C is an additional cause of catalyst deactivation. Twenty-micron Fe powder has been shown to be less active per unit concentration than 3-μ powder. Moreover, while 3-μ particles catalyzed the gasification reaction at 850°C, 20-μ particles did so only at 900°C and were merely oxidized to magnetite at 850°C. This behavior is strikingly similar to that of the Fe carburized at 1300°C for long periods of time. The fact that the catalyzed gasification for the 1300°C samples occurred at 950°C and conversion to magnetite without C gasification occurred as high as 900°C suggests that the agglomerated particle size probably exceeded 20 μ.

The reactivity of samples containing ca. 300 ppm of 3-μ Fe carburized to varying degrees was determined at 850°C. The results presented in Fig. 28 reveal no significant difference in general reactivity behavior or reaction rates between heat-treated samples and the un-heat-treated sample, regardless of the extent of carburization. The concentration of C in the catalyst phase was estimated for the samples represented by the open circle and open triangle in Fig. 28 by analogy with previously observed carburizing behavior at 850°C (Fig. 20). The C concentration for the sample represented by a cross was determined magnetically and is the steady-state C concentration at 850°C. The closed circle sample was maintained in a CO_2 atmosphere at all times during placement in the furnace and reaction in order to preclude carburization of the catalyst. The open-square sample, unlike the previous four, had been preheated at 1300°C for 1 hr; and although the C concentration was quite similar to that of the sample carburized to a steady state at 850°C, the reaction rate was somewhat lower. The lower rate probably resulted primarily from agglomeration of catalyst particles at this higher heat-treatment temperature.

In an independent (although less direct) check on the oxide-phase identification made by magnetic analysis, a mixture of 20%, 3-μ Fe powder and 80% SP-1 graphite was prepared and pelletized. Two samples

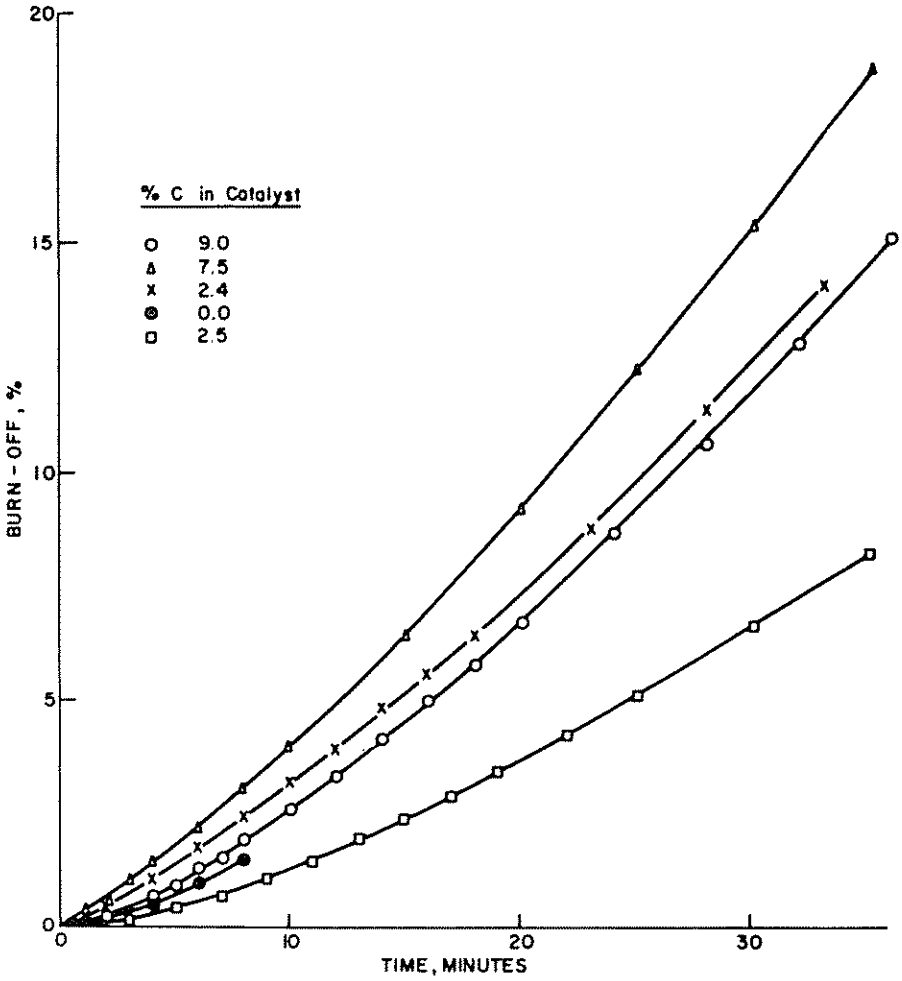

Fig. 28. Graphite reactivity at 850°C showing effect of different precarburizing treatments on subsequent rates.

were obtained and subjected to treatment in CO_2. Afterward the samples were reground and examined by X-ray diffraction. In one case the sample was rapidly reacted at 850°C, and then the temperature was lowered to 750°C, where the gasification rate approached zero. The rate of C burn-off was about six times faster than for samples containing ca. 300 ppm of Fe at 850°C. As soon as the 750°C temperature was attained, the sample

was rapidly cooled to room temperature in He. Only metallic Fe and wüstite were identified. The interpretation of these results is that the catalyst was maintained in a primarily metallic state during reaction at 850°C, and that oxidation of the catalyst probably started at 750°C. This description is qualitatively the same as that given for oxide formation in Fig. 21, where a partially metallic phase was maintained during reaction at 900°C but oxidation of the Fe occurred at 800°C without the occurrence of graphite gasification. Some variation of the conditions under which these phenomena occur may be expected because of the vastly higher catalyst concentration used in the present experiment.

Heat treatment of the other sample was started at 750°C and a gain in weight was observed, indicating formation of an Fe oxide. The temperature was decreased to 700°C before cooling to room temperature in an effort to ensure that C gasification was a minimum and not being masked by weight changes occurring because of Fe oxidation. Total treatment time was 35 min. X-ray diffraction peaks were obtained only for magnetite, no peaks being observed for wüstite or Fe. Although this high Fe concentration may not be completely analogous to the systems containing a few 100 ppm of Fe, this added evidence once again confirms that oxidation of Fe to magnetite can occur at relatively low temperatures in CO_2 without incurring graphite gasification.

4. Relative catalytic activities of Fe, Co, and Ni

Samples were prepared as described in Section III.B.2. The impurity level of each additive was kept constant at 300 ppm of 10-μ material. Figures 29–31 present results for the reaction of graphite with CO_2, as affected by the presence of Fe, Co, and Ni. In most cases, the gasification rate (i.e., the slope of the plots) increased initially up to ca. 15% burn-off and the rate then remained constant over a considerable additional burn-off range, the extent of this range depending upon the temperature and catalyst employed. The increase in gasification rate over the low burn-off range has been considered at length by Walker and co-workers (*105*,*106*); it is generally attributed to some initial increase in surface area of the sample to a more or less steady-state value. First, it is to be emphasized that Fe, Co, and Ni are all very active catalysts. That is, the gasification rate of the pure graphite in CO_2 at 1000°C, in the constant burn-off region, is only 0.008% burn-off/min (*41*). The overall E for the gasification of the pure graphite in the temperature range studied here is ca. 87 kcal/mole (*8*).

The leveling off of the curves, after some period of constant gasification rate, was most pronounced for the samples containing Fe. It is significant

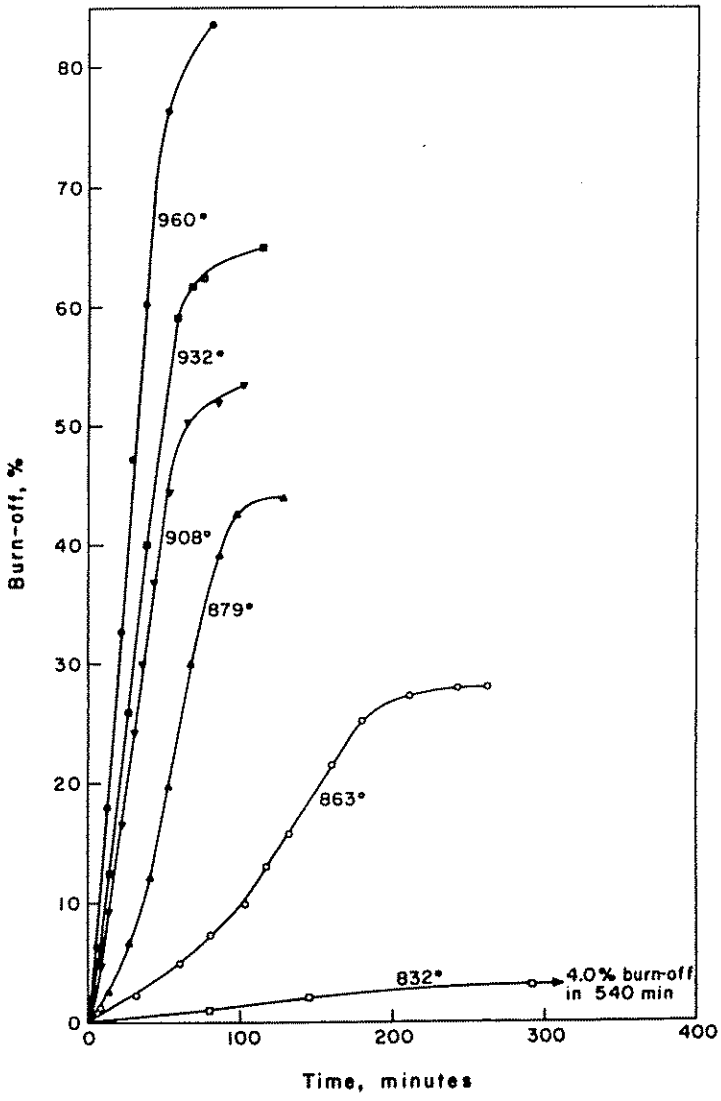

Fig. 29. Reactivity plots for graphite doped with 300 ppm of 10-μ Fe powder.

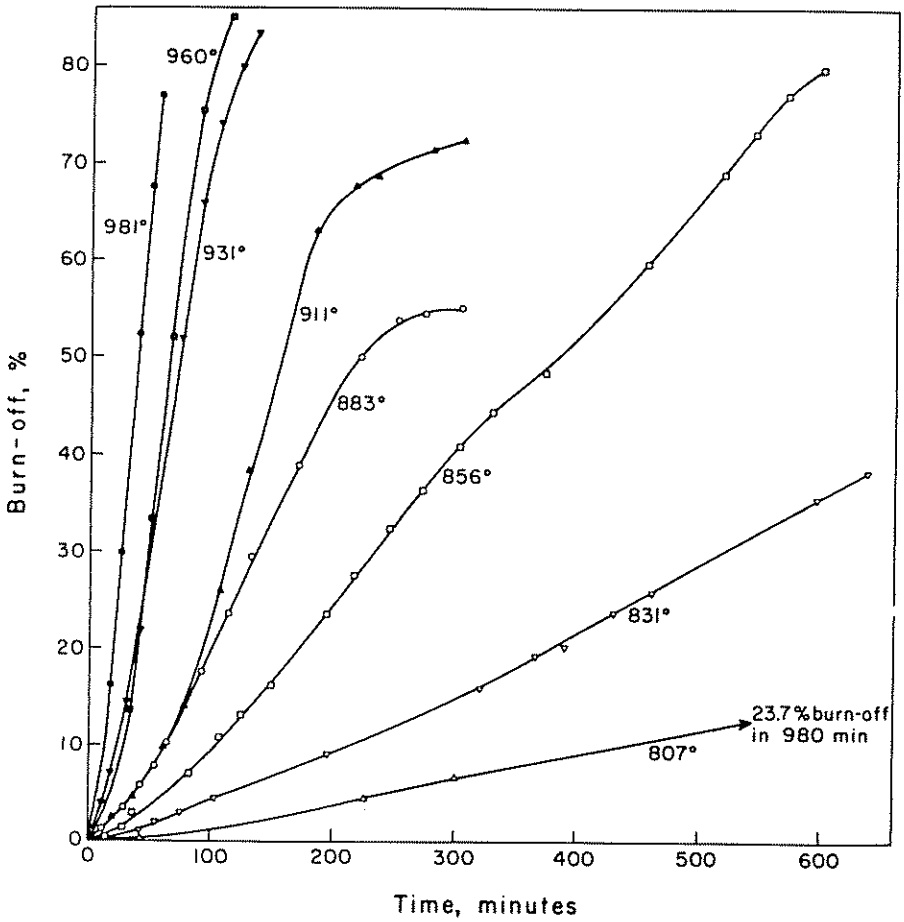

Fig. 30. Reactivity plots for graphite doped with 300 ppm of 10-μ Co powder.

that Fe was the most active catalyst in the region of constant-gasification rate before this leveling off of rate, or catalyst deactivation, occurred. With increasing temperature, the fall-off of the gasification rate occurred at shorter times but due to the faster reaction rate the burn-off achieved was higher.

For Co, catalyst deactivation was clearly evident for gasification temperatures of 883 and 911°C, but deactivation commenced at burn-offs significantly higher than in the case of the Fe catalyst. At gasification temperatures of 931°C and higher, little evidence of catalyst deactivation

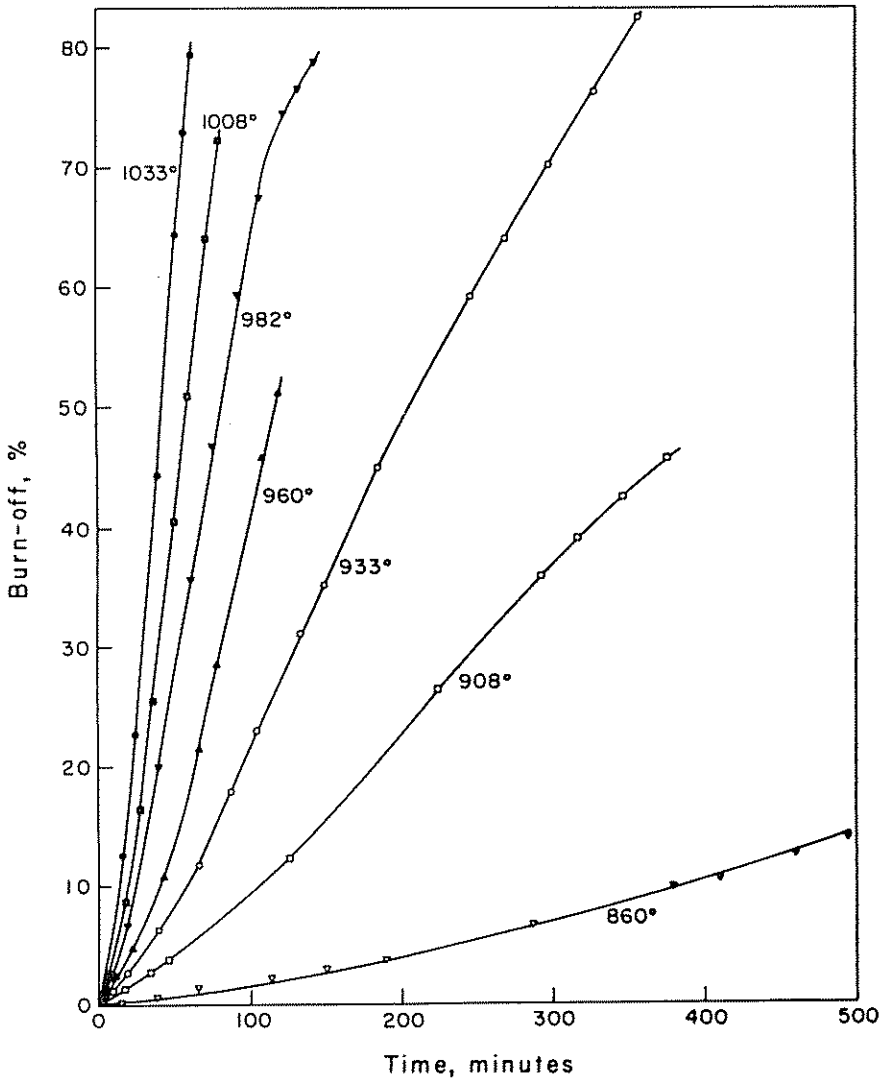

Fig. 31. Reactivity plots for graphite doped with 300 ppm of 10-μ Ni powder.

is seen. For burn-offs greater than ca. 75%, a slowly decreasing gasification rate is attributed to a concurrent decreasing total surface area available for reaction (*106,107*). Therefore, at these higher burn-off levels the slowly decreasing gasification rates, as observed, are not thought to be associated primarily with catalyst deactivation.

The activity of the Ni catalyst, which was the lowest of the three elements, was not significantly impaired over the entire temperature range studied, 884–1033°C.

As first discussed in Section III.C.3, the Fe catalyst could be reactivated by H_2, CO, or by bringing the sample to a sufficiently high temperature. Figure 32 shows a run where gasification was started at 867°C for a sample containing 300 ppm of 10-μ Fe. Significant catalyst deactivation occurred after only ca. 5% burn-off. Exposure of the sample to CO for 20 min resulted in marked catalyst reactivation. Subsequent catalyst deactivation, following burn-offs to 45 and 53%, were reversed by H_2 and CO treatments, respectively. Subsequent catalyst deactivation at 60% burn-off was reversed by raising the reaction temperature to 961°C.

The gasification rates in the constant-rate region, taken from Figs. 29–31, are shown on Arrhenius plots in Fig. 33. The interpretation of these plots is complicated by the catalyst deactivation phenomenon occurring simultaneously with gasification. That is, the high E in the dashed regions shown for the Fe- and Co-containing samples are thought to be anomalous. The Arrhenius plot for gasification of the Ni-containing sample (in which catalyst deactivation was not observed) appears more reasonable. It is suggested that an E of 76 kcal/mole is applicable to the chemical control region (zone I), the E being less than the E for gasification of the high-purity graphite in zone I. The fall-off in E at higher temperatures is attributed to partial internal diffusion control becoming operative (*1*). An E of 52 kcal/mole for gasification of the Co-containing sample over the temperature range 856–981°C may be representative of the temperature dependence in zone I. The E of 38 kcal/mole for the Fe-containing samples over the temperature range 879–960°C is thought to be representative of the temperature dependence close to zone II. It suggests that the true E in zone I for gasification of the Fe-containing samples is close to the E for gasification of the Ni-containing samples (that is, 2×38 or ca. 76 kcal/mole). It is to be emphasized again, however, that interpretation of Arrhenius plots for gasification of graphite samples containing significant concentrations of added impurities is difficult. Catalyst deactivation, agglomeration of catalyst particles (*18*), and in some cases production of a liquid catalyst upon its oxidation (*18*) (for example,

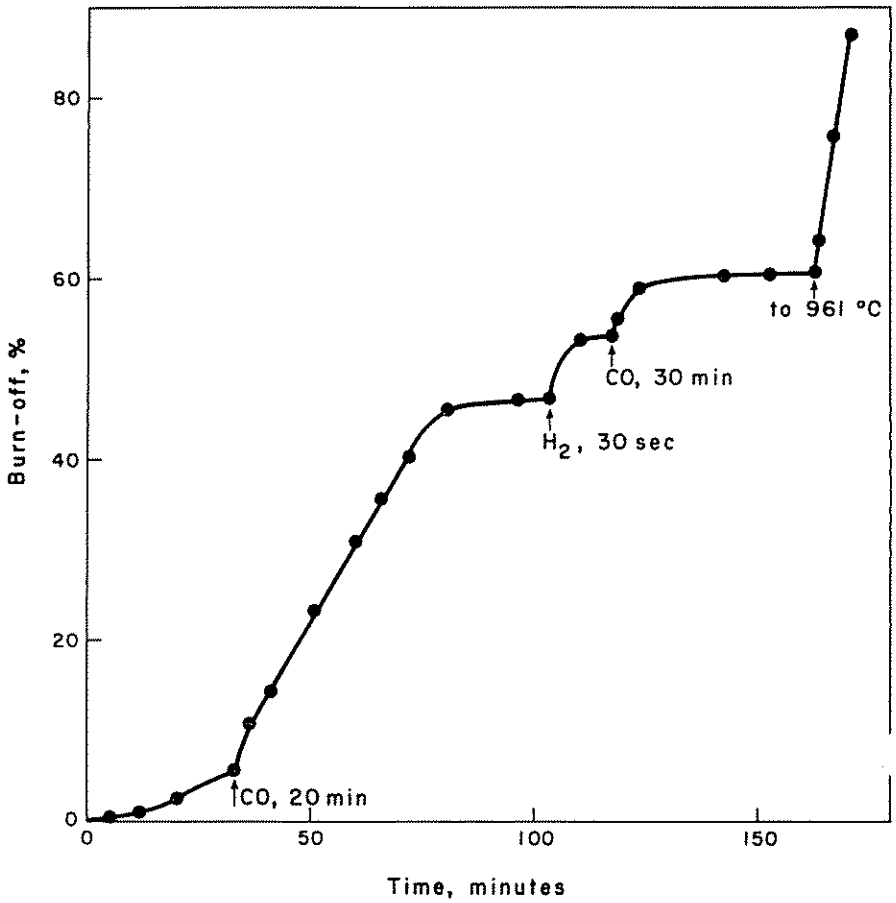

Fig. 32. Reactivation of Fe catalyst for C—CO_2 reaction at 867°C upon its reduction by CO, H_2, and carbon.

V_2O_5, MoO_3, and B_2O_3) make reliable interpretation of the dependence of gasification rates on temperature most questionable.

D. Discussion

1. Catalyzed versus uncatalyzed gasification reactions

It is of interest that the effect of the products in the C—CO_2 and C—H_2O reactions on gasification rate is markedly dependent upon whether we are primarily observing the uncatalyzed or catalyzed reaction. In the

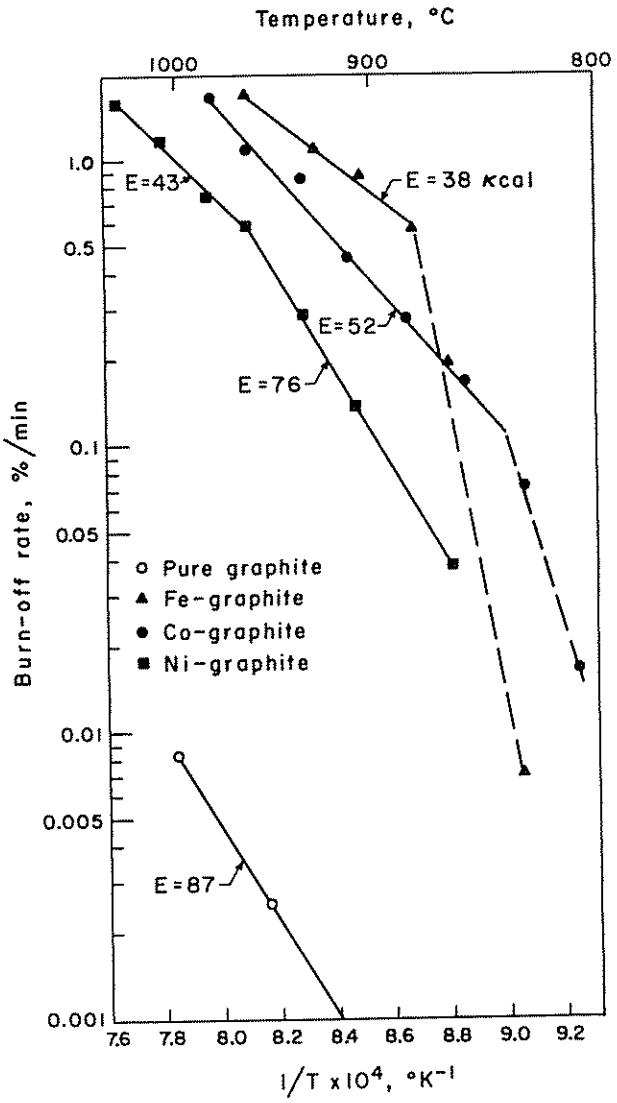

Fig. 33. Arrhenius plots for gasification of pure graphite and samples containing Fe, CO, and Ni in CO_2.

case of the uncatalyzed reaction, the reaction products CO and H_2 are marked inhibitors to gasification (*1*). This inhibition is attributed to a reduction in the steady-state concentration of oxygen complex which breaks down to product, either by the product reacting with the complex to produce the reactant or by the product chemisorbing and blocking active sites for the reaction. In the case of the catalyzed reaction, it is seen that the reaction products effectively serve as accelerators (using the usual catalysis nomenclature). That is, their presence in sufficient amounts maintains the catalyst in a more reduced and active state.

There is another interesting difference between the uncatalyzed and catalyzed gasification reactions. In the uncatalyzed C—O_2 reaction, as discussed by Austin and Walker (*108*), nonuniformity of gasification through a porous carbon body is to be expected even at low reaction rates because of the strong inhibiting effect of CO. Since the concentration of the CO will go from a maximum at the center of the body to a minimum at the outer surface, the gasification rate will go from a minimum at the center of the body to a maximum at the outside. Thus following some total overall gasification, the body would show a nonuniform density profile—highest density at the center and lowest density at the outer surface. In our present studies on the catalyzed C—CO_2 reaction, a different situation was sometimes found. Following gasification of the graphite cylinders to relatively high burn-offs, the inner portion was porous and friable (of low density). This inner portion was surrounded by a coherent outer shell which apparently had undergone little or no reaction. This outer shell was in contact with the highest CO_2 concentrations, which would tend to produce and maintain the noncatalytic magnetite phase. CO concentrations would be highest at the inner portions of the cylindrical sample, tending to maintain a less oxidized and more catalytically active phase there. Emission spectrographic analysis showed that the inertness of the outer shell was not caused by loss of Fe. Over a period of years, the presence of an apparently unreacted outer shell has been observed many times in this laboratory following the partial gasification of reasonably impure artificial electrode graphites.

2. Thermodynamic considerations

It was clearly shown in Figs. 29–31 that the Fe catalyst is much more susceptible to deactivation than is the Co catalyst, which in turn is more susceptible to deactivation than is the Ni catalyst. To the extent that oxidation of the metal results in catalyst deactivation, the results are

TABLE VII

Standard-State Free Energies of Formation of Compounds in Reactions (a)–(c), kcal/mole

Temp., °K	NiO	CoO	$Fe_{0.95}O$	CO	CO_2
1000	−35.70	−39.75	−47.35	−47.86	−94.63
1100	−33.60	−38.10	−45.70	−49.96	−94.66
1200	−31.60	−36.45	−43.95	−52.05	−94.68
1300	−29.55	−34.65	−42.35	−54.13	−94.70

predictable on thermodynamic grounds. Consider the reactions

$$Ni + CO_2 \rightarrow NiO + CO \quad (a)$$

$$Co + CO_2 \rightarrow CoO + CO \quad (b)$$

$$0.95Fe + CO_2 \rightarrow Fe_{0.95}O^* + CO \quad (c)$$

Table VII summarizes data for the standard-state free energy of formation of the compounds in the above reactions taken from (*110–112*). Using these data, equilibrium constants can be calculated for the reactions. Table VIII summarizes the per cent CO in the equilibrium mixture, calculated from the equilibrium constants, also given in Table VIII. Calculations

TABLE VIII

Equilibrium Constants and Equilibrium CO Concentrations for Reactions (a)–(c)

	Reaction (a)		Reaction (b)		Reaction (c)	
Temp., °K	K_p	% CO	K_p	% CO	K_p	% CO
1000	3.60×10^{-3}	0.359	2.91×10^{-2}	2.88	1.72	63.3
1100	6.20×10^{-3}	0.556	4.88×10^{-2}	4.65	2.13	68.1
1200	9.75×10^{-3}	0.965	7.46×10^{-2}	6.95	2.58	72.0
1300	1.39×10^{-2}	1.377	1.01×10^{-1}	9.15	2.77	73.4

* In this chapter so far, we have referred to wüstite as FeO for simplicity. In fact, even though wüstite exhibits a wide homogeneity range, the stoichiometric composition, FeO, is unstable (*109*). In equilibrium with Fe, the composition of wüstite above 800°C corresponds closely to $Fe_{0.95}O$.

show that an amount of CO in the gas mixture of the order of 1% is sufficient, in the temperature range investigated, to maintain Ni in the metallic state. This amount is probably always exceeded as a result of carbon gasification in the interior of the sample, even when pure CO_2 is flowing over the sample. Thus deactivation of the Ni catalyst is not expected. Data in Table VIII show that Co is more susceptible to deactivation by oxidation in CO_2 than is Ni. Experimentally, as is seen in Fig. 30, deactivation of Co is evident at reaction temperatures of 883 and 911°C. At the lower and higher reaction temperatures studied, no deactivation (as indicated by a sharp decrease in gasification rate) is evident. At temperatures below 883°C, either sufficient CO was produced by carbon gasification to maintain the Co in a reduced state or the rate of Co oxidation is sufficiently slow to not be able to observe its deactivation over the time period studied. At temperatures above 911°C, it is thought that sufficient CO is produced by carbon gasification to maintain the Co in a reduced state. The equilibrium amount of CO produced by the C—CO_2 reaction at 1200 and 1300°K is considerably in excess of the amount of CO required to maintain Co metal (*1*).

As is seen from Table VIII, large concentrations of CO are required to prevent the oxidation of Fe to wüstite. These data for Fe and also equilibrium data for the oxidation of Fe_xO to Fe_3O_4, taken from Fast (*109*), are summarized in Fig. 34. The equilibrium for the oxidation of Fe_3O_4 to Fe_2O_3 does not appear on Fig. 34, since it lies so far on the CO_2 side that the curve representing it almost coincides with the upper horizontal axis. That is, thermodynamically, Fe_2O_3 is not expected to be formed under the conditions used in this study. Over the temperature range 1000–1300°K, the equilibrium amount of CO in the oxidation of wüstite to Fe_3O_4 decreases from 31.7 to 15.0%. Clearly, with increasing reaction temperature, the catalyst is less likely to be oxidized to Fe_3O_4 both because less CO is needed to maintain Fe in a less oxidized state and because increasing amounts of CO will be produced by carbon gasification.

3. Probable catalytic iron phases

The successful use of magnetic susceptibility measurements to follow changes in the chemical form of Fe dispersed in graphite during gasification of the graphite has been demonstrated in this study. The method is not without its shortcomings, however, as we will discuss presently.

Clearly magnetite is not an active catalyst for the C—CO_2 reaction. Consistently, when reactivities decreased to low values immediately

following relatively high gasification rates magnetite was identified (see the 850°C runs, Figs. 22 and 23, for example).

It is concluded that hematite is not an active catalyst for the C—CO_2 reaction. Evidence is not as direct to substantiate this conclusion, since magnetite susceptibility cannot be used to identify the paramagnetic hematite. However, as described earlier, in one run 300 ppm of hematite

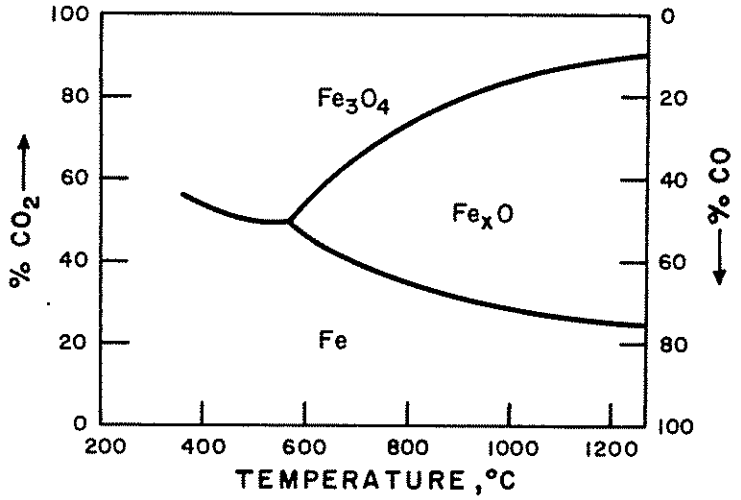

Fig. 34. Oxidation and reduction equilibrium of Fe and Fe oxides with mixtures of CO and CO_2. [From Fast (*109*).]

was added to the graphite. In CO_2 at 850°C for 20 min, negligible gasification was observed. Further, there was no progressive decrease in gasification as the hematite was converted to magnetite. The question of the catalytic activity of hematite for the C—CO_2 reaction is academic in any case, since it is thermodynamically not favored.

If it is agreed that hematite is not an active catalyst, and indeed not even stable under the conditions of this study, then it is concluded that Fe particles of an intermediate oxidation state between Fe and magnetite have some catalyst activity. That is, catalysis of the C—CO_2 reaction is observed when the specific magnetization of the Fe phase is less than that of magnetite (see the 850°C run, Figs. 21 and 22, for example). As indicated previously, the specific magnetization of the Fe phase could be reduced below that of magnetite by the presence of hematite and/or wüstite. Since hematite is catalytically inactive, it is concluded that Fe particles containing some wüstite are still catalytically active.

At this point it is well to reflect on what information the magnetic susceptibility measurement is giving us and what pertinence it may have in the case of the gasification of a porous carbon. The measurement reflects an average situation of the state of the Fe particles within the graphite matrix. However, the Fe particles may exist in varying states of oxidation depending upon their radial location within the graphite cylinders. Their oxidation state can be highest at the outside of the cylinder and lowest at the center of the cylinder because of nonuniformity in the CO_2/CO ratio. A result of this is the observation of an unreacted outer graphite shell surrounding an inner reacted graphite core, as described previously. However, a varying CO_2/CO ratio in the radial direction will not necessarily mean that the state of oxidation of the Fe particles in the radial direction will be nonuniform. This is because there are wide limits of the CO_2/CO ratio over which the oxide phases are stable. For example, magnetite is stable at 800–900°C for CO_2/CO ratios ranging between ca. 3 to 3×10^4. Thus nonuniformity of oxidation of Fe particles in the radial direction would be expected during the unsteady-state period, for example, while particles of Fe are being oxidized to magnetite, but probably uniformity of oxidation of the Fe particles in the radial direction is expected once the Fe particles have obtained their equilibrium condition.

While oxidation or reduction of the Fe particles is occurring, a particle itself will not be in a uniform state of oxidation. For example, in the oxidation of Fe to Fe_3O_4, discrete phases of Fe, wüstite, and Fe_3O_4 will be observed from the center to the outside of the particle (*113*). Hence, again during the unsteady-state period (or the period of oxidation or reduction of the Fe particles) the magnetic susceptibility measurement represents an average value for the phases present.

In this regard, it is of interest to focus our attention once again on Figs. 21 and 22. Consider the 850°C run. Susceptibility results indicate that after 30 min in CO_2 the Fe particles have almost been oxidized to Fe_3O_4. Certainly the majority of the Fe particles would be expected to consist of a thick outer layer of Fe_3O_4 surrounding an inner layer of wüstite. Despite this, the Fe particles remained as somewhat active catalysts between 30 and 50 min, at which time an *abrupt* decrease in catalytic activity occurred. Other examples of very abrupt changes in catalytic activity were observed in Figs. 23, 25, and 27. Thus it is concluded that an Fe particle has some catalyst activity as long as it is not completely oxidized to Fe_3O_4, even though the Fe_3O_4 phase is present on the exterior of the particle.

As evident from the results and discussion to date, the catalytic activity

of wüstite needs further clarification. Correlation of reactivity with magnetic susceptibility data indicates that wüstite does have some catalytic activity. On the other hand, results presented in Fig. 27 appear to contradict this conclusion. That is, even though up to 66% CO was introduced into the gas mixture at 850°C, reactivation of the Fe catalyst was not achieved. At this concentration of CO, wüstite is the stable phase. Introduction of 82% CO, where Fe is the stable phase, did reactivate the catalyst. That the results reflected rate and not equilibrium considerations, however, is suggested by the fact that the subsequent decrease in CO concentration to 42% (where wüstite is the stable phase) resulted in continuing catalyst activity.

Figure 35 presents reactivity runs for SP-1 graphite containing 300 ppm of 3-μ Fe. The samples were prepared some $2\frac{1}{2}$ years prior to the reactivity runs, and hence some surface oxidation of the Fe particles may have occurred over this time period. These runs were performed in a static reactor at starting CO_2 pressures between 600 and 630 torr. Prior to reactivity studies at 862°C, the samples were pretreated in vacuo ($<10^{-6}$ torr) for various times and temperatures above 1000°C to more or less reduce the Fe by reaction with carbon. The sample gasified in initially pure CO_2 reacted at a constant rate up to ca. 47% burn-off. The rate then very abruptly decreased to a low value. At 47% burn-off the CO concentration in the reacting gas would be ca. 7%; at this concentration Fe_3O_4 is the equilibrium oxide phase and presumably was formed. The sample gasified in a gas mixture containing 22.5% CO initially also reacted at a rapid rate up to ca. 47% burn-off before undergoing an abrupt and large rate decrease. At the initial CO concentration of 22.5%, Fe_3O_4 is the equilibrium oxide phase at 862°C. However, at 47% burn-off the CO concentration in this reacting gas would be ca. 30%, or wüstite would now be the stable oxide phase. Either Fe_3O_4 which was formed in the initial part of the run was not reduced to wüstite over the latter period of the run (which seems unlikely considering the extended duration of the run) or this is direct confirmation that wüstite is a much poorer catalyst than metallic Fe. It should be emphasized again, though, that catalyst deactivation occurs very suddenly in spite of the fact that oxidation of Fe to wüstite is presumably occurring over most of the burn-off range up to 47%. This will be considered later. The samples gasified in a gas mixture containing 37.5% CO, initially, react at a rapid rate up to 75% burn-off, and then gradually decrease in rate. The concentration of CO in the gas mixture at 87% burn-off would be ca. 50%; that is, wüstite was the equilibrium oxide over the entire burn-off range. The Fe was apparently not entirely

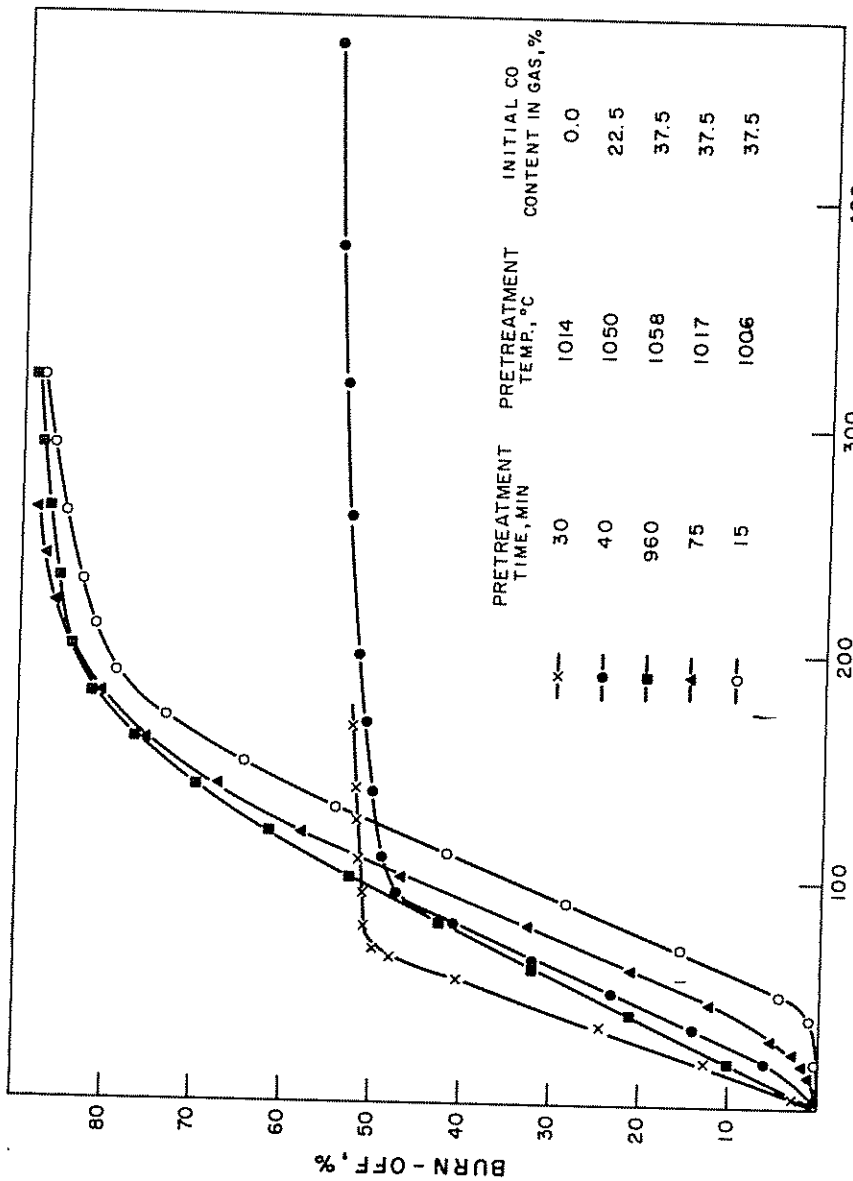

Fig. 35. Reactivity plots for graphite doped with 300 ppm of 3-μ Fe powder at 862°C in various CO/CO_2 mixtures.

converted to wüstite over most of the gasification run, however, possibly because of a diminished oxidation rate at the lower CO_2 concentration.

When previously considering the Arrhenius plots for carbon gasification, Fig. 33, it was concluded that the Fe-catalyzed reaction between 879 and 960°C was occurring in zone II. The reaction would be expected to continue in zone II to somewhat lower temperatures provided the Fe catalyst remained active. It is felt that the abrupt decreases in gasification rate, noted in Fig. 35 can be explained on this basis. As previously discussed in detail (*1*), gasification in zone II means that the concentration of the reacting gas decreases to its equilibrium value (or close to zero in this case) at some point between the outer surface and interior center line of the sample. If the reaction is well into zone II, the concentration will go to a low value close to the outside surface. Consider now the gasification run for the sample reacted in initially pure CO_2. As reaction proceeds, the Fe catalyst in the reaction region is oxidized and deactivated. The result is that the reaction region progressively moves in toward the center of the sample, with the overall reaction rate remaining constant. It is suggested that between ca. 47% and 51% burn-off the Fe in this last reaction region (that is, its inner boundary is the center line of the sample) is oxidized sufficiently to deactivate it. This oxidation appears rapid, because the reaction region is thin, and there is, consequently, relatively little Fe to oxidize.

It is felt that the abrupt increase in rate at the beginning of some gasification runs (Fig. 35, for example) can be explained in a similar manner. A pretreatment time of 15 min in high vacuo at 1006°C was apparently insufficient to reduce the Fe to a very active state. Upon exposure of the sample to the CO_2/CO mixture, sufficient additional CO was produced initially by gasification that reduction of the Fe at the center of the sample occurred. The process is autoaccelerating in that reduction of Fe would still further increase the gasification rate, providing more CO and leading to continued production of the Fe progressively closer to the outside of the sample. A constant high rate would result when a reaction region of constant thickness (as discussed above) developed.

The catalytic activity of wüstite can be determined by measuring gasification rates for prolonged periods following the abrupt decrease in rate provided the original gas mixture is selected so that wüstite is the thermodynamically stable phase. A starting gas mixture containing between 25 and 37.5% CO at 862°C is suitable for this purpose. Figure 36 presents the results of two runs. In runs A and B 300 ppm of 3-μ and 10-μ Fe, respectively, were added to the SP-1 graphite. In run A the temperature

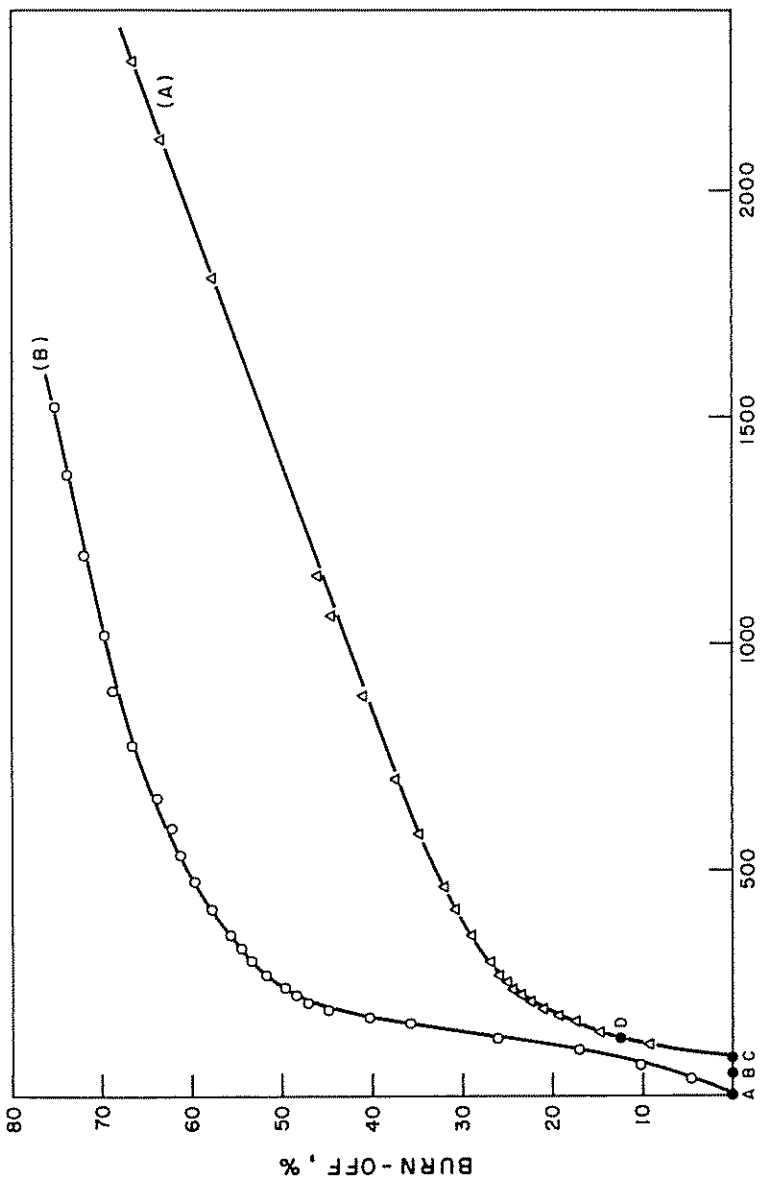

Fig. 36. Reactivity plots for graphite doped with 300 ppm of Fe powder at 862°C Reactivities were measured over an extended time period to particularly show catalysis by wüstite.

history in CO_2 was A–B, 862°C; B–C, 945°C; C–D, 1005°C; D onward, 862°C. This temperature cycle resulted in the catalyst being all converted to wüstite at a relatively low burn-off (ca. 33%) and gave ample opportunity to follow the gasification reaction as catalyzed by wüstite. In run B, the entire run was conducted at 862°C.

Table IX summarizes results for gasification rates at 862°C for pure SP-1 and SP-1 containing 3- and 10-μ Fe. The Fe-containing samples were reacted in CO_2/CO mixtures where wüstite is the stable phase. For the fast

TABLE IX

Gasification Rates of Pure and Iron Containing SP-1 Graphite at 862°C

	Carbon burn-off, %/min	
Sample	Rapid	Slow
SP-1 plus 300 ppm 3-μ Fe	0.5–0.6[a]	0.013[a]
SP-1 plus 300 ppm 10-μ Fe	0.3–0.4[a]	0.012[a]
Pure SP-1	—	0.002[b]

[a] From Fig. 36.
[b] From Fig. 33.

rates, the catalyst (in the reaction region) is thought to be Fe. For the slow rates, the catalyst is thought to be wüstite. The rate of gasification of the pure graphite in pure CO_2 was obtained by extrapolating the Arrhenius plot shown in Fig. 33 to 962°C. It is seen that the gasification rate when the reaction is catalyzed by metallic Fe is some 30- to 40-fold greater than the rate catalyzed by wüstite. The difference is still much greater if it is concluded that the gasification catalyzed by metallic Fe is occurring over a narrow reaction region, whereas that catalyzed by wüstite is occurring over the entire sample. The pure graphite is seen to have about a 6-fold lower gasification rate than the sample containing wüstite.

The extent of catalytic activity of carburized Fe for catalysis of the C—CO_2 reaction could not be clearly determined from these studies, since decarburization occurred in oxidizing atmospheres. At gasification temperatures in a CO_2 atmosphere, the carburized Fe was progressively oxidized. Certainly, as seen from Fig. 28, samples containing carburized Fe underwent immediate gasification in CO_2 at 850°C. The increase in

gasification rate with time possibly could be attributed to the conversion of the carburized Fe to a more active catalyst, but also could be related to an increase of active surface area of the graphite upon its gasification.

4. Mechanism of catalysis

The authors approach this difficult subject of mechanism with some trepidation but have concluded that their remarks may suggest to the reader new, significant experiments which will lead to a final quantitative understanding of this problem.

Consider our system. Flake-like particles of graphite, having ca. 96% of their surface composed of basal planes, are mixed with a small concentration of metal particles. It is concluded that the metal particles primarily make contact with the basal-plane surfaces of the graphite particles. Microcinematographic studies of Fe catalysis of the oxidation of the basal plane of graphite single crystals have shown that etching occurs at each location where an Fe particle resides on the surface (*18,55*). This one-to-one correspondence between number of Fe particles and etch pits formed is attributed to the strong probability that over an area occupied by an Fe particle one or more defects exist in the graphite where carbon gasification with an oxygen species can occur. A similar mode of attack is expected to occur in our studies. The question now is by what mechanism do Fe, Co, and Ni promote such attack. We will consider Fe in particular but feel that our remarks can also be qualitatively applied to catalysis by Co and Ni.

As we discuss in Section II.I, two general theories of catalysis of the gasification of carbon by impurities have been proposed—the oxygen-transfer and the electron-transfer mechanisms. For our particular system, the electron-transfer mechanism says that Fe has unpaired electrons in its *d* band and when Fe is in contact with graphite, π electrons in the graphite will pair up with these electrons in the *d* band. The result will be to localize π electrons and, consequently, decrease the number of mobile π electrons in the graphite. This will result in a weakening of the average strength of the bonds between peripheral carbon atoms and carbon–oxygen complexes; or gasification of the carbon–oxygen complexes will be enhanced.

As discussed previously (*81*), the number of negative carriers in graphite closely equals the number of positive hole carriers (each ca. 10^{18} cm^{-3} of graphite). Consequently, the thermoelectric power (TEP) of graphite, which is proportional to the difference in the number of negative and positive carriers, is very sensitive to any process which changes the carrier balance, such as that proposed above between Fe and graphite. In this

laboratory, TEP studies have been made on identical materials as used in this gasification study. The introduction of 0.3% by weight of 3-μ Fe powder to SP-1 graphite had no detectable effect on the TEP of the system over that of the pure graphite (*81*). This is not taken to mean that no π electrons in the graphite were localized by the Fe but that the number was small. With gasification, graphite is etched and particles of Fe reside in the etch pits where their area of contact with the graphite is enhanced. Thus the possibility of enhanced π-electron localization, per weight of Fe, would seem to be possible. However, concurrently etching increases the number of edge carbon atoms (that is, surrounding the etch pits) which themselves can localize π electrons (*114*). Therefore, the contribution of the Fe to the overall localization of π electrons could, in fact, diminish as carbon gasification proceeds. It is concluded that the mechanism of catalysis by Fe in our studies cannot be primarily attributed to an electron-transfer process.

Let us consider the possible mechanism of catalysis by an oxygen-transfer process. This discussion will be primarily phenomenological, since at this time sufficient information does not exist to make it otherwise. A number of workers have studied the interaction of CO_2/CO mixtures with Fe (*115–120*). They find that chemisorption of CO_2 over Fe is dissociative down to 20°C (*119*) forming CO and an adsorbed oxygen atom (or ion). The adsorbed oxygen atom has at least three fates: Either it can be incorporated into the oxide lattice, can combine with a second oxygen atom and desorb as O_2, or recombine with CO to yield CO_2. These possibilities are given below:

$$xCO_2 + yFe \rightarrow Fe_y(O)_x + xCO \qquad \text{(d)}$$

$$Fe_y(O)_x \rightarrow Fe_yO_x \qquad \text{(e)}$$

$$Fe_y(O)_x \rightarrow yFe + xO_2/2 \qquad \text{(f)}$$

$$Fe_y(O)_x + xCO \rightarrow xCO_2 + yFe \qquad \text{(g)}$$

When Fe is in contact with graphite, the oxygen atom has another possible fate. It can diffuse across the Fe surface to the Fe–graphite interface, can there react with the graphite to form CO, or can diffuse along the graphite surface until reaching an active site and there react to form CO.* Field ion microscope studies have shown that oxygen has

* Very recently, L'Homme and co-workers (*120a*) have suggested a similar mechanism for the catalysis by Pt of the oxidation of the channel black, Spheron 6. They concluded that two parallel paths of reaction are operative with the platinized samples. At low temperatures, the rate of oxidation is limited by surface diffusion of adsorbed oxygen

considerable mobility on metal surfaces at elevated temperatures (*121*). Recently studies of Robell and co-workers (*122*) show surface diffusion of hydrogen atoms on carbon, following their dissociation and diffusion over Pt particles, to occur at temperatures as low as 350°C. Vastola and co-workers (*123*) and others (*124,125*) have shown that oxygen atoms are highly reactive with carbon; activation energies for gasification are low. Thus Fe is acting as a catalyst for the C—CO_2 reaction by dissociating CO_2 and thereby producing an active species—oxygen atoms (or ions). Smeltzer (*116,117*) finds that the E for the oxidation of Fe by CO_2 in the very early stages, between 760 and 910°C, is 60.6 ± 7 kcal/mole. He notes the close agreement between this figure and the dissociation energy of CO_2 of 67.6 kcal/mole. No agreement would be expected between the E reported for the C—CO_2 reaction catalyzed by Fe in our studies and the above value, since competing reactions and diffusion processes, with their own E, would affect our experimental value.

For surface diffusion to be the effective medium for transport of oxygen atoms from the Fe to the graphite, physical contact of these two materials is required. It might be thought that with oxidation, gasification of carbon surrounding the Fe particles would sharply reduce this contact. In fact, many workers have shown that metal particles at gasification temperatures continue to be in contact with the carbon atoms where gasification is occurring (*35,55,56*). In some cases, as with Fe, the metal particles continue to fall into etch pits; in other cases, they travel parallel to the basal-plane surfaces (probably along edges and grooves). In the latter case, it is suggested that surface tension effects are operative in promoting particle mobility (*56*).

The marked reduction in catalytic activity of the Fe when it is oxidized to wüstite and Fe_3O_4 appears consistent with the above reasoning. Dissociative chemisorption of CO_2 on outgassed metal oxide surfaces has not been reported to the authors' knowledge. In fact, Stone (*126*) even reports negligible nondissociative chemisorption. Chemisorption of CO_2 is reported if oxygen has been preadsorbed; but in this case CO_3 complex formation is believed to occur (*126*). The wüstite surface does have some catalytic activity, since, in fact, the surface does contain a small fraction of Fe atoms. That is, oxidation to wüstite proceeds by transport of Fe ions through the oxide to the oxide/gas interface (*115,116*). The oxidation

atoms to the prismatic faces of the carbon lattice. The atoms are supplied by the fast dissociation of O_2 on the Pt crystals. At higher temperatures, a direct reaction between oxygen atoms and carbon atoms at the Pt–carbon interface predominates.

to Fe_3O_4 also proceeds by a similar mechanism. However, since the diffusion rate of Fe ions in Fe_3O_4 is much smaller than their diffusion rate in wüstite (*115*), the concentration of Fe atoms (or ions) at the oxide/gas interface would be expected to be much less when the outer oxide is Fe_3O_4. Thus Fe_3O_4 appears to have no detectable catalytic activity.

It is interesting to compare the rate of wüstite formation in 1 atm of CO_2 with the catalytic activity of wüstite for the C—CO_2 reaction. Smeltzer (*117*) reports that at 862°C the weight gain during wüstite formation is ca. 3 mg of oxygen/cm² of surface/hr. The surface area of 3-μ Fe from N_2 adsorption at 77°K is 2.5×10^4 cm²/g. Thus for a 0.2-g sample of graphite containing 300 ppm of 3-μ Fe powder, the amount of oxygen atoms produced by CO_2 decomposition would be at least 4.5 mg/hr. If all these atoms were to react with carbon to produce CO, the carbon burn-off would be ca. 0.03%/min. This is to be compared with the experimental gasification rate reported in Table IX of 0.013%/min in roughly a 1:1 CO_2/CO mixture. The close agreement might be fortuitous, but the authors feel that the approach has interesting possibilities.

In conclusion, it is well to emphasize that the oxidation of all metals does not lead to their deactivation as catalysts for the gasification of carbon by oxidizing gases. Vanadium, which forms a liquid oxide readily at gasification temperatures (V_2O_5), is a very active catalyst for the C—O_2 reaction (*56*). Molybdenum, which also forms a liquid oxide (MoO_3), is a remarkable catalyst for the C—O_2 reaction (*55*). It has high mobility on the basal plane of graphite, traveling in crystallographic directions and catalyzing carbon gasification as it moves. These metal oxides, however, can be reduced relatively easily by carbon (*127,128*). Thus it is suggested that a significant rate of solid-state reduction of these oxides by carbon to produce CO occurs at gasification temperatures and through this route they are participating in the oxygen-transfer process. The rate of solid-state reduction is further enhanced since, in the liquid state, these oxides afford a greater contact area between themselves and the carbon surface for reaction to occur.

ACKNOWLEDGMENTS

Our interest in catalysis of carbon gasification was prompted primarily through concern about the gasification of moderator graphite in high-temperature, gas-cooled nuclear reactors. The continuing financial support of the U.S. Atomic Energy Commission under Contract AT(30-1)-1710 made the preparation of this chapter a reality.

REFERENCES

1. P. L. Walker, Jr., F. Rusinko, Jr., and L. G. Austin, *Advan. Catalysis*, **11**, 133 (1959).
2. R. N. Smith, *Quart. Rev. (London)*, **13**, 287 (1959).
3. G. D. Blackwood, *Coke Gas*, **22**, 190, 250, 293 (1960).
4. T. J. Clark, R. E. Woodley, and D. R. De Halas, *Nuclear Graphite*, Academic Press, New York, 1962, pp. 387–437.
5. S. Ergun and M. Mentser, *Chemistry and Physics of Carbon*, Vol. I (P. L. Walker, Jr., ed.), Dekker, New York, 1966, pp. 203–263.
6. C. Kröger, *Z. Angew. Chem.*, **52**, 129 (1939).
7. J. F. Strange, Ph.D. thesis, Pennsylvania State University, University Park, 1964.
8. D. L. Biederman, Ph.D. thesis, Pennsylvania State University, University Park, 1965.
9. V. A. Evropin, N. V. Kul'kova, and M. I. Temkin, *Zh. Fiz. Khim.*, **30**, 398 (1956).
10. P. V. N. Ramachandra Rao and E. E. Petersen, *Ind. Eng. Chem.*, **50**, 331 (1958).
11. W. M. Tudenham and G. R. Hill, *Ind. Eng. Chem.*, **47**, 2129 (1955).
12. C. Heuchamps, Thèse Ingénieur-Docteur, Université de Nancy, 1960.

12a. C. Heuchamps and X. Duval, *Carbon*, **4**, 243 (1966).

13. C. Heuchamps, X. Duval, and M. Letort, *Compt. Rend.*, **260**, 1657 (1965).
14. L. Bonnetain, *J. Chim. Phys.*, **56**, 266, 486 (1959).
15. G. Hoynant, F. Collart, X. Duval, and M. Letort, *Compt. Rend.*, **246**, 2889 (1958).
16. F. M. Lang, P. Magnier, and S. May, *Carbon*, **1**, 33 (1963).
17. M. Letort and G. Martin, *Bull. Soc. Chim. France*, **14**, 400 (1947).
18. J. M. Thomas and P. L. Walker, Jr., Carbon, **2**, 434 (1965).
19. H. Amariglio, Thèse Docteur Science, Université de Nancy, 1960.
20. H. Hering, S. Keraudy, F. M. Lang, and S. May, *Proceedings of the Fourth Conference on Carbon, Buffalo, 1959*, Pergamon Press, New York, 1960, pp. 115–122.
21. J. T. Gallagher and H. Harker, *Carbon*, **2**, 163 (1964).
22. H. Harker, *Proceedings of the Fourth Conference on Carbon, Buffalo, 1959*, Pergamon Press, New York, 1960, pp. 125–139.
23. S. Patai, E. Hoffman, and L. Rajbenbach, *J. Appl. Chem.*, **2**, 306, 311 (1952).
24. J. F. Rakszawski and W. E. Parker, *Carbon*, **2**, 53 (1964).
25. G. C. Bond, *Catalysis by Metals*, Academic Press, New York, 1962.
26. F. J. Long and K. W. Sykes, *Proc. Roy. Soc. (London)*, **A215**, 100 (1952).
27. J. G. King and J. H. Jones, *J. Inst. Fuel*, **5**, 39 (1931).
28. G. E. Goring, G. P. Curran, R. P. Tarbox, and E. Gorin, *Ind. Eng. Chem.*, **44**, 1051 (1952).
29. E. A. Gulbransen and K. F. Andrew, *Ind. Eng. Chem.*, **44**, 1048 (1952).
30. J. F. Rakszawski, F. Rusinko, Jr., and P. L. Walker, Jr., *Proceedings of the Fifth Conference on Carbon, Penn State, 1961*, Vol. 2, Pergamon Press, New York, 1962, pp. 243–250.

30a. J. Lothe and S. Melsom, *Dragon Project Rept.* **372**, A.E.E., Winfrith, England, Aug. 1965.

31. H. S. Taylor and H. A. Neville, *J. Am. Chem. Soc.*, **43**, 2055 (1921).
32. N. Bach and I. Lewitin, *Kolloid-Z.*, **64**, 22 (1933).
33. N. Bach and I. Lewitin, *Kolloid-Z.*, **68**, 152 (1934).